universität wien

MASTERARBEIT / MASTER'S THESIS

Titel der Masterarbeit / Title of the Master's Thesis

„Optimization of Special Magnets for the MedAustron Accelerator"

verfasst von / submitted by

Florian Hinterschuster, BSc

angestrebter akademischer Grad / in partial fulfilment of the requirements for the degree of

Master of Science (MSc)

Wien, 2020 / Vienna, 2020

Studienkennzahl lt. Studienblatt / degree programme code as it appears on the student record sheet:	A 066 876
Studienrichtung lt. Studienblatt / degree programme as it appears on the student record sheet:	Masterstudium Physik UG2002
Betreut von / Supervisor:	Univ.-Prof. Dipl.-Ing. Dr. Robin Golser

Contents

Introduction

The EBG MEDAUSTRON GmbH [1] is building, and will later operate, the MEDAUSTRON centre for ion-therapy and research in Wiener Neustadt in the county of Lower Austria. The centre comprises an accelerator facility based on a synchrotron for the delivery of protons and light ions to irradiation stations for cancer treatment and for clinical as well as non-clinical research. EBG MEDAUSTRON is owned and financed by the County of Lower Austria with financial contributions from the Federal Republic of Austria and the City of Wr. Neustadt.

Figure 1 – Artists impression of the MEDAUSTRON medical centre.

The accelerator complex consists of the injector with ion sources and an ion linac that will accelerate particles up to the synchrotron injection energy of 7 MeV/u, this is followed by a synchrotron capable of accelerating particles to the planned extraction energy, ranging from 60 MeV to 250 MeV for protons and 120 MeV/u to 400 MeV/u for carbon ions, suitable for the medical application. For non-clinical research only a proton energy extended up to 800 MeV is also possible. Figures 11, 12 and 13 show preliminary schematic pictures of the MEDAUSTRON centre.

During the past few decades mainly cyclotrons were built for radiation treatment but having the disadvantage that the energy cannot be altered as well as it is only possible to us one particle type. MEDAUSTRON will use a linac and a synchrotron as accelerators. This has the advantage that it is possible to use different particle types and to vary the magnetic field strength of the magnets. Thus it is possible to alter the energy of the particle beam and hence the depth of penetration. For injection, acceleration and extraction of the particles in the synchrotron a variety of magnets are used. These magnets are designed in cooperation with CERN [2] and the concepts and developments for CNAO (a similar facility being built in Italy) [3] are used as a baseline. After DANFYSIK [4] built the magnets for CNAO, measurements

[1] EBG MedAustron GmbH, Viktor Kaplan-Straße 2, 2700 Wiener Neustadt, Austria
[2] CERN CH-1211, Geneve 23, Switzerland
[3] Fondazione CNAO, Strada Campeggi 53, 27100 Pavia, Italy
[4] DanFysik A/S, Gregersensvej 8, DK-2630 Taastrup, Denmark

showed that some of these were not performing as predicted. Hence it was necessary to do new simulations of the magnets as they were designed to verify the measurements and identify possible modifications to reach the required specifications again.

For 3d-simulations three different types of magnets, namely the injection bumpers, the dump bumpers and the chopper dipoles, were modelled and analysed. After the problems were identified, the magnets have been modified accordingly and new simulations have been done to verify these improvements.

Chapter 1 consists of a short introduction to synchrotron concepts as well as the layout of the MEDAUSTRON accelerator. Further the Lorentz force will be explained since this force will act on the particles and deflect the beam. Furthermore the most important parameters for designing fast-pulsed magnet systems are explained.

Chapter 2 presents the simulation models and results for all of the magnets. Based upon the specifications of the CNAO project, possible methodical improvements and modifications for the MEDAUSTRON accelerator are investigated in order to minimize or eventually avoid completely the technological problems, which occurred during the experimental realization of the CNAO project. Furthermore the program suite OPERA from COBHAM VECTORFIELDS [5] is introduced which was used for modelling and analysing the magnets in 3-dimensions.

Finally *Chapter 3* summarizes and concludes the results presented in chapter 2.

[5] Cobham CTS Limited, 24 Bankside, Kidlington Oxfordshire, UK

1 Basics

This chapter contains a short introduction to synchrotron concepts and basic mathematics, which are important for the design of magnets. Furthermore the most important parameters for designing fast-pulsed magnet systems are explained.

1.1 Synchrotron Accelerator

A synchrotron is a circular accelerator using magnetic fields of dipole magnets to keep the particles on track while quadrupole magnets are used to focus the beam in transversal direction and sextupoles in longitudinal direction. A section with a time varying electrical field (RF section) is used to accelerate the particles by increasing the magnetic field appropriately to the particles energy gain, the particles can be held constant on the reference trajectory during acceleration.

Since accelerators have a certain energy range, particles have to be pre-accelerated before entering the synchrotron. After they are extracted from the source the particles are usually accelerated in a linear accelerator and then injected into the main ring. After the particles gained the foreseen energy in the synchrotron they are extracted and delivered to the target. For injection and extraction several special magnets are needed. Also for dumping the beam special dedicated magnets are needed.

1.1.1 Example: MedAustron

The MEDAUSTRON synchrotron supports the acceleration of carbon ions and protons. Starting from the source and accelerated in a linear accelerator they are injected using multi-turn injection to fill the phase space at an energy of 7 MeV/[A]. Therefore a special concept has to be applied as it is impossible to inject on top of an already filled orbit (law of Liouville according the phase-space) and thus the beam already in the synchrotron has to be bumped from its orbit using injection bumpers. In the main ring the beam can be dumped every time by two dump bumpers. After the beam was extracted to deliver it to the treatment rooms there is one more option to abort the beam. Four chopper magnets route the beam around a dump. For safety reasons the arrangement is constructed in a way that the magnets have to be active for the beam to go around the dump.

The positions of the two injection bumpers (with the letters mki in the end), the two dump bumpers (with the letters mks in the end) and the four chopper dipoles (with the letters mkc in the end) can be seen in Figure 2.

A design of the MEDAUSTRON accelerator layout can be seen in Figure 3.

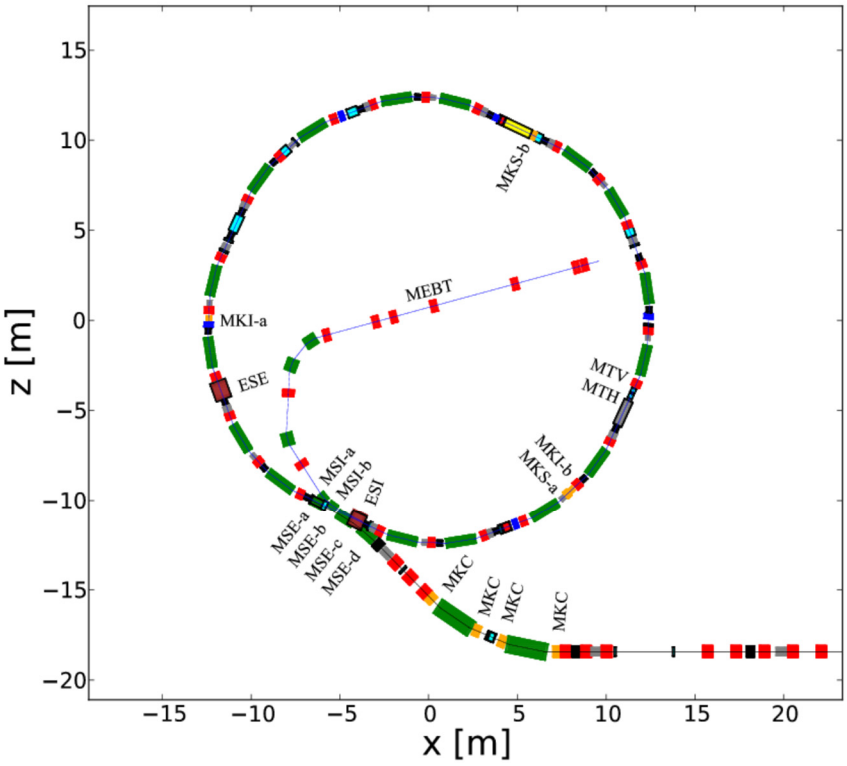

Figure 2 – Layout of the MEDAUSTRON accelerator cutting of the right hand side of the beam delivery to the treatment rooms.

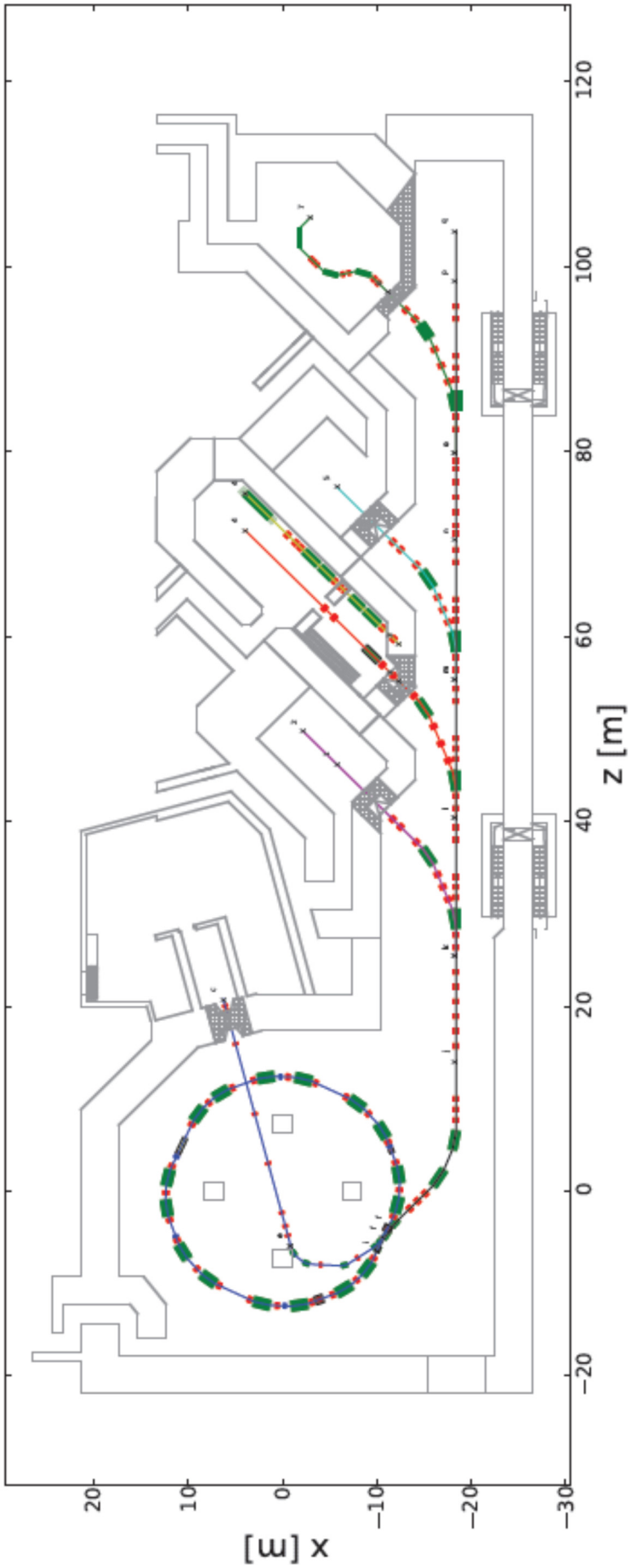

Figure 3 – Design of the MedAustron accelerator layout.

1.1.2 Particles in Magnetic Fields – Lorentz Force

Particles in an accelerator are kept on their trajectory using magnets. The force that is applied on a particle by electric and magnetic fields is the Lorentz force:

$$\vec{F}_{Lorentz} = q\left(\vec{E} + \vec{v} \times \vec{B}\right)$$

Since the electrical fields do not play a role in a bending magnet the Lorentz force can be written in an easier form:

$$\vec{F}_{Lorentz} = q\left(\vec{v} \times \vec{B}\right)$$

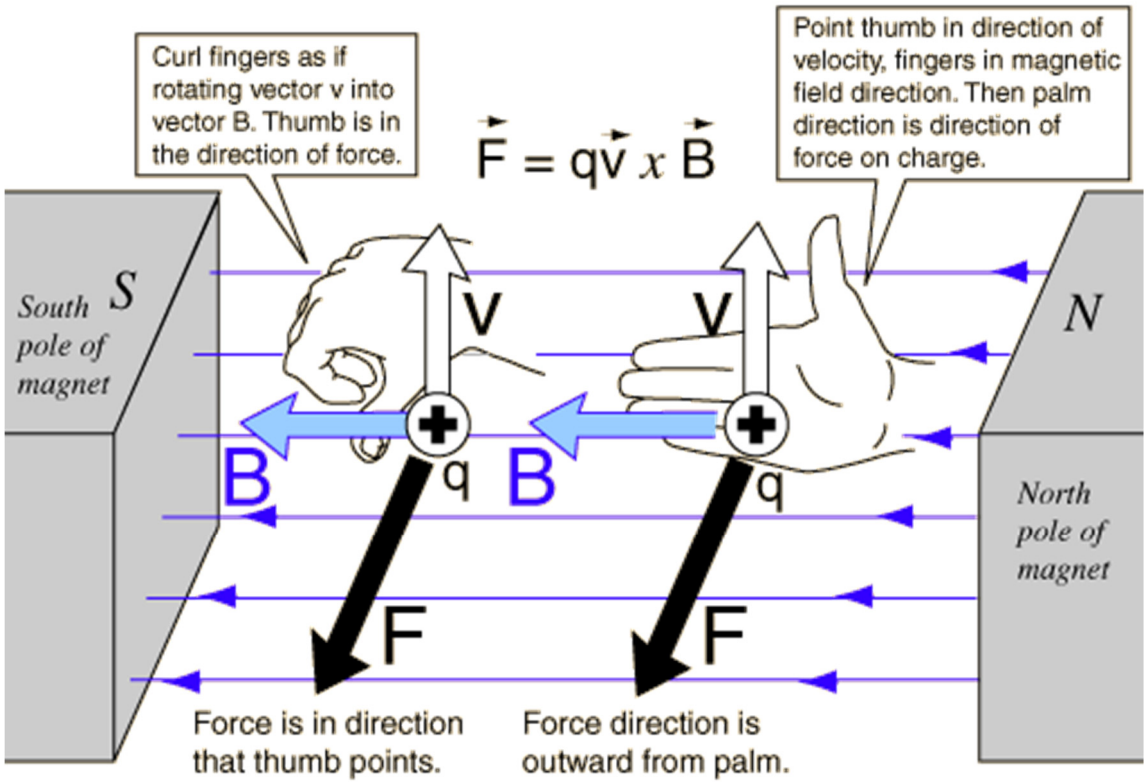

Figure 4 - Lorentz force and right hand rule in a magnetic field [6].

[6] http://hyperphysics.phy-astr.gsu.edu/hbase/magnetic/imgmag/rthnd.gif

1.2 Parameters for magnets and terms

Physical Length [m]

The physical length of a magnet contains everything which is built inside the magnet in beam direction i.e. yoke, conductors and shielding box on the outside which is the borderline of the magnet to the next element in the accelerator. Flanges or vacuum chambers on the outside of the box are not included. See Figure 5.

Maximum magnetic field B_0 [T]

Though the magnetic field strength is higher next to the conductors or inside the yoke, the maximum magnetic field is measured in the centre of the magnet since this is the region of interest and the magnetic field, which acts on the beam at this point. See Figure 5.

Integrated magnetic field $\int Bdl$ [Tm]

Since particles are supposed to follow along the reference trajectory through the magnet, a magnetic field acts on a particle over a certain distance. Integrating the field B_x or B_y along the line of beam direction gives the integrated length. This value can differ strongly depending on the borders of the integral. See Figure 5.

Effective length L_{eq} [m]

The effective magnetic length or equivalent length is the ratio between integrated magnetic length and the maximum magnetic field. See Figure 5.

$$L_{eq} = \frac{\int_{z1}^{z2} Bdl}{B_0}$$

Beam rigidity $B\rho$ [Tm]

The rigidity of a beam can be derived starting at the Lorentz force $F_{Lorentz}$ with q as the charge and v the velocity.

$$\vec{F}_{Lorentz} = q\left(\vec{E} + \vec{v} \times \vec{B}\right)$$

Without an electric field and assuming a homogeneous magnetic field perpendicular to the particle velocity this simplifies to

$$F_{Lorentz} = qvB$$

The bending of the particle provokes a centrifugal force F_{centr} due to the centrifugal acceleration a_{centr}

$$F_{centr} = ma_{centr} = \frac{mv^2}{\rho}$$

where ρ represents the radius of the curvature of the particle trajectory.

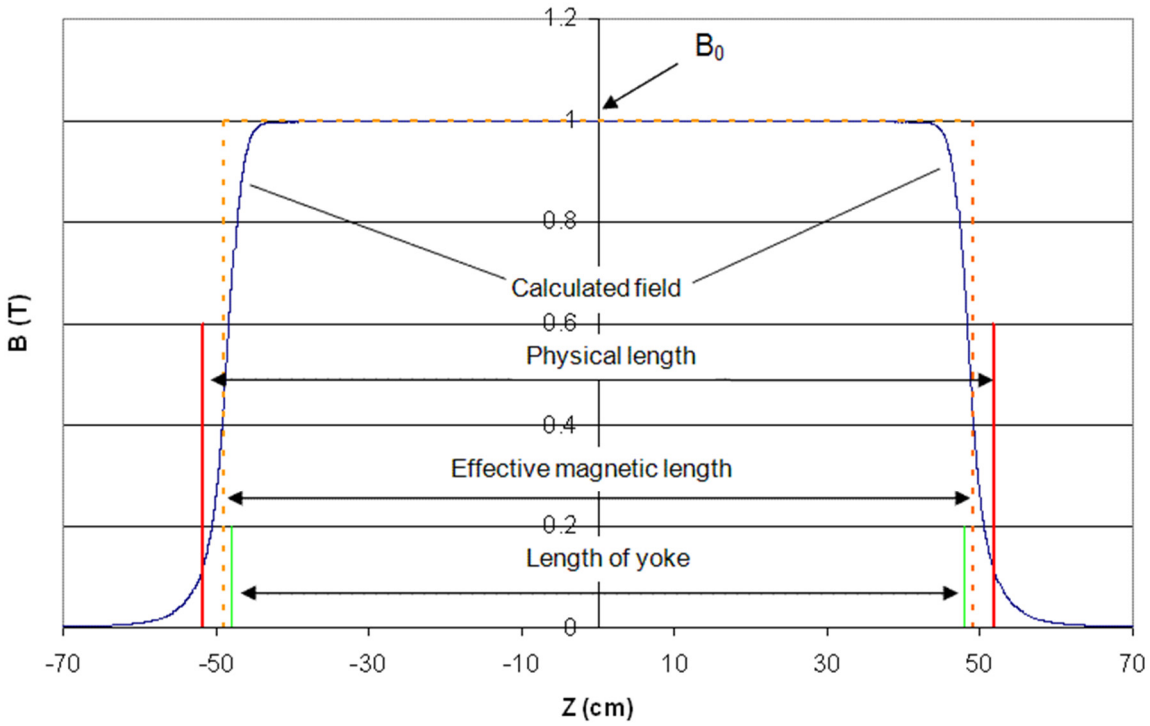

Figure 5 – Example for a calculated field over 140 cm along the beam direction in the center of a magnet showing the maximum field, physical, effective and yoke length. Integrating the calculated field over a certain distance is giving the integrated field [7].

For equilibrium of the Lorentz force and the centrifugal force the following expressions can be deduced

$$F_{Lorentz} = F_{centr}$$

$$qvB = \frac{mv^2}{\rho}$$

$$B\rho = \frac{p}{q}$$

$B\rho$ is then called the beam rigidity or magnetic beam rigidity.

For a beam momentum p not given in SI units but as common in particle physics in GeV/c and with the charge $q=ne$ the beam rigidity can be written as

$$B\rho[\mathrm{SI}] = \frac{10^9}{nc} p[\mathrm{GeV/c}]$$

[7] T. Stadlbauer, "Optimization of special magnets", page 21, University of Applied Sciences Kaiserslautern, Kaiserslautern, 2010

Deflection angle *Θ*

Using the Lorentz force without an electrical field and the magnetic field perpendicular to the velocity *F=qvB* and Newton's law *F=ma* the acceleration *a* can be expressed by

$$a = \frac{qvB}{m}$$

The time period the particle sees the maximum field can be written as

$$t = \frac{l_{eq}}{v}$$

Substituting these two terms into

$$s = \int vdt = \iint adt^2 = \frac{a}{2}t^2$$

gives

$$s = \frac{1}{2}\frac{qvB}{m}\frac{l_{eq}^2}{v^2}$$

The deflection angle Θ as it can be seen in Figure 6 is

$$\tan\Theta = \frac{ds}{dl} = \frac{qB}{m}\frac{l_{eq}}{v} = \frac{q}{mv}\int Bdl = \frac{\int Bdl}{B\rho}$$

Since small angles can be approximated by *tan Θ= Θ* if *Θ<<1* the formula for the deflection angle is

$$\Theta = \frac{\int Bdl}{B\rho}$$

Pole gap [mm]

The pole gap is the height of the distance within the yoke.

Aperture [mm.mm]

The aperture is the area of the cross section within the vacuum chamber.

Good field region [mm.mm]

The good field region specifies the cross section in which the integrated magnetic length shall have a certain field quality i.e. the integrated magnetic length at all positions within the good field region has to be within the specified field quality of the integrated length of the reference trajectory.

Field quality [%]

The percentage of allowance of different values for the integrated field length referred to the reference trajectory in within the good field region.

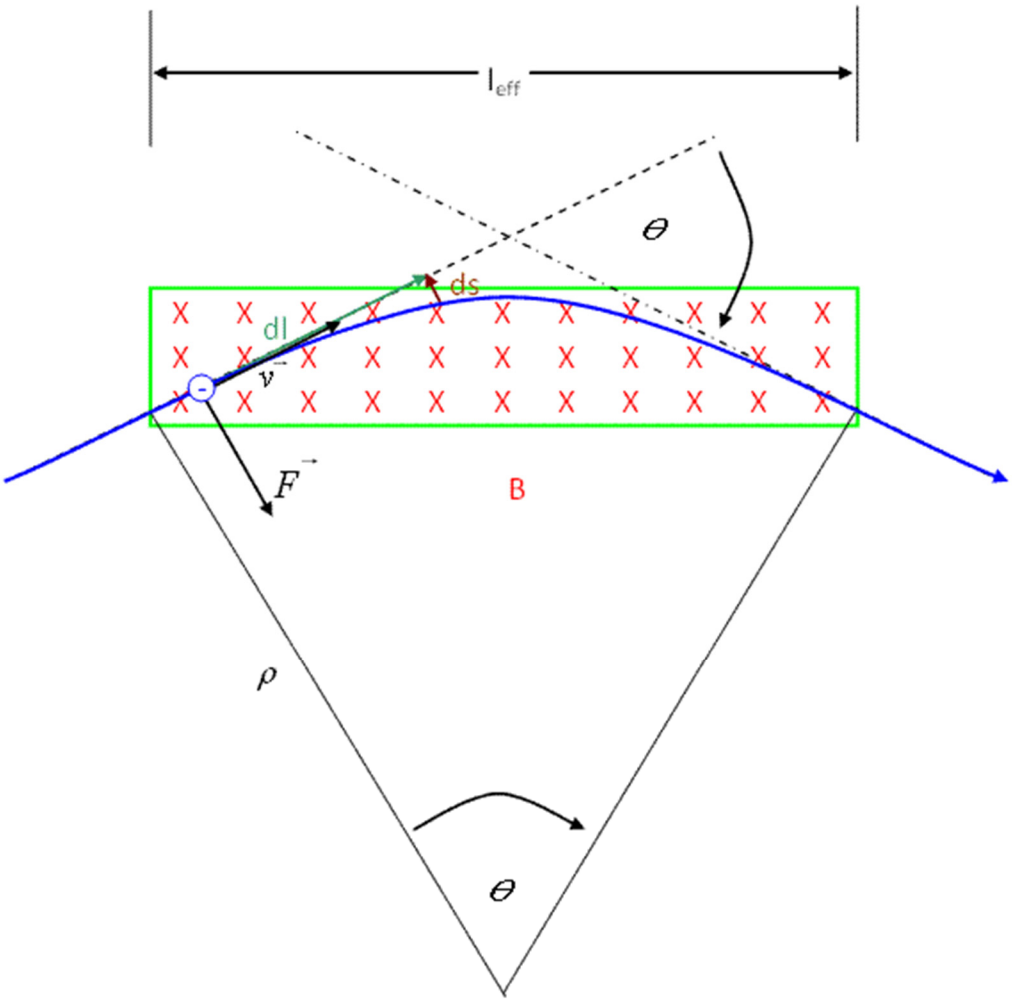

Figure 6 – Deflected beam by a magnetic field [8].

Current *I* [A]

The given current *I* feeds the conductors.

Current density [A/mm²]

The current density *J* is the current divided by the cross section of one turn of the conductor. The magnetic field rises with the current density in dependence of the hysteresis. The higher the current density over a certain time, the hotter the conductor gets and cooling is required.

$$J = \frac{I}{A}$$

[8] T. Stadlbauer, "Optimization of special magnets" page 24, University of Applied Sciences Kaiserslautern, Kaiserslautern, 2010

Ramp time [µs]

The ramp time is the time in which the magnet has to be powered to the maximum current or lowered to zero current.

Stored Energy *W* [J]

The stored energy is the energy density of the electromagnetic field. It can be derived from the Maxwell equations and the Lorentz force acting on a particle with the charge q. This is done in the cgs-system. For the displacement of $d\vec{s} = \vec{v}dt$ the mechanical work is

$$dA_{mech} = \vec{F}d\vec{s} = q\left(\vec{E} + \frac{\vec{v}}{c} \times \vec{B}\right)\vec{v}dt = q\vec{E}\vec{v}dt$$

In a volume it is then

$$\frac{dA_{mech}}{dt} = \int_V d^3r\, \rho(\vec{r},t)\vec{v}(\vec{r},t)\vec{E}(\vec{r},t) = \int_V d^3r\, \vec{j}(\vec{r},t)\vec{E}(\vec{r},t)$$

with $\rho(\vec{r},t)$ as charge density $\vec{j}(\vec{r},t)$ as current density.

Using the two Maxwell equations

$$\text{curl}\,\vec{E} + \frac{1}{c}\frac{\partial}{\partial t}\vec{B} = 0 \qquad |\vec{B}$$

$$\text{curl}\,\vec{B} - \frac{1}{c}\frac{\partial}{\partial t}\vec{E} = \frac{4\pi}{c}\vec{j} \qquad |\vec{E}$$

and multiply them with $\vec{B}$ and $\vec{E}$ as well as subtracting them from each other. $\vec{j}\vec{E}$ can then be expressed as

$$\vec{j}\vec{E} = -\frac{c}{4\pi}\left(\vec{B}\,\text{curl}\,\vec{E} - \vec{E}\,\text{curl}\,\vec{B}\right) - \frac{1}{4\pi}\left(\vec{E}\frac{\partial\vec{E}}{\partial t} + \vec{B}\frac{\partial\vec{B}}{\partial t}\right)$$

$$= -\frac{c}{4\pi}\text{div}\left(\vec{E}\times\vec{B}\right) - \frac{1}{4\pi}\frac{\partial}{\partial t}\frac{1}{2}\left(\vec{E}^2 + \vec{B}^2\right)$$

Considering that $\frac{c}{4\pi}\text{div}\left(\vec{E}\times\vec{B}\right)$ is the Poynting vector $\text{div}\,\vec{S}(\vec{r},t)$ and substituting this expression in the formula of the work, it delivers

$$\frac{dA_{mech}}{dt} = -\int_V d^3r\,\text{div}\,\vec{S}(\vec{r},t) - \frac{d}{dt}\int_V d^3r\frac{1}{8\pi}\left(\vec{E}(\vec{r},t)^2 + \vec{B}(\vec{r},t)^2\right)$$

$$\frac{d}{dt}\left(A_{mech} + \int_V d^3r\frac{1}{8\pi}\left(\vec{E}(\vec{r},t)^2 + \vec{B}(\vec{r},t)^2\right)\right) = -\int_V d^3r\,\text{div}\,\vec{S}(\vec{r},t)$$

$$\frac{d}{dt}\left(A_{mech} + A_{field}\right) = -\oint_F d^2\vec{f}\vec{S}$$

This formula is the law of conservation of energy of electrodynamics. The term $A_{field} = \int_V d^3r\frac{1}{8\pi}\left(\vec{E}(\vec{r},t)^2 + \vec{B}(\vec{r},t)^2\right)$ is the field energy in a given volume while

$\frac{1}{8\pi}\left(\vec{E}(\vec{r},t)^2+\vec{B}(\vec{r},t)^2\right)$ can be understood as energy density of the electromagnetic field. Hence the stored energy *W* is

$$W=\int_V d^3r\frac{1}{8\pi}\left(\vec{E}(\vec{r},t)^2+\vec{B}(\vec{r},t)^2\right)$$

Inductance *L* [µH]

Taking the result for the field energy the formula simplifies for a magneto static case to

$$W=\frac{1}{8\pi}\int_V d^3r\,\vec{B}(\vec{r})^2$$

Using the vector potential $\vec{A}$ for a magnetic field $\vec{B}=\operatorname{curl}\vec{A}$ and the Maxwell equation $\operatorname{curl}\vec{B}-\frac{1}{c}\frac{\partial}{\partial t}\vec{E}=\frac{4\pi}{c}\vec{j}$ with $-\frac{1}{c}\frac{\partial}{\partial t}\vec{E}=0$ since a static case is assumed, the energy for the magneto static field can be written as

$$W=\frac{1}{8\pi}\int_V d^3r\,\vec{B}(\vec{r})^2 W=\frac{1}{8\pi}\int_V d^3r\vec{B}\left(\vec{\nabla}\times\vec{A}\right)$$

$$=\frac{1}{8\pi}\int_V d^3r\vec{\nabla}\left(\vec{A}\times\vec{B}\right)+\frac{1}{8\pi}\int_V d^3r\vec{A}\left(\vec{\nabla}\times\vec{B}\right)$$

$$=\frac{1}{8\pi}\oint_F d^2\vec{f}\left(\vec{A}\times\vec{B}\right)+\frac{1}{2c}\int_V d^3r\vec{A}\vec{j}$$

The surface integral vanishes due to natural boundary conditions and with the general solution for magneto static problems $\vec{A}=\frac{1}{c}\int d^3r'\frac{\vec{j}(\vec{r}\prime)}{|\vec{r}-\vec{r}\prime|}$ the field energy is then

$$W=\frac{1}{2c^2}\iint d^3rd^3r'\frac{\vec{j}(\vec{r})\vec{j}(\vec{r}')}{|\vec{r}-\vec{r}'|}$$

The current density can be distributed into single complexes due to the linearity of the Maxwell equations $\vec{j}(\vec{r})=\sum_n\vec{j}_n(\vec{r})$. The calculation of the field energy results into two sums that can be divided again into an equation for self-energy and mutual energy. For natural border conditions this results in

$$W_{self}=\sum_n\frac{1}{2c^2}\iint d^3rd^3r'\frac{\vec{j}_n(\vec{r})\vec{j}_n(\vec{r}')}{|\vec{r}-\vec{r}'|}$$

$$W_{mutual}=\sum_{n<m}\frac{1}{c^2}\iint d^3rd^3r'\frac{\vec{j}_n(\vec{r})\vec{j}_m(\vec{r}')}{|\vec{r}-\vec{r}'|}$$

Assuming several current loops with the current I_n in loop *n* and no current density $\vec{j}(\vec{r})$ between the loops, hence $d^3r\vec{j}_n(\vec{r})\xrightarrow{yields}I_nd\vec{r}$ the formula for the total field energy *W* results in

$$W = \frac{1}{2}\sum_{n,m} I_n I_m \frac{1}{c^2} \oiint_{Cm,Cn} \frac{d^3\vec{r}_n d^3\vec{r}_m}{|\vec{r}_n - \vec{r}_m|} = \frac{1}{2}\sum_{n,m} I_n I_m L_{mn}$$

The induction coefficients L_{mn} are only depending on the geometrical dimensions (length of a turn) and the distribution of the current loops. For calculating the induction coefficients, it has to be integrated along every single loop C_n. L_{nn} are the self-induction coefficients and L_{mn} are the mutual induction coefficients. The magneto static energy of such an electrical system for *N* circuit loops (i.e. *N* turns of the conductor) can then be written as

$$W = \frac{1}{2}\sum_{n,m}^{N} I_n I_m L_{mn}$$

The induction *L* for a magnet can then be calculated by

$$L = \frac{2W}{I^2}$$

This can be done since VECTORFIELDS provides calculation tools for the stored field energy.

Voltage *U* [V]

The voltage *U* that is needed is given by the electromotive force $\mathcal{E}$ described by Faraday's law of induction in each turn. The change of a magnetic flux Φ, when powering the magnet causes an electromotive force and therefore a current in the conductor. Due to Lenz law the changes in the magnetic flux over time and the electromotive force have opposing signs.

$$U = -N\mathcal{E} = -N\frac{d\Phi}{dt} = -N\oint_{\partial\Sigma(t)} d\vec{l}\left(\vec{E}(\vec{r},t) + \vec{v}\times\vec{B}(\vec{r},t)\right)$$

Φ is the flux through a surface with an opening bounded by a curve $\partial\Sigma(t)$.

$\partial\Sigma(t)$ is a closed contour that can change with time and the electromotive force is found around this contour, while the contour is a boundary of the surface over which Φ is found.

$d\vec{l}$ is an infinitesimal vector element of the contour $\partial\Sigma(t)$ and finally $\vec{v}$ is the velocity of the segment $d\vec{l}$.

The magnetic flux can also be described by the inductance *L*, the current *I* and the number of turns *N* of the conductor.

$$\Phi = \frac{LI}{N}$$

The voltage needed is then

$$U = L\frac{dI}{dt}$$

Conductor size [mm x mm], conductor length and turns

The conductor size is the cross section of one turn of the conductor. A high conductor size means less current density and cooling requirements are reduced.

The length of the conductor and the number of turns has a huge impact on the inductance and therefore on the voltage needed to power the magnet.

2 Simulations

In this chapter the simulation models and results for all of the magnets are presented. Based upon the specifications of the CNAO project, analyses have been done and possible methodical improvements and modifications for the MEDAUSTRON accelerator are investigated in order to minimize or eventually avoid completely the technological problems, which occurred during the experimental realization of the CNAO project. Furthermore the program suite OPERA from COBHAM VECTORFIELDS [9] is introduced which was used for modelling and analysing the magnets in 3-dimensions.

2.1 Vectorfields–Opera

For analyzing the magnets from CNAO and improve the design the program OPERA from COBHAM VECTOR FIELDS has been used. A short description of the program and a introduction how to use finite element mesh will now be presented.

2.1.1 Pre- and Post Processor, Finite Element Mesh

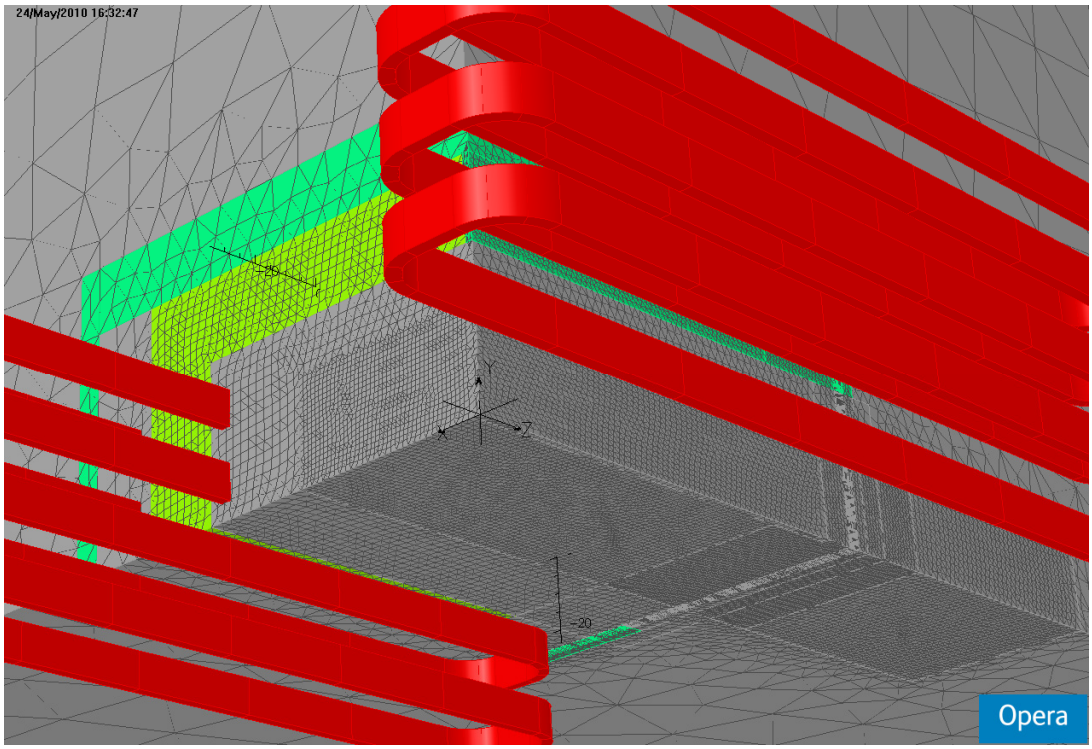

Figure 7 - Surface mesh of one eighth of the injection bumper.

[9] Cobham CTS Limited, 24 Bankside, Kidlington Oxfordshire, UK

For simulation COBHAM VECTOR FIELDS OPERA 3d is used. OPERA 3d consists of a pre and post processing system for electromagnetic analyses programs. This includes the programs TOSCA, ELEKTRA, SCALA, CARMEN, SOPRANO, DEMAG, QUENCH and Tempo. For all the simulations only TOSCA for static and ELEKTRA for transient simulations were used.

For designing the models the OPERA 3d Modeller was used and the OPERA 3d Post-Processor to analyse them. The infinite element solver (modified Newton-Raphson method) provides the analysed data to the Post-Processor to be graphically displayed.

Near the region of interest the concentration of the element size was set to smaller values in order to increase the number of surface elements and more accurate simulation results in these regions.

'Finite element discretization forms the basis of the methods used in these analysis programs. This widely applicable technique for the solution of partial differential equations requires special enhancements to make it applicable to electromagnetic field calculations. Access to these features is supported by the Geometric Modeller and Pre-Processor. These programs provide facilities for the creation of finite element models, specification of complicated conductor geometry, definition of material characteristics (including nonlinear, anisotropic and hysteretic materials) and graphical displays for interaction and examination of data.

Similarly, the Post-Processor provides facilities necessary for calculating electromagnetic and temperature fields, displaying them as graphs and contour maps. The Post-Processor can also calculate and display many derived quantities and can plot particle trajectories through electromagnetic fields.' [10]

2.1.2 Creating a Model

For all the models all dimensions were taken from the technical drawings from CNAO and DANFYSIK respectively but have been simplified in the model to the important parts for the electromagnetic field, i.e. yoke, aluminium box and the conductors. The connections to the power supply isolation plates between conductors and yoke as well as to the aluminium are omitted.

As it was possible, the symmetry of a magnet was used and only one eighth or one quarter of the magnet was modelled. This reduces the required computation time. The conductors are made of copper and the values are set automatically by OPERA 3d. For the yoke a ferrite namely CMD 5005 [11] produced by Ceramics Magnetics Inc. [12] has been used for all magnets and was set to be an isotropic nonlinear material with low conductivity, which is neglected in the simulations and an BH-curve provided by OPERA as it can be seen in Figure 8.

[10] Opera-3d User Guide, V.13, 2009
[11] Datasheet available under http://www.magneticsgroup.com/pdf/CMD5005.pdf
[12] Ceramic Magnetics, Inc., 16 Law Drive, Fairfield, New Jersey 07004, USA

For DC simulations in TOSCA and AC simulations in ELEKTRA material properties of aluminium are a relative permeability of μ_r=1 H/m, a conductivity of σ=3.77*10^7 Sm^{-1} and a coercivity of H_c=0 Am^{-1}.

To allow eddy currents in the ELEKTRA transient calculations, 10 layers layered the aluminium endplates of the shielding box. The offset for the layers was derived by a quarter of the skin depth *d*, which is calculated by

$$d = \left(\frac{\rho}{\pi \mu_0 f} \right)^{1/2}$$

where ρ is the specific resistance, μ_0 is the magnetic constant and *f* is the frequency of the current. The resistivity off aluminium is ρ_{Al}=26.4*10^{-9} Ωm. The current pulse length for the injection bumper and the dump bumper respectively can be read from Figure 13 and Figure 44. For the chopper dipole the ramp time was not fixed yet but assumed with 90 µs. As example the current pulse of the injection bumper is approximately 200 µs which is the half sine period time and therefore the frequency is *f*=1/400 µs^{-1}. The skin depth is then 1.64 mm and the offset was set to 0.4 mm.

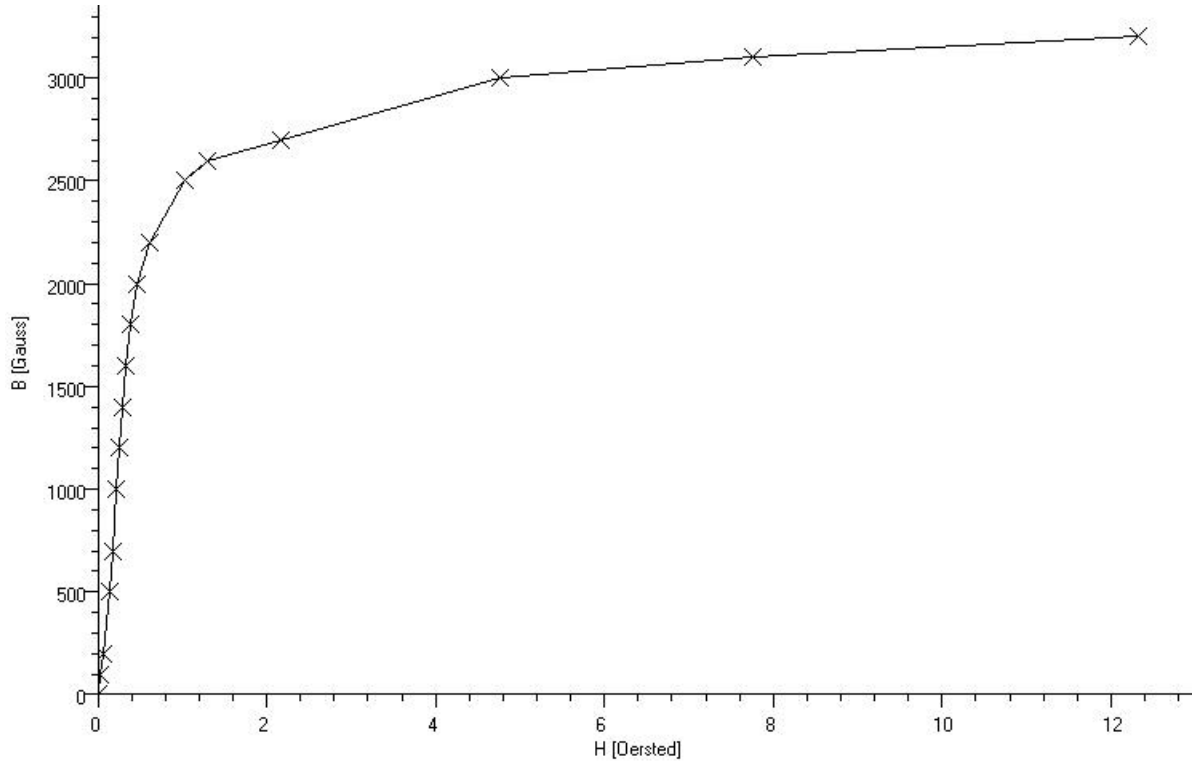

Figure 8 - BH-curve of CMD 5005 from Ceramics Magnetics Inc.

Since simulations in TOSCA are much faster than in ELEKTRA, due to it is not necessary to compute different time steps and no eddy currents exist, first approximations for ELEKTRA have

always been done as DC simulations. In addition it was not possible to make ELEKTRA simulations for the dump bumper due to limitations of the CPU capacity. However it was somehow necessary to simulate eddy currents (which occur within AC operation) and therefore the shielding effects of the aluminium box in TOSCA. Hence the relative permeability of aluminium was set to μ_r=0.0001 H/m. That this approximation works quite well has been verified in an example of the injection bumper, which was once calculated in TOSCA and once in ELEKTRA with reduced permeability.

2.1.3 AC and DC Simulations

In this section it shall be shown that using TOSCA, when changing one parameter of the properties of aluminium can approximate AC simulations in ELEKTRA. Therefore results from the injection bumper, namely the maximum magnetic field, the integrated field over 600 mm and the effective magnetic length are compared using ELEKTRA transient simulation in AC mode and the static TOSCA simulation. For AC and DC simulation the same model has been used as described in section 2.2.2 with 500 A of maximum current. Calculating this model with DC in TOSCA gives different results because no eddy currents are calculated in the aluminium box. The results are given in Table 1.

Table 1 - Results from the ELEKTRA and TOSCA simulation with a relative permeability of μ_r=1 H/m in DC and AC simulations.

	TOSCA with μ_r=1 H/m	**ELEKTRA**	**Deviation [%]**
B0 [T]	0.0262	0.0278	5.97
Bdl over 600 mm [mTm]	8.092	7.715	4.67
Leq [mm]	308.37	277.41	10.04

Simulating the effects of eddy currents by setting the relative permeability to μ_r=0.0001 H/m in the TOSCA simulation while the relative permeability in ELEKTRA remains the same with μ_r=1 H/m gives the results shown in Table 2.

Table 2 - Results from the ELEKTRA simulation with μ_r=1 H/m and the TOSCA simulation with a relative permeability of μ_r=0.0001 H/m.

	TOSCA with μ_r=0.0001 H/m	**ELEKTRA**	**Deviation [%]**
B0 [T]	0.0278	0.0278	0.01
Bdl over 600 mm [mTm]	7.686	7.715	0.38
Leq [mm]	276.34	277.41	0.39

Table 2 compares the results of the AC simulation and the modified TOSCA model. In this DC simulation the deviation is less than 0.4 %. Therefore results for ELEKTRA can be approximated in a satisfying way by using TOSCA simulations. This can save a lot of time for first approximations before starting time consuming ELEKTRA calculations and can also be used for more complex models, which exceeds calculation capacities in AC-mode.

2.2 Injection Bumper

The two identical injection bumpers for CNAO were designed at CERN [13] and built and measured by DANFYSIK [14]. These measurements showed an inhomogeneous field. Hence it was necessary for the MEDAUSTRON accelerator to have a closer look onto these bumpers and rework the design if necessary.

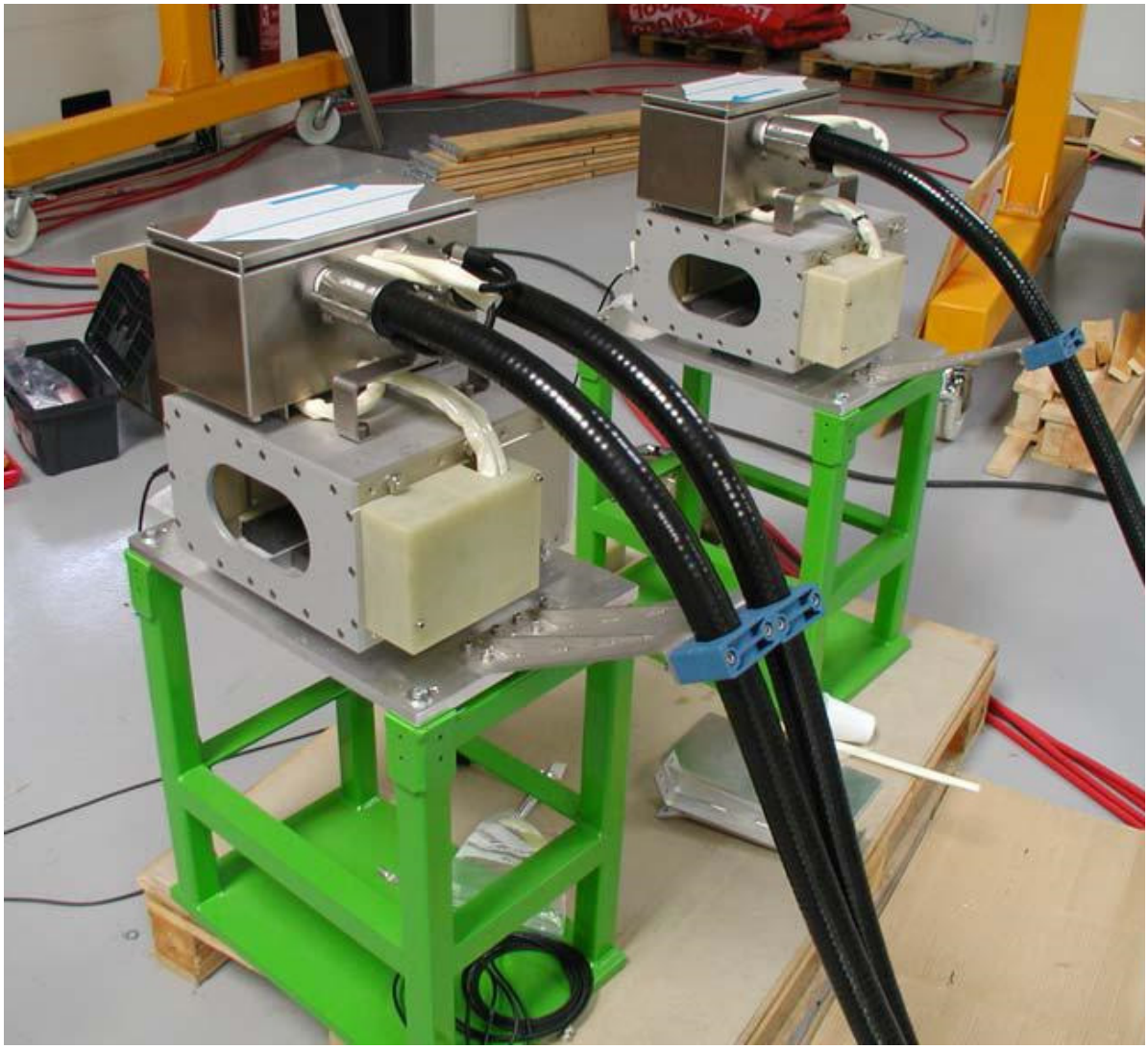

Figure 9 - Complete Assembly of the CNAO injection bumper magnet.

[13] "Final Design, Special Magnets" CAN-TNDP-006WXX-00231, 21th July 2003, J. Borburgh et.al (CNAO-CERN)
[14] "Quality Assurance Report" CNA-SPDF-007WXX-00234, 15th May 2007, N. Hauge (DanFysik)

2.2.1 Parameter List

Table 3 - Magnet parameter list predicted by CERN for the CNAO injection bumper build by DANFYSIK.

Injection Bumper	
Function	Injection bump
Dismantling	Horizontal
Effective magnetic length [m]	0.3
Total physical length [m]	0.295
Ferrite physical length [m]	0.22
Maximum integrated field ∫Bdl [Tm]	0.0076
Maximum field B [T]	0.0254
Maximum beam rigidity [Tm]	0.763
Deflection angle [mrad]	10
Pole gap [mm]	90
Aperture w × h *[mm^2]	166 × 90
Coil 2 in series, copper conductor,	2 in series, copper conductor, 4 turns
Conductor size [mm^2]	3 × 10
Space between turns [mm]	10
Good field region (rectangle) [mm^2]	120 × 60
Field quality [%]	± 1
Current for maximum field [A] (nominal)	454
Voltage [V] (max.)	280
Current density [A/mm^2]	15.13
Number of turns	8 (4 per coil)
Average turn length [m]	0.552
Cooling	Air, not forced
DC power dissipation [W]	-
Estimated inductance [µH]	20

Estimated stored energy [J]	15
Maximum coil voltage to ground [V]	~ 1000
Rise time [µs]	Whatever
Rise shape	Whatever shape
Flat top [µs]	-
Uniformity on flat top [%]	-
Fall time [µs]	20 < t < 70 selectable
Fall Shape	Linear shape
Repetition rate [s]	1.2

2.2.2 CNAO Design

The required horizontal deflection of 10 mrad provided by an effective magnetic length of 0.3 m corresponds closely to an existing design for ion injection into the CERN LEIR synchrotron [15]. The magnet is constructed from two C-shaped ferrite cores, mounted face to face, to form a window frame magnet. The two 8-turns magnets are powered in series and require a peak current of 454 A. The magnets are build-up from identical 4-turns open C-magnet halves, as shown in Figure 10, Figure 11 and Figure 12. The main parameters are given in Table 3.

[15] "The Injection Bumper System for LEIR Ion Test" T. Fowler, Kd. D. Metzmacher PS/CA/Note 98-22 (Tech.).

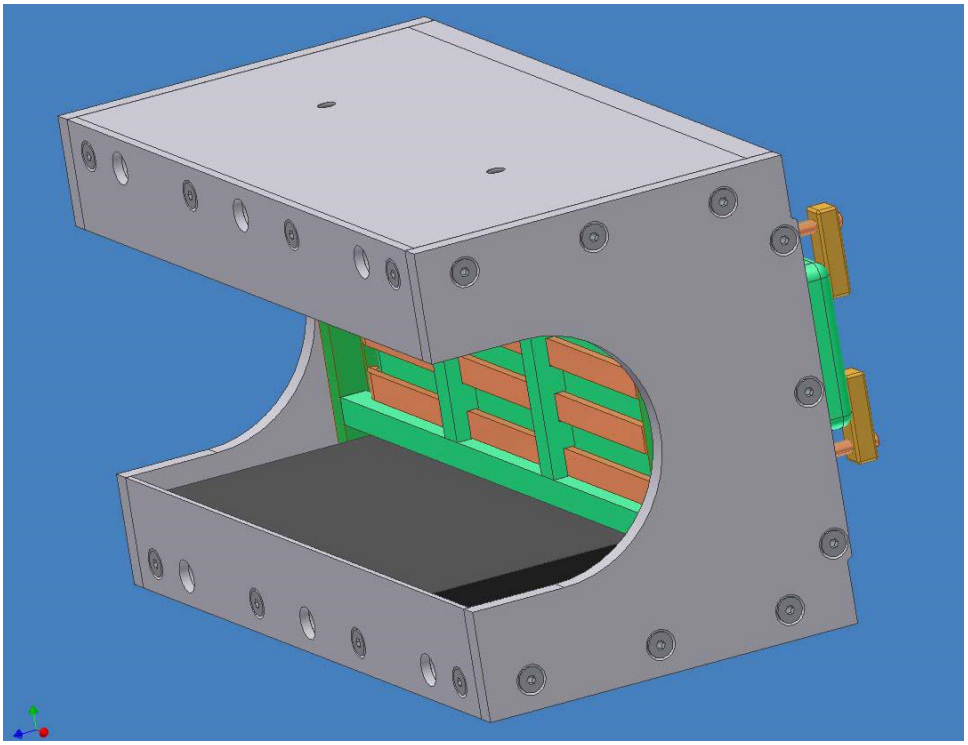

Figure 10 - Open C-shape 4-turns half magnet for injection bumpers.

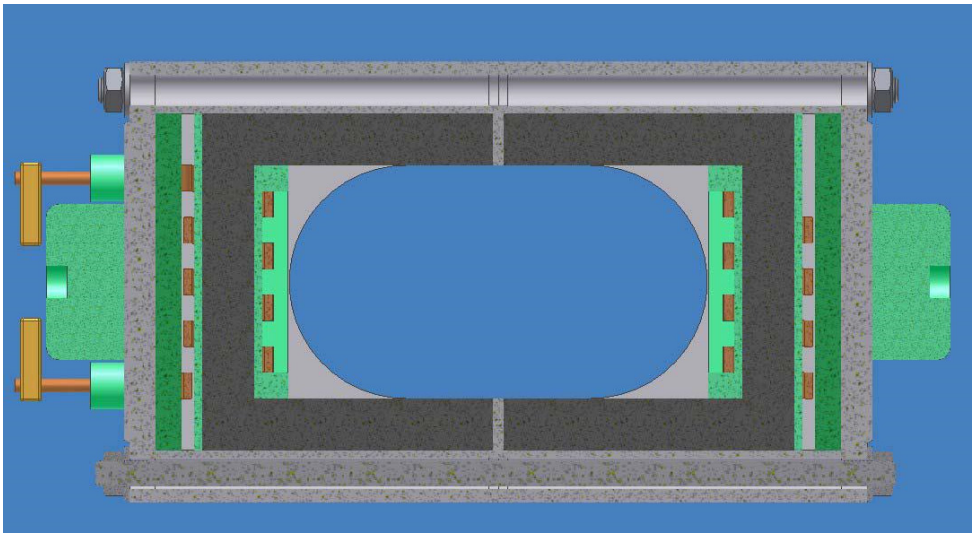

Figure 11 - Cut through the assembled half magnets of the injection bumper.

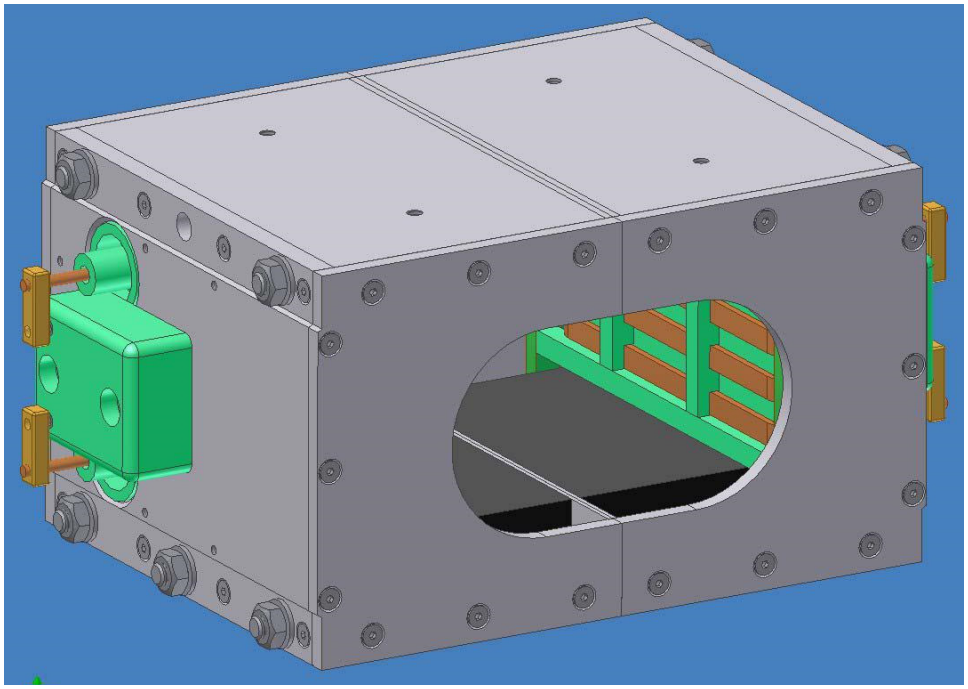

Figure 12 - A 3-D view of an assembled injection bumper magnet.

Figure 13 shows the current waveforms for the minimum and maximum pulse lengths (corresponds to falling times of 20 µs and 70 µs). The use of controlled switching of the primary current avoids the need for any high voltage resonant techniques to establish the peak current and allows implementation of a circuit using the semiconductor switches and avoids high voltage power. DANFYSIK tested the magnet built by them at a current of 500 A. Simulations were done with 500 A as well as 600 A to verify if the necessary deflection angle of 10 mrad can be reached for higher injection energies up to 10 MeV. However it was not verified if the power supply system also works with these higher currents.

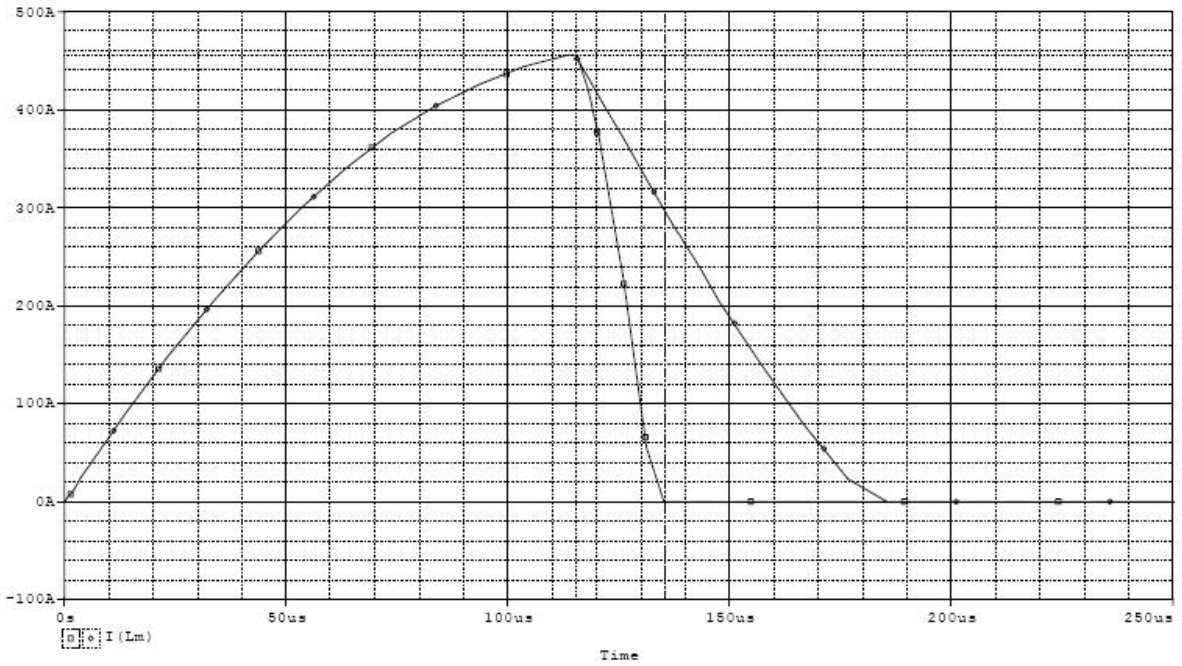

Figure 13 - Injection Bumper magnet current vs. time for two possible operating modes.

The model was designed by using technical drawings from CNAO and DANFYSIK [16]. Simplifications, layering of the aluminium end plates, symmetry and settings for ELEKTRA simulations as well as the material properties have been done and set as described in 2.1.2. The model as designed in the OPERA Modeller is shown in Figure 14 and Figure 15.

[16] The files of the technical drawings can be found under \\cern.ch\dfs\Projects\medaustron\CNAOdocs\docs\Special magnets\special magnets and PS - final documentation\Drawings\B.D.I

Technical Drawings used:

CNAO, Injection Bumpers Assembly, CNA-DRDF-BDIMSS-01000, 23th April 2004

CNAO, Injection Bumpers Sub Assembly, CNA-DRDF-BDIMSS-01001, 23th April 2004

CNAO, Injection Bumper Iron, CNA-DRDF-BDIMSS-02432, 23th April 2004

DanFysik, Half Part Assembly, 14878.104.009.B, 30th August 2005

DanFysik, Coil - 4 Turns, 14878.104.051.B, 30th August 2005

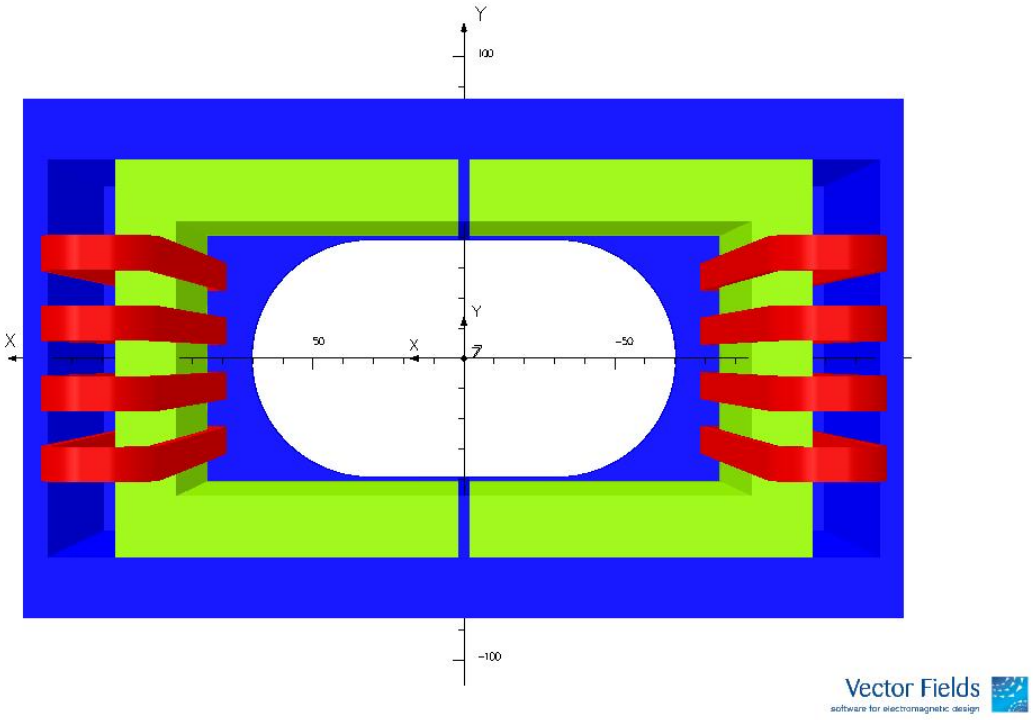

Figure 14 - Cut through the injection bumper in VECTORFIELDS (green parts are the yoke, blue is the aluminium and red are the conductors).

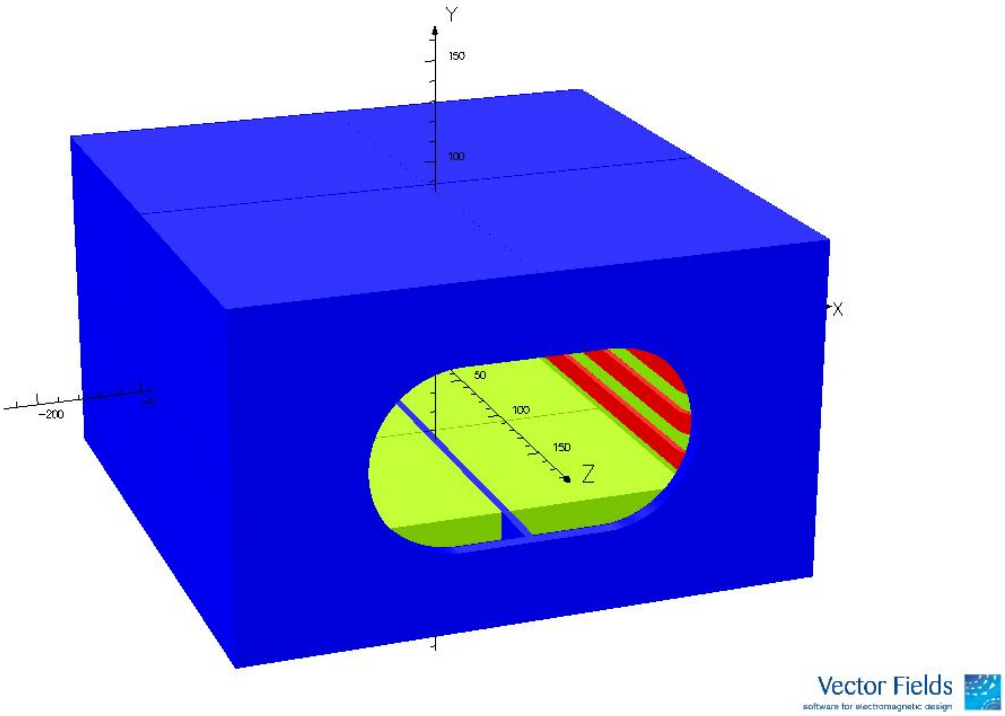

Figure 15 - A 3-D view of an injection bumper magnet in VECTORFIELDS (green parts are the yoke, blue is the aluminium and red are the conductors).

2.2.3 DANFYSIK Measurements Compared to Simulation

CNAO Measurements

Measurements have been done by using a strip line air probe in the centre of the magnet (along the *z*-axis in simulations, which is the particle reference trajectory). The magnet has been excited with a low voltage 10 kHz sine wave using a current of 500 A instead of the 454 A specified.

The maximum magnetic field measured by DANFYSIK is 26.5 mT and 26.2 mT respectively in a second measurement as well as an effective magnetic length of 305 mm and 302 mm [17].

Otherwise to the simulations where the yoke completely consists of CMD 5005, the yoke in the measurements is a mixture of various materials [18]. This also explains magnetic field inhomogeneities in the DANFYSIK magnet.

Simulations in VECTORFIELDS

Simulations calculated for AC are done in VECTORFIELDS OPERA-ELEKTRA-Transient for various time steps during the current rising and falling time. As in DANFYSIK measurements the peak current is 500 A instead of the specified 454 A. This corresponds to a peak current density of 16.67 A/mm^2. The pulse is triangular with a rise time of 150 µs and a fall time of 70 µs. Therefore the total pulse time is 220 µs.

Effective Magnetic Length

The effective magnetic length at maximum current of 500 A is given in Table 4 in various positions of one quarter of the magnet and being symmetric in the other three quarters. The effective length varies strongly from the middle of the magnet to the outer parts due to the proximity of the conductors and the yoke. The effective magnetic length of 305 mm and 302 mm in the centre, which was measured by CNAO, is only reached in simulations removing the aluminium shielding plates. The effective length in simulations is then between 306 mm and 309 mm. The magnetic strength in the centre of the magnet is 27.8 mT. The effective magnetic length is calculated over 300 mm, which is slightly more than the physical length of the magnet. Integrated length further outside is lost which is up to 8% but was not calculated because of other close elements and the possibility of interfering magnetic fields. In worst case the integrated field is higher and therefore it is a safety margin. B_0 is always taken from the centre of the magnet.

[17] "Quality Assurance Report" CNA-SPDF-007WXX-00234, 15th May 2007, N. Hauge (DanFysik)
[18] According to Luc Sermeus in private communication, 13th January 2009

Table 4 - Effective magnetic length in one quarter of the frame window.

Effective magnetic length [mm]			
x/y	0	15	30
-60	276.68	282.98	304.56
-50	276.82	282.61	301.88
-40	277.04	282.57	300.83
-30	277.22	282.59	300.35
-20	277.34	282.63	300.13
-10	277.42	282.63	299.97
0	277.41	282.64	300.01

Homogeneity of the Magnetic Field

As it can be seen in the line map in Figure 16 the magnetic field is nearly homogenous at the plane z=0 within a region of 40*50 mm^2 between 27.7 mT and 27.85 mT. For the difference of Δ0.15 mT the beam receives a differing kick of Δ0.11 mrad for protons and Δ0.05 mrad for $^{12}C^{6+}$-ions at 7 MeV/[A].

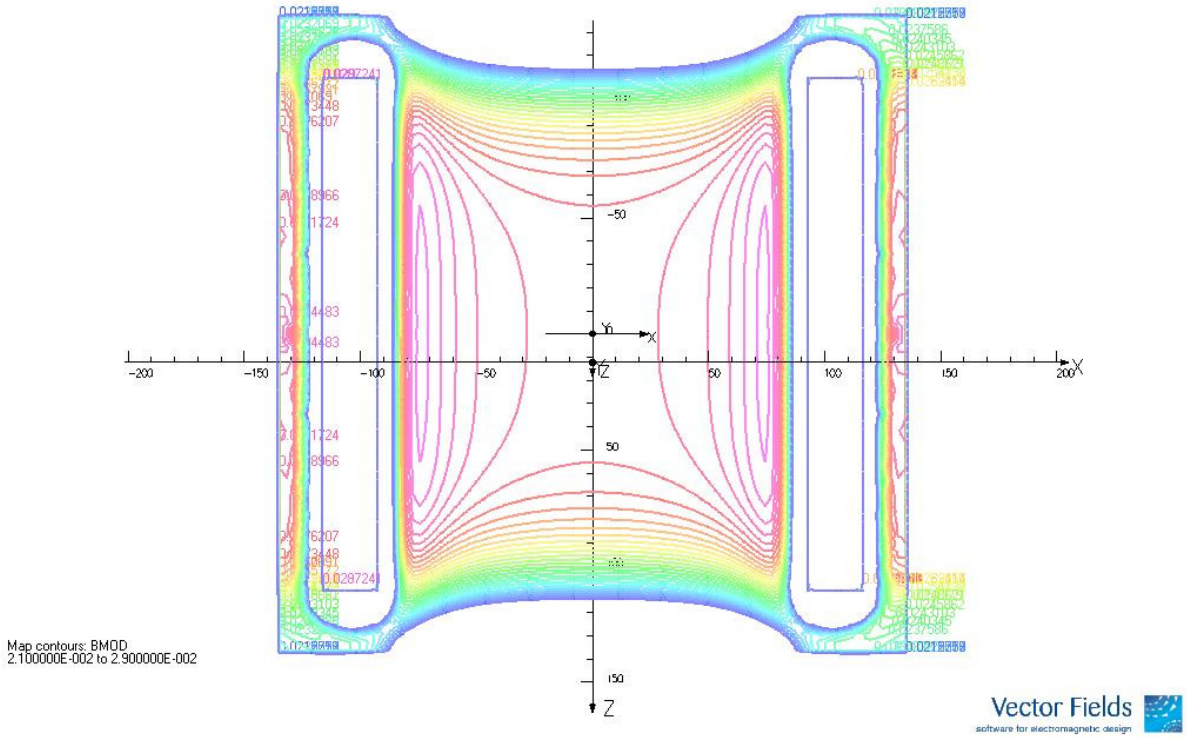

Figure 16 - Equivalent field-lines of the B-field in the x-z plane.

Rise and Fall Time

The time development over the 220 µs current pulse with the maximum of 500 A at 150 µs can be seen in Table 5. It shows the B-field at the various time steps in the centre of the magnet as well as the integrated field over 300 mm along the z-axis, which refers to the reference trajectory.

Table 5 - B_0 and *Bdl* over 300 mm along the reference trajectory at various time steps. Rising the current from 0 to 150 µs to its maximum of 500 A and the falling to 0 A at 220 µs.

Rise-Time [µs]	B_0 [T]	Bdl over 300 mm [mTm]
100	0.0185	4.7792
150	0.0278	7.1717
160	0.0238	6.1508
170	0.0199	5.1263
200	7.92E-03	2.05
220	1.00E-05	0.0106

The integrated field is also shown as chart in Figure 17 and for the single time steps in Figure 18, Figure 19, Figure 20, Figure 21, Figure 22 and Figure 23, where the shown length in Figure 23 has been extended to see the small magnetic field, which arises at both ends of the magnet, due to eddy currents in the aluminium plates.

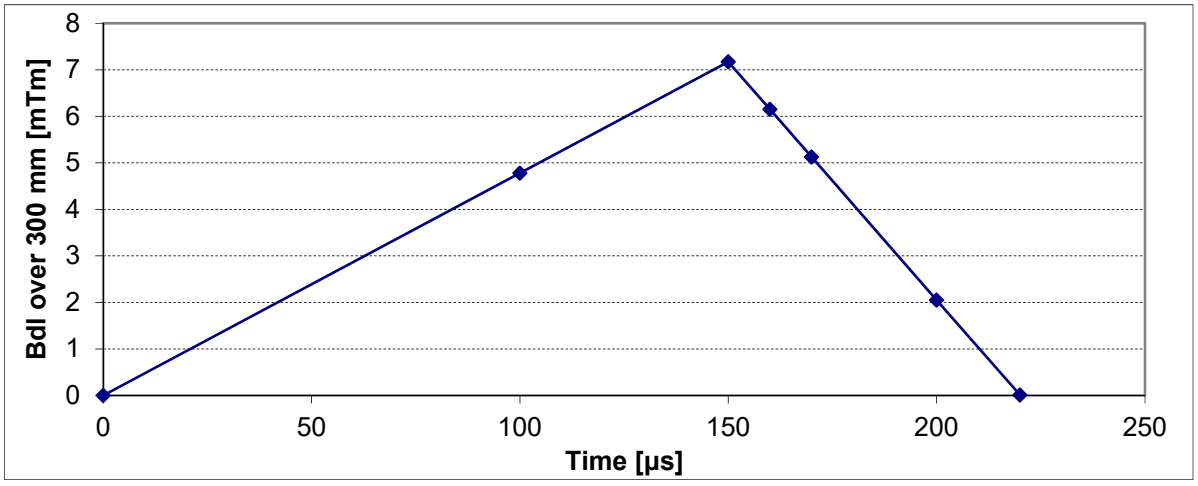

Figure 17 - *Bdl* over 300 mm in mTm over time in µs.

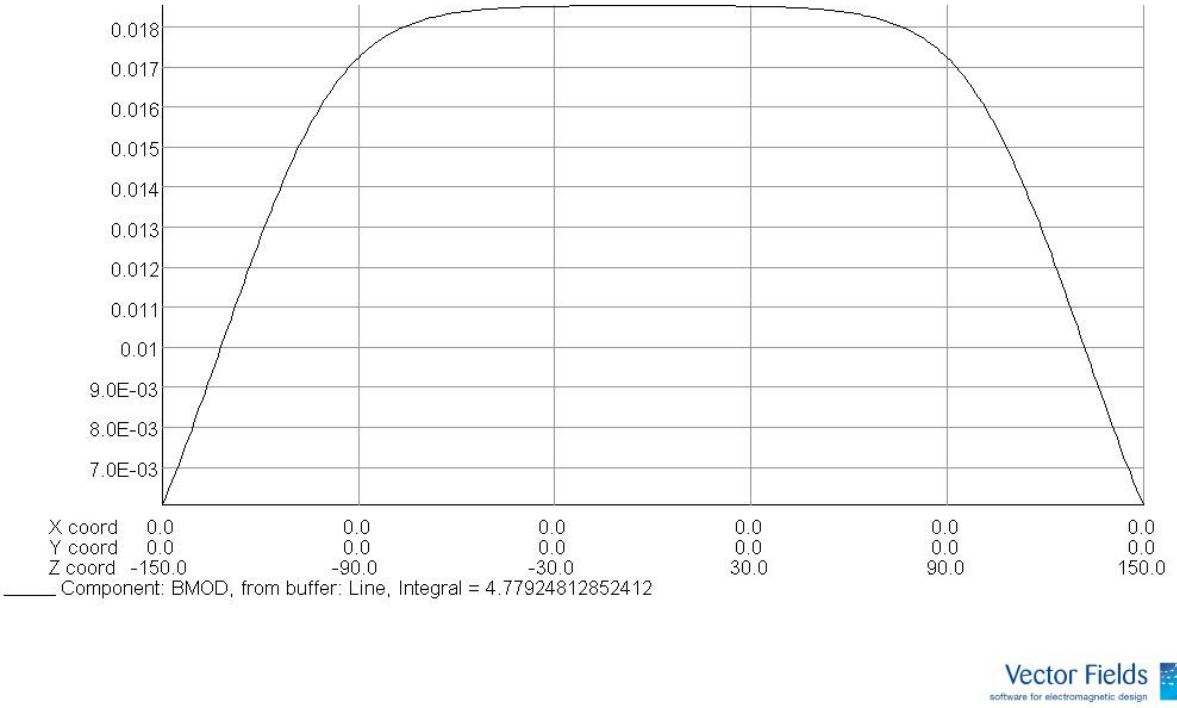

Figure 18 - *Bdl* at 100 µs.

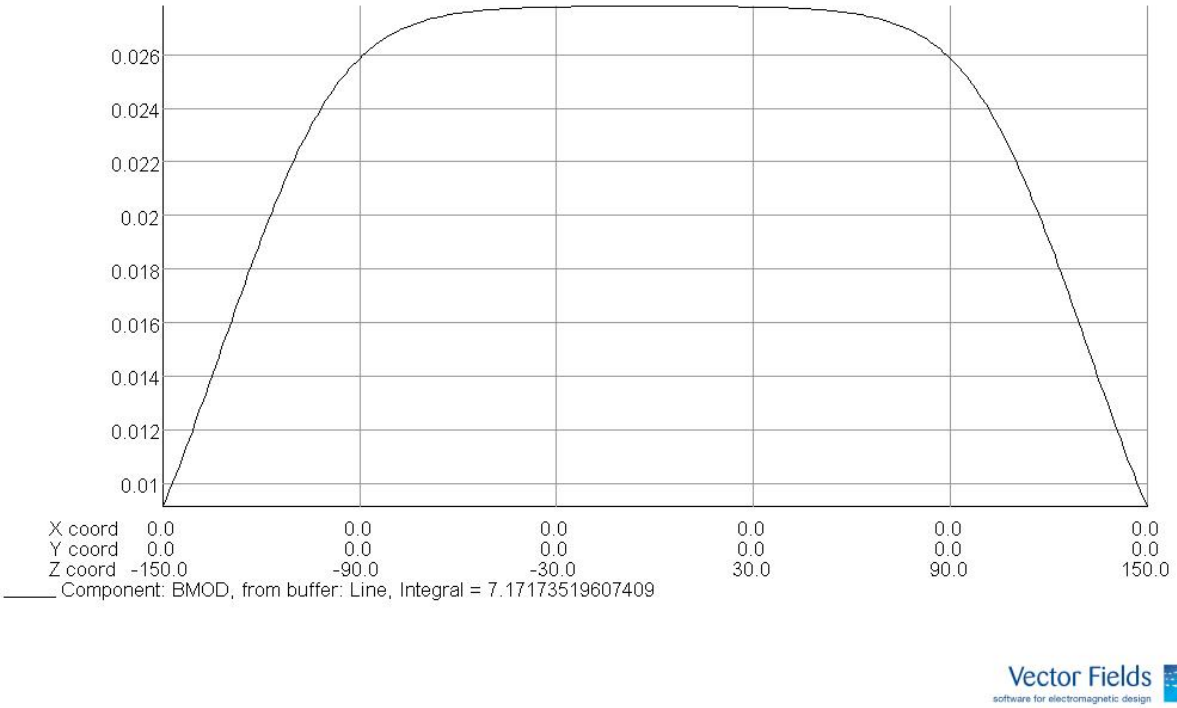

Figure 19 - *Bdl* at 150 µs (maximum peak at 500 A).

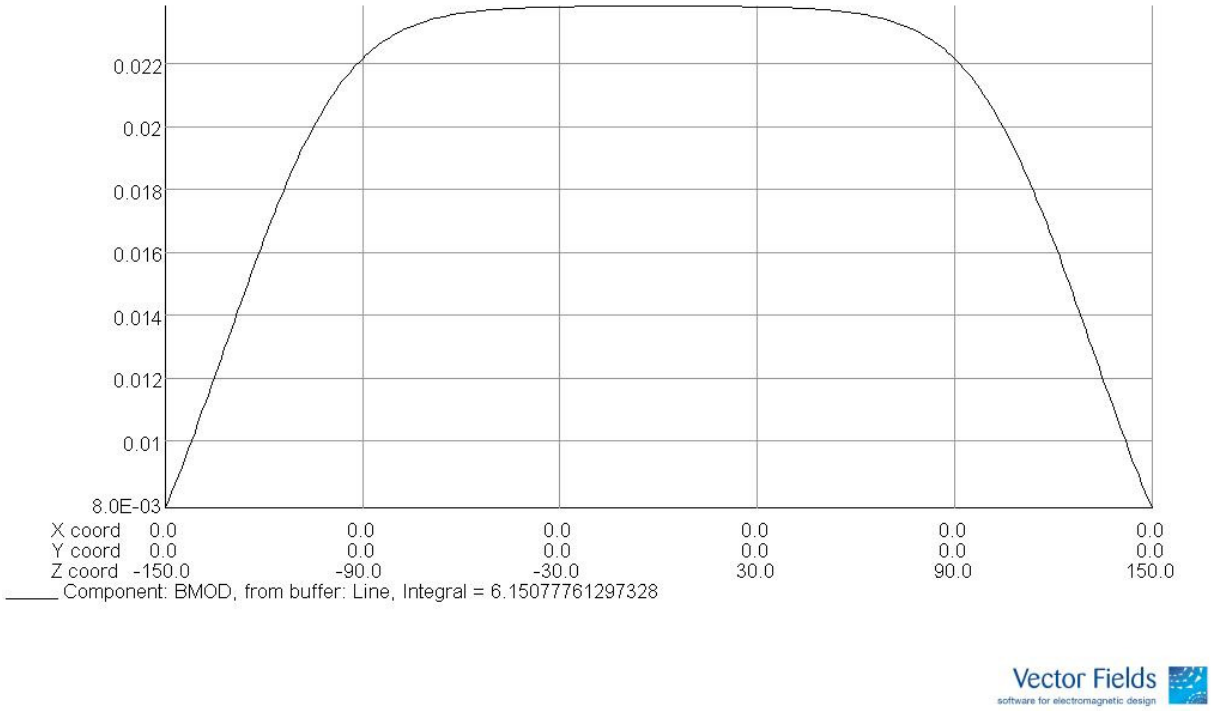

Figure 20 - *Bdl* at 160 µs.

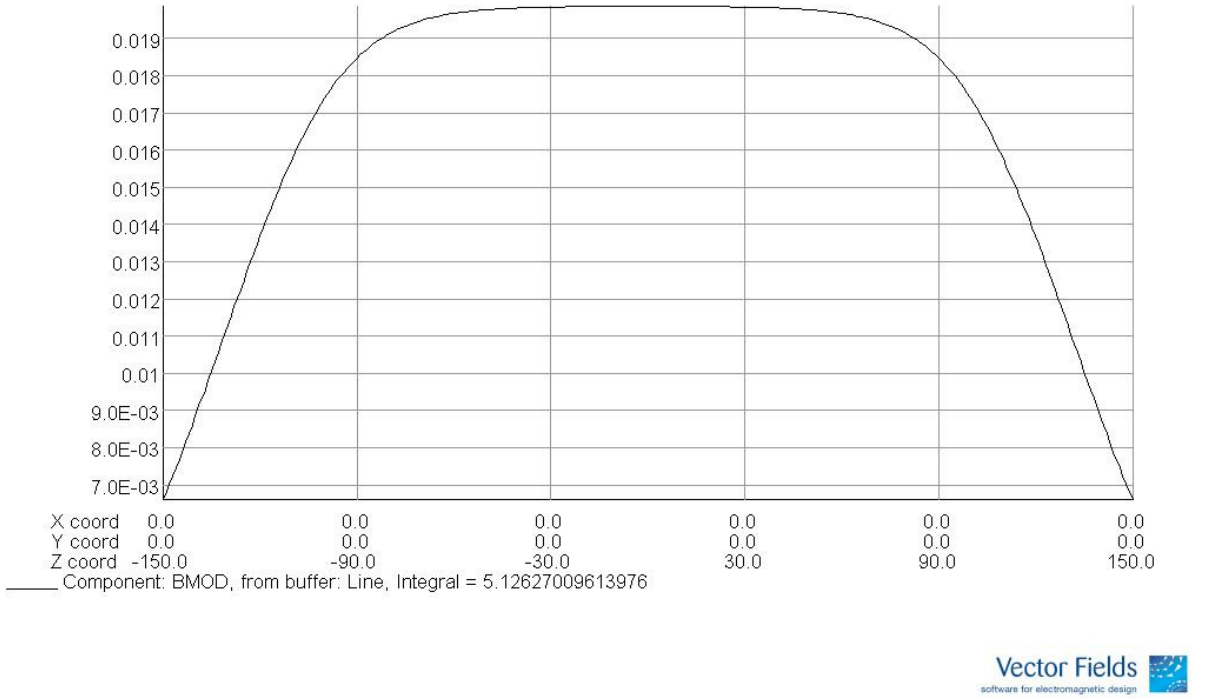

Figure 21 - *Bdl* at 170 µs.

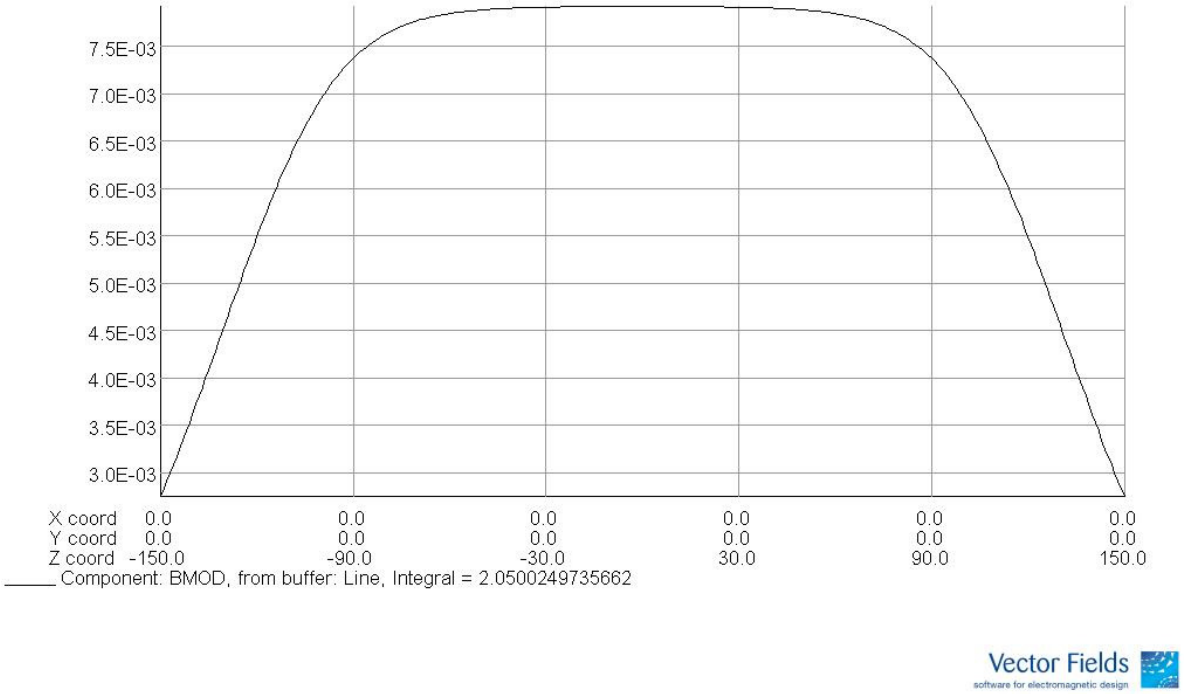

Figure 22 - *Bdl* at 200 µs.

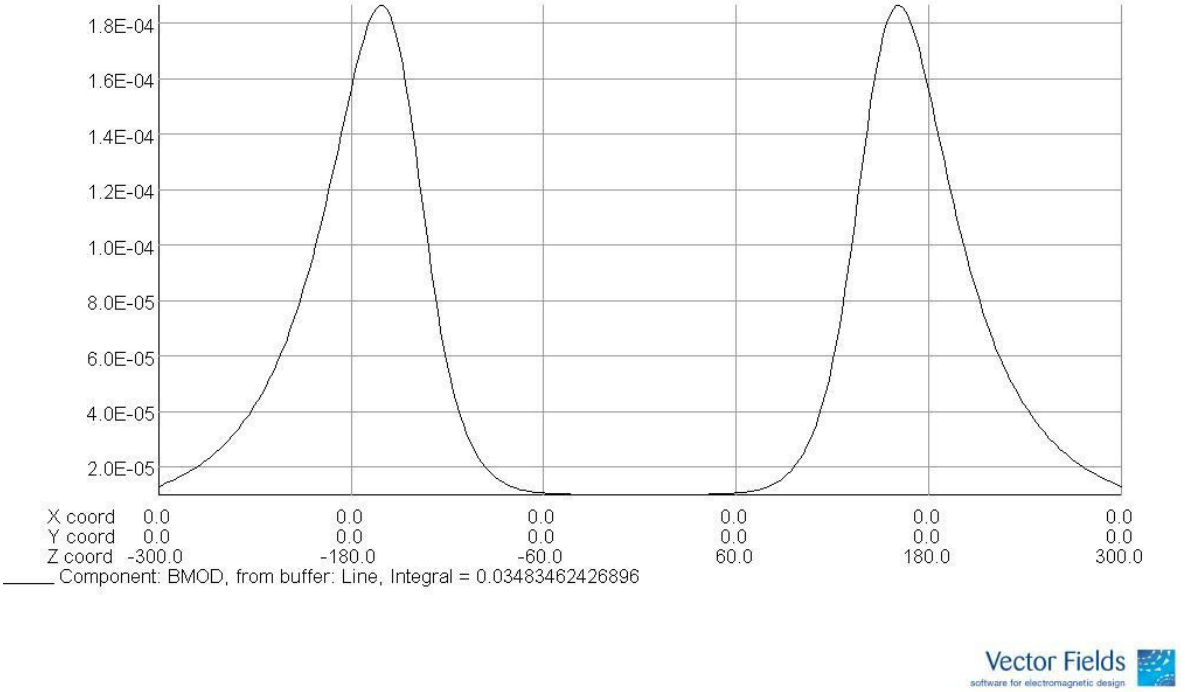

Figure 23 - *Bdl* at 220 µs.

Yoke and Aluminium Box

The highest magnetic field occurs in the yoke in the inner corners as it could be expected. The field can there obtain a maximum strength of 210 mT at a current of 500 A. Also some small fields are produced at the side between the aluminium plates and the yoke (see Figure 24).

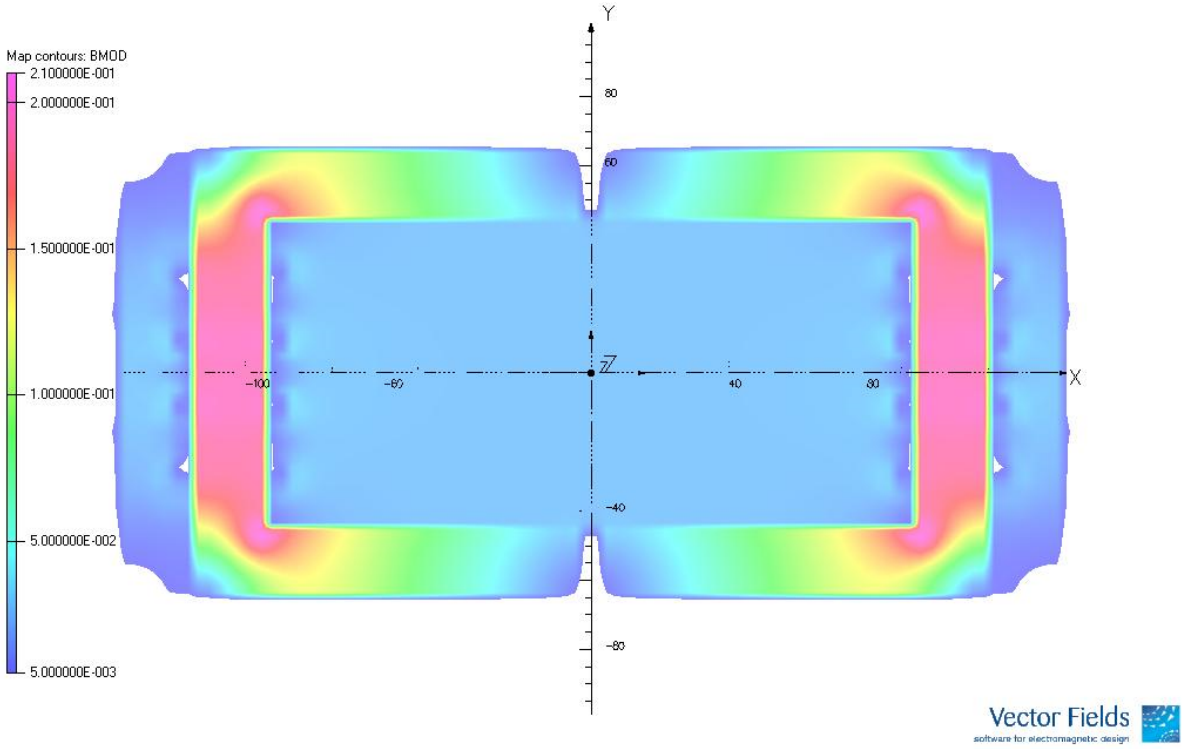

Figure 24 - Magnetic field within the yoke and between yoke and side plates in the x-y plane at z=0.

There are also some eddy currents in the aluminium box which are strongest near to the conductors with 6.5 A/mm^2 in the x-y plane at z=0 and in the gap between the two C-shaped half yokes at the end plates, where *J* reaches a strength up to 14.5 A/mm^2 (see Figure 25 and Figure 26).

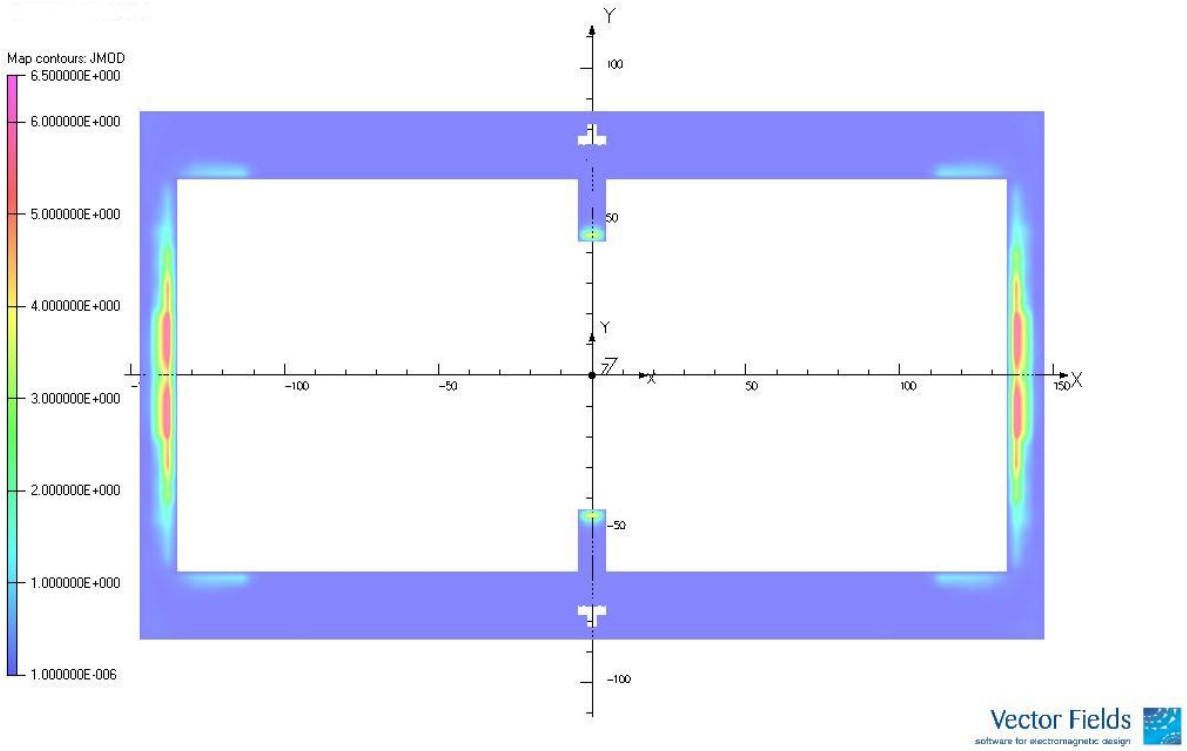

Figure 25 - Current density within the aluminium box in the x-y plane.

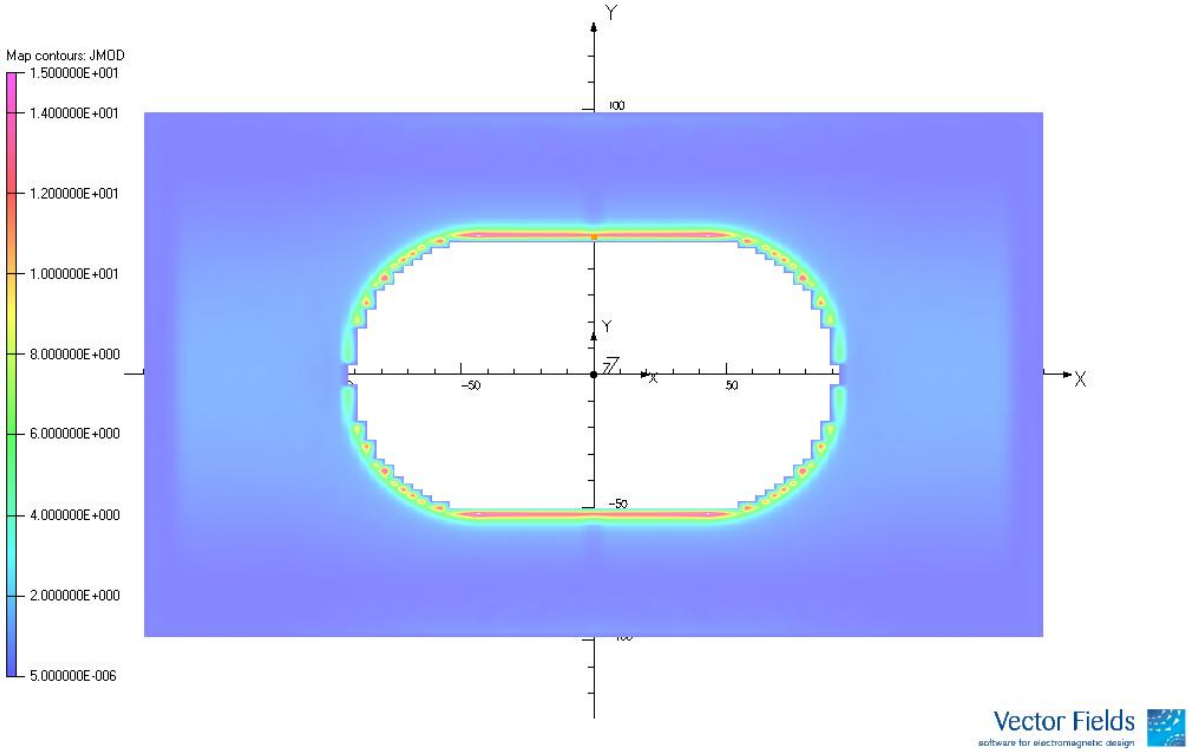

Figure 26 - Current density within the aluminium box in the x-y plane at the aluminium end plate.

Yoke and Aluminium Box at 600 A

To obtain higher deflection angles also simulations with a higher current namely 600 A were done. It shall be shown that it is also possible to work with this higher current.

Figure 27 shows that by increasing the maximum current to 600 A, the integrated field still grows linear, which means that the ferrite still does not saturate.

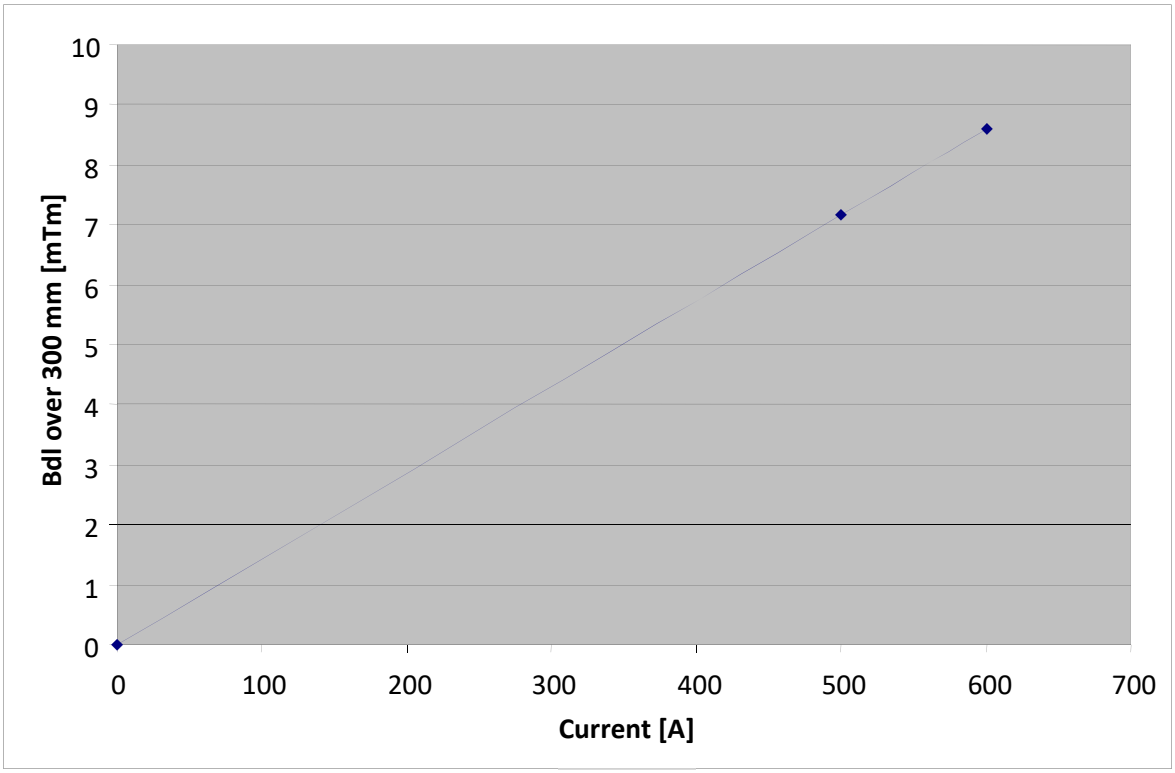

Figure 27 - Behaviour of the integrated field over 300 mm at rising current.

The highest magnetic field can be found again in the inner corners of the yoke with strength up to 240 mT. See Figure 28.

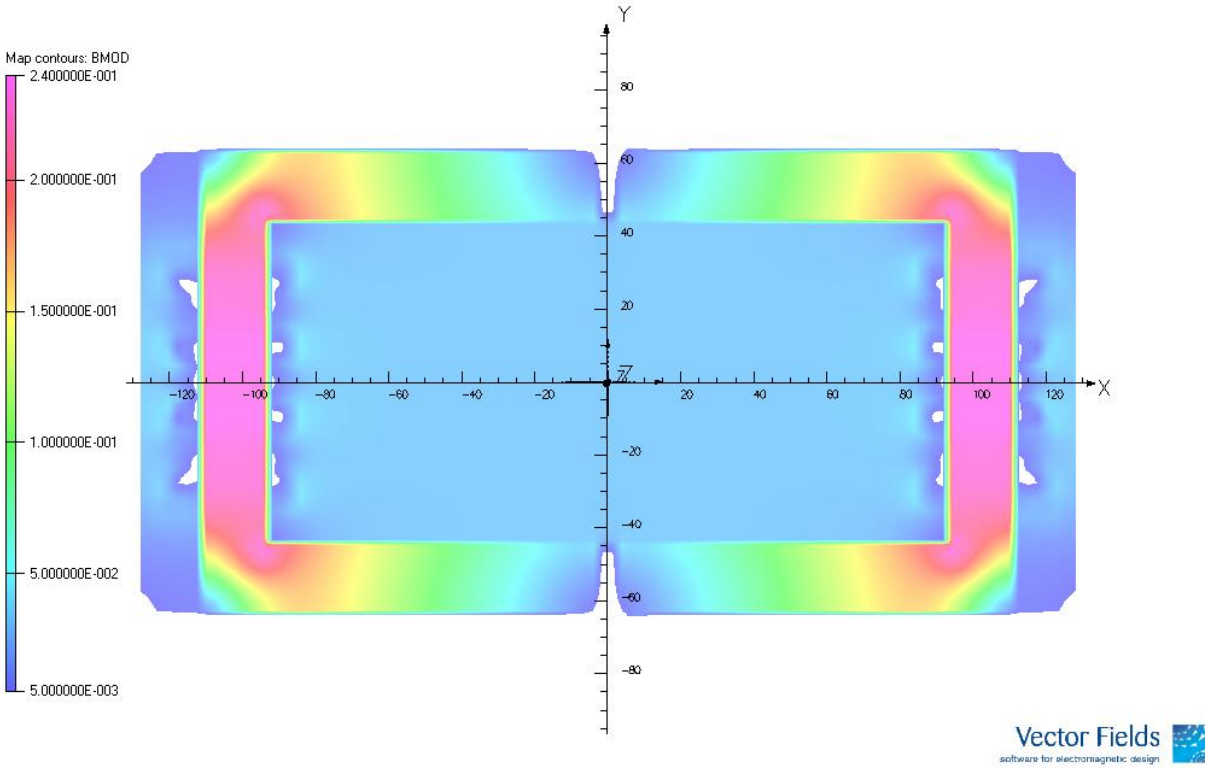

Figure 28 - Magnetic field within the yoke and between yoke and side plates in the x-y plane at z=0 and a current of 600 A.

The eddy currents in the aluminium box in the 600 A simulation are as in the simulation with 500 A strongest near to the conductors here with 8.1 A/mm^2 in the x-y plane at z=0 and in the gap between the two C-shaped half yokes at the end plates with 24 A/mm^2 (see Figure 29 and Figure 30).

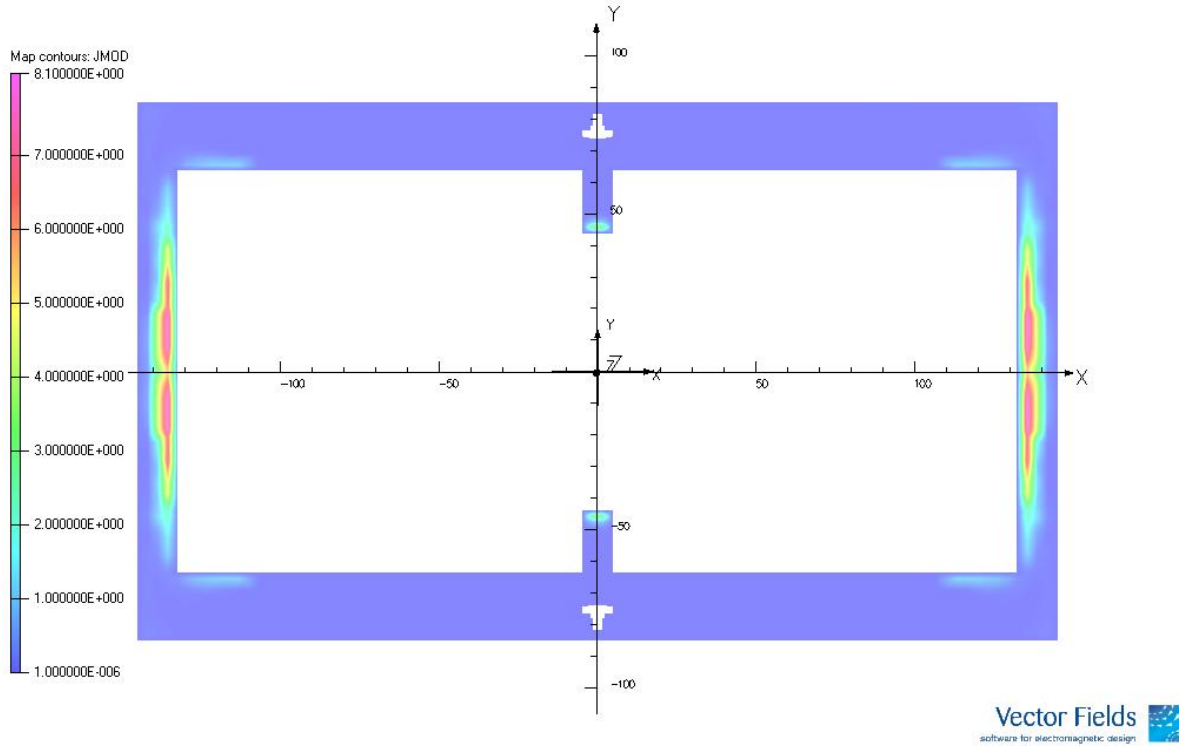

Figure 29 - Current density within the aluminium box in the x-y plane at 600 A.

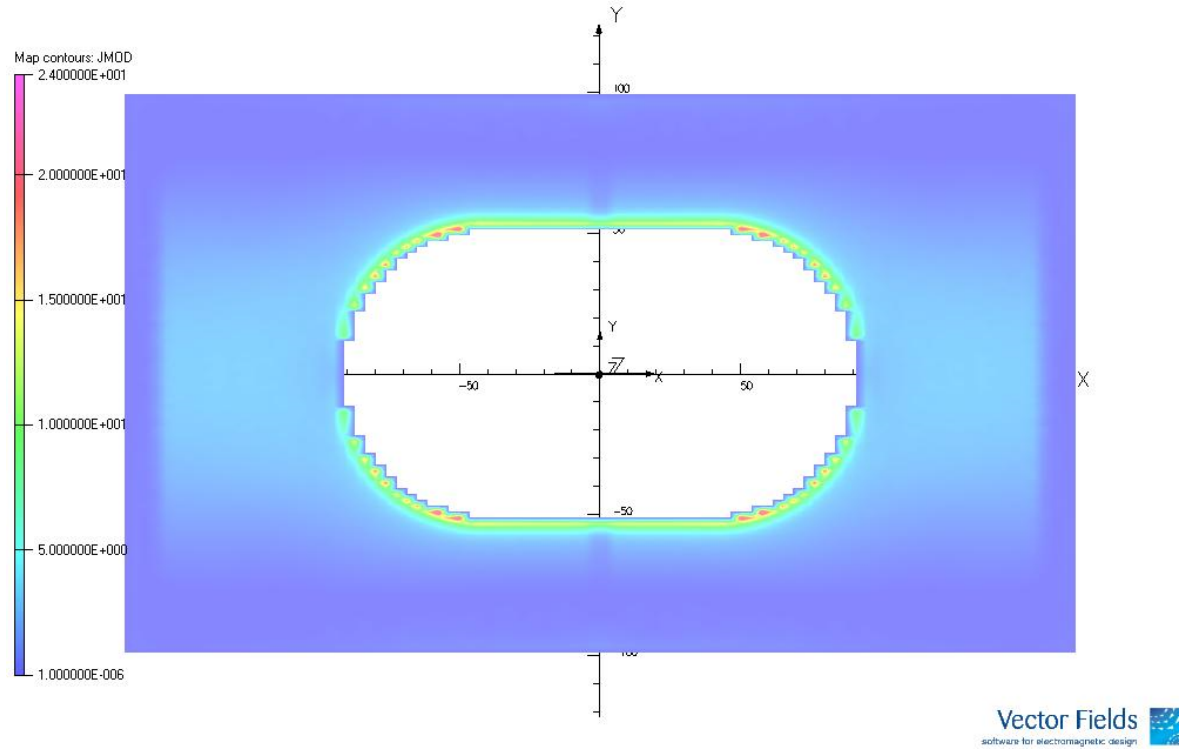

Figure 30 - Current density within the aluminium box in the x-y plane at the aluminium end plate at 600 A.

Deflection Angle

It is of interest to see, if it is possible to reach the specified deflection angle of 10 mrad also with higher injection energies than 7 MeV/[A].

The deflection angle can be calculated by

$$\Theta = \int \frac{Bdl}{B\rho}$$

The *Bdl* along the effective length is 0.006933 Tm, and Bρ is calculated for the energies 7, 8, 9 and 10 MeV/[A] by

$$B\rho(\mathrm{Tm}) = \frac{10}{2.998}\beta E_{Total}(\mathrm{GeV})$$

The deflection angles for protons and $^{12}C^{6+}$-ions respectively for the different energies can be obtained from Table 6 and Table 7 [19].

Table 6 - Deflection angle for protons with kinetic energies from 7 MeV/[A] to 10 MeV/[A] at a current of 500 A.

Deflection angle for protons		
Kinetic Energy [MeV/[A]]	Bρ [Tm]	θ [mrad]
7	0.383	18.101
8	0.409	16.928
9	0.434	15.955
10	0.458	15.132

Table 7 - Deflection angle for $^{12}C^{6+}$-ions with kinetic energies from 7 MeV/[A] to 10 MeV/[A] at a current of 500 A.

Deflection angle for carbon ions		
Kinetic Energy [MeV/[A]]	Bρ [Tm]	θ [mrad]
7	0.763	9.085
8	0.816	8.496
9	0.866	8.008
10	0.912	7.595

Increasing the maximum current from 500 A to 600 A changes B_0 to 0.03335 T, the effective magnetic length to 277.41 mm and the integrated field over the effective length is then 0.008314 Tm. Deflection angles for the increased current are given in Table 8 and Table 9.

[19] Values for protons and carbon needed for calculation are taken from: http://physics.nist.gov/cuu/constants

Table 8 - Deflection angle for protons with kinetic energies from 7 MeV/[A] to 10 MeV/[A] at a current of 600 A.

Deflection angle for protons		
Kinetic Energy [MeV/[A]]	Bρ [Tm]	θ [mrad]
7	0.383	21.708
8	0.409	20.3
9	0.435	19.134
10	0.458	18.147

Table 9 - Deflection angle for $^{12}C^{6+}$-ions with kinetic energies from 7 MeV/[A] to 10 MeV/[A] at a current of 600 A.

Deflection angle for carbon ions		
Kinetic Energy [MeV/[A]]	Bρ [Tm]	θ [mrad]
7	0.763	10.895
8	0.816	10.188
9	0.866	9.603
10	0.913	9.108

2.2.4 Adjustments for MEDAUSTRON

Since the yoke is saturated up to 250 mT at a current of 600 A, it should be discussed to make a slight adjustment by increasing the yoke thickness so that there is a safety margin before saturation effects take over.

Changes and Simulation in VECTORFIELDS

Therefore the cross-section of the upright parts of the ferrite between the coils is increased by 4 mm in outwards direction so that the space between the ferrite remains the same. The width of the turns of the conductor is increased by the same value to keep the space between conductor and yoke. Also the aluminium side plates have been shifted by these 4 mm so that the distance between conductor and shielding box remained the same (Figure 31). Applying this changes on both sides the total width of the magnet is increased by 8 mm. Due to the higher cross-section of 24 mm instead of 20 mm of the sides of the yoke there will be a higher magnetic flux which allows to lower the current. The new current in the following simulation will be 530 A, which corresponds to a current density of 17.67 A/mm^2. As the models before, the simulation was done in ELEKTRA-Transient with 10 layers in the aluminium end plate with an offset of 0.4 mm. The current pulse is triangular but rise and fall time has been altered to

100 µs each, giving a total pulse length of 200 µs. The materials and their properties remain the same.

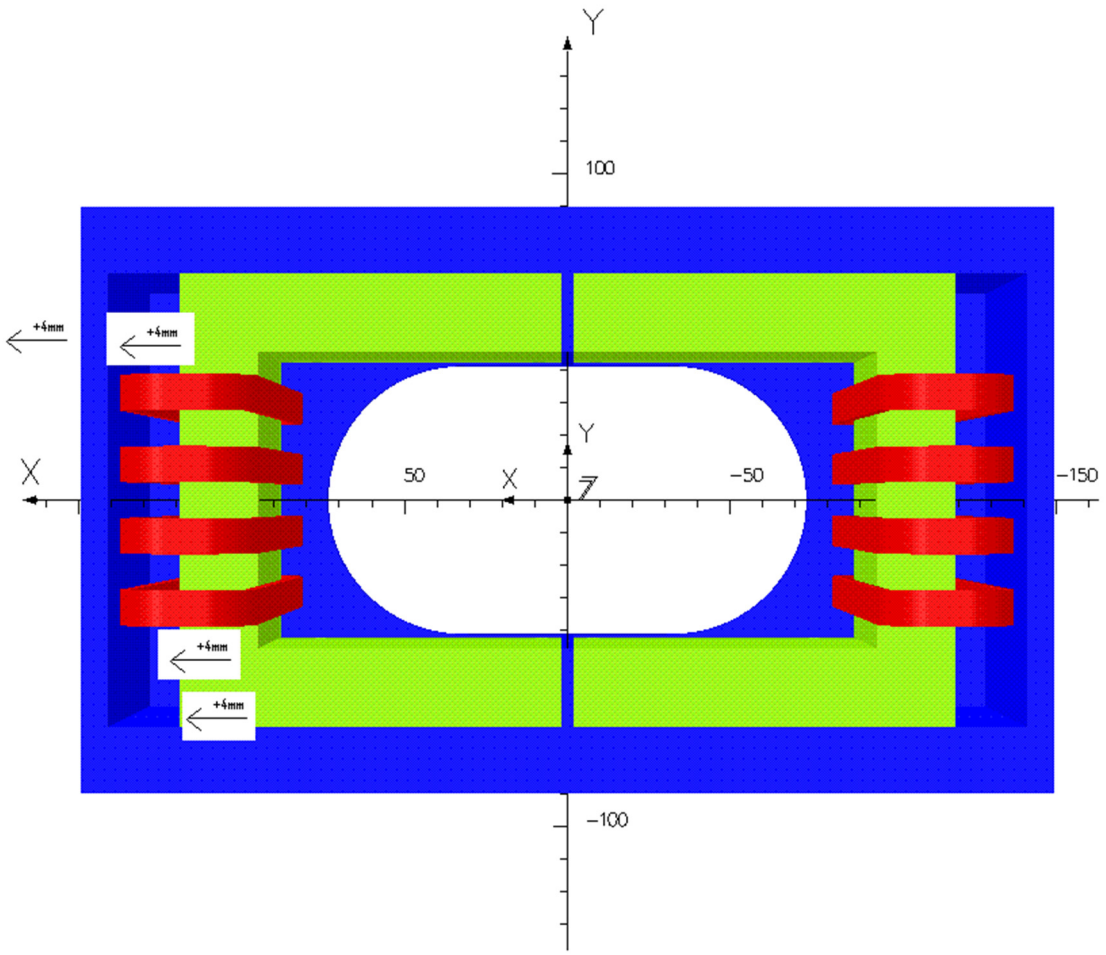

Figure 31 – Changes for increasing the cross section of the ferrite.

Effective Magnetic Length

The development of the integrated field, the maximum field and the effective length can be seen in Table 10. The deviation of the effective length at 200 µs from the values at other time steps can be explained by measuring B_0 in the centre of the magnet, where the magnetic field almost vanished, while the eddy currents in the aluminium end plates still give a recognizable amount of flux at the outside of the magnet, which effects dominate the integrated field. This effect can also be seen in the simulation for the CNAO model in Figure 23.

The integrated field is also shown as chart over time for different time steps in Figure 32.

Table 10 - B_0, *Bdl*, and effective magnetic length at various time steps.

Time step [µs]	B_0 [T]	Bdl over 300 mm [mTm]	Effective magnetic length [mm]
50	0.0147	3.7959	258.05
100	0.0294	7.5949	258.06
150	0.0147	3.7963	258.06
200	1.33E-06	4.89E-04	368.10

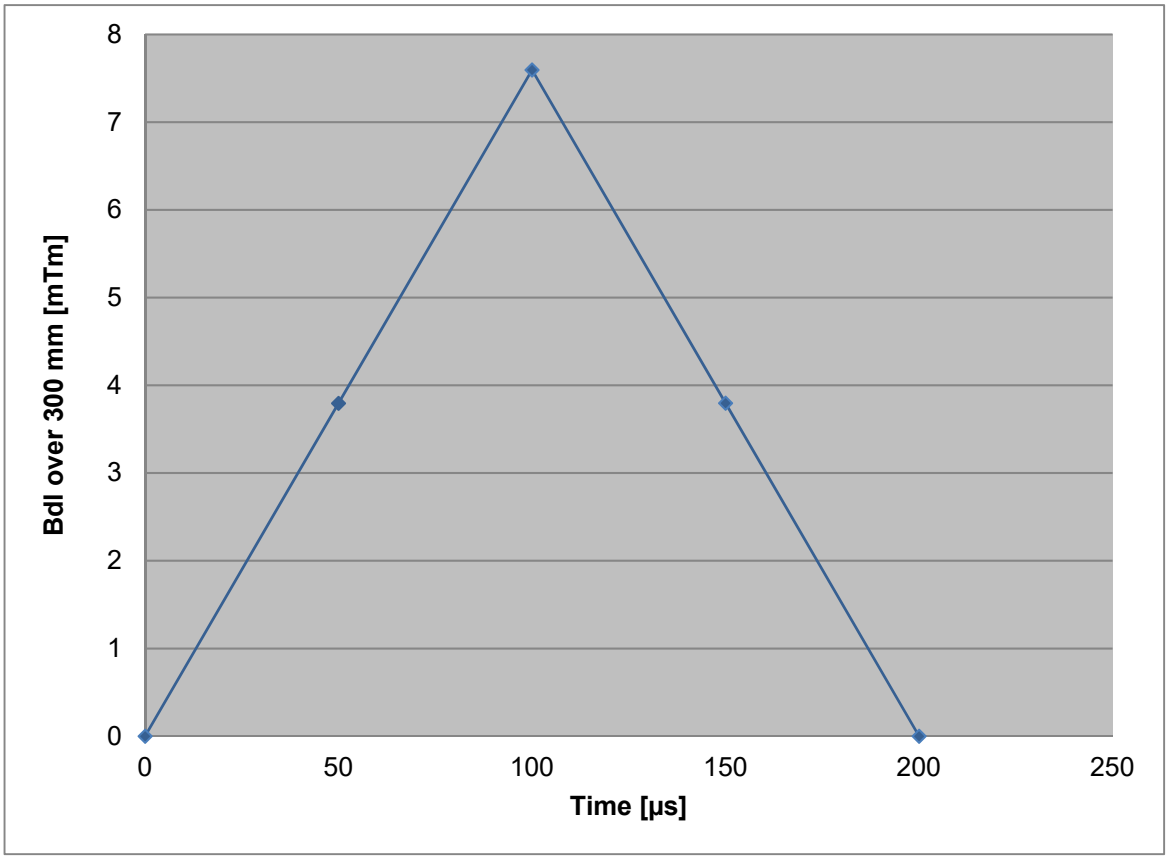

Figure 32 - Bdl over 300 mm in mTm over time in µs.

Saturation

The saturation of the ferrite is decreased with respect to the simulations before with the thinner cross-section of the yoke. The highest values are still in the corners and next to the conductors. On the outside of the ferrite the magnetic flux is up to 212 mT. Figure 33.

Cuts through the x-z plane at different levels of y show that the flux density within the ferrite is even lower. Figure 34 shows the x-z plane at y=0 (i.e. in the centre of the magnet). Figure 35 and Figure 36 show the flux density at y=10, which is a cut plane to one of the turns of the conductor and at y=45 cutting through the first bit of the top ferrite. The saturation is highest in the corners of the ferrite and even there it does not exceed 207 mT. Hence it is possible to raise the current if necessary for higher injection energies without having saturation effects.

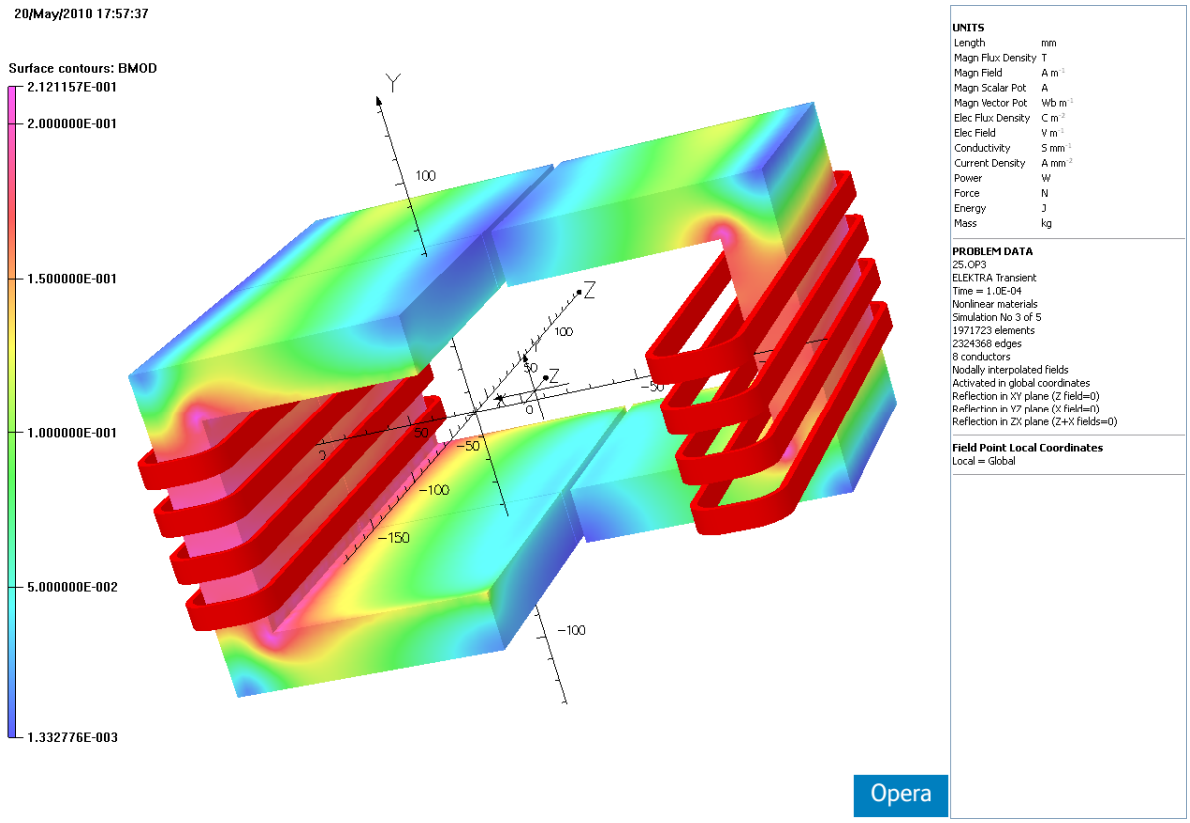

Figure 33 - Saturation on the ferrite surface and in the x-y plane at z=0, showing three quarter of the magnet without the aluminium box.

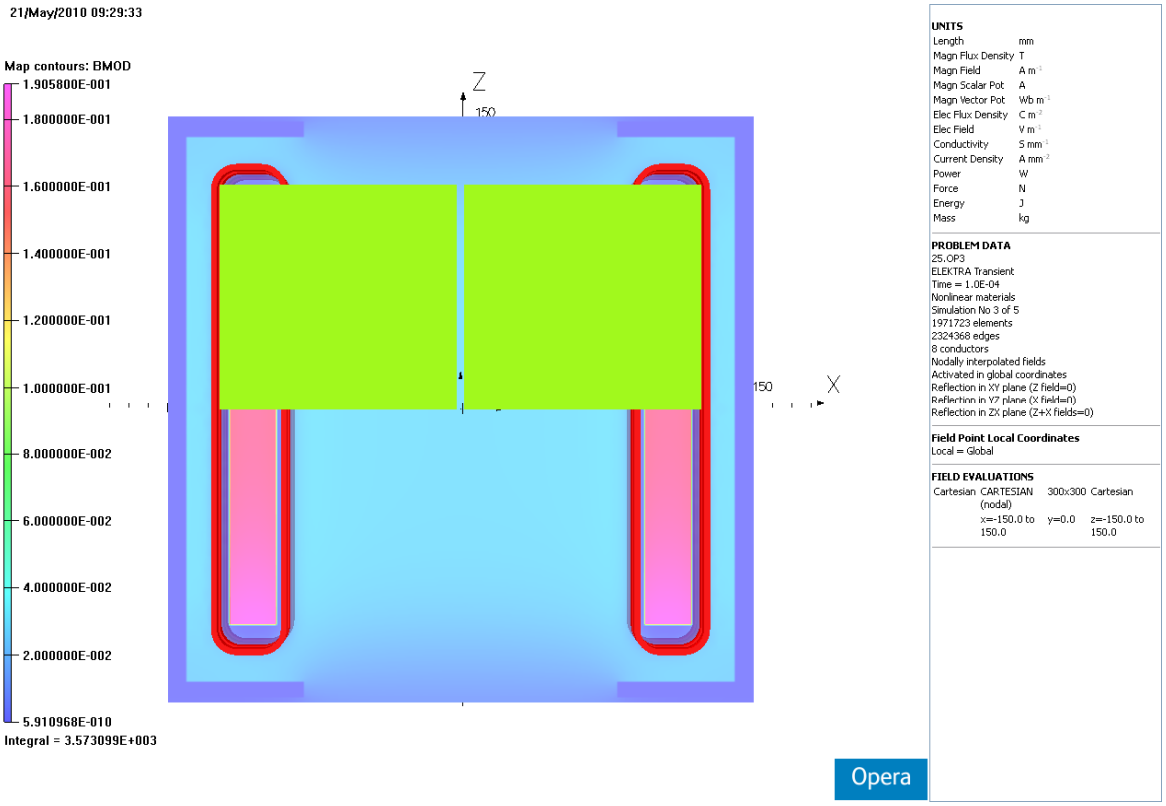

Figure 34 - Magnetic flux density on the x-z plane at y=0.

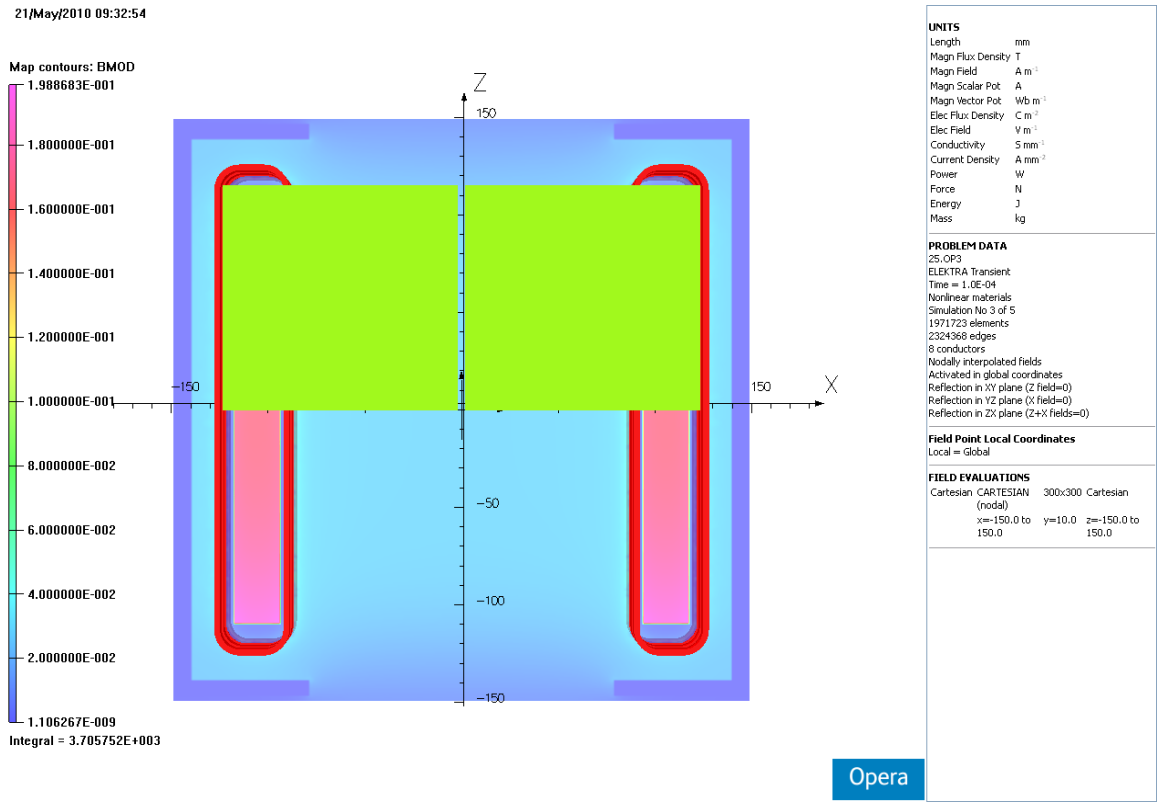

Figure 35 - Magnetic flux density on the x-z plane at y=10.

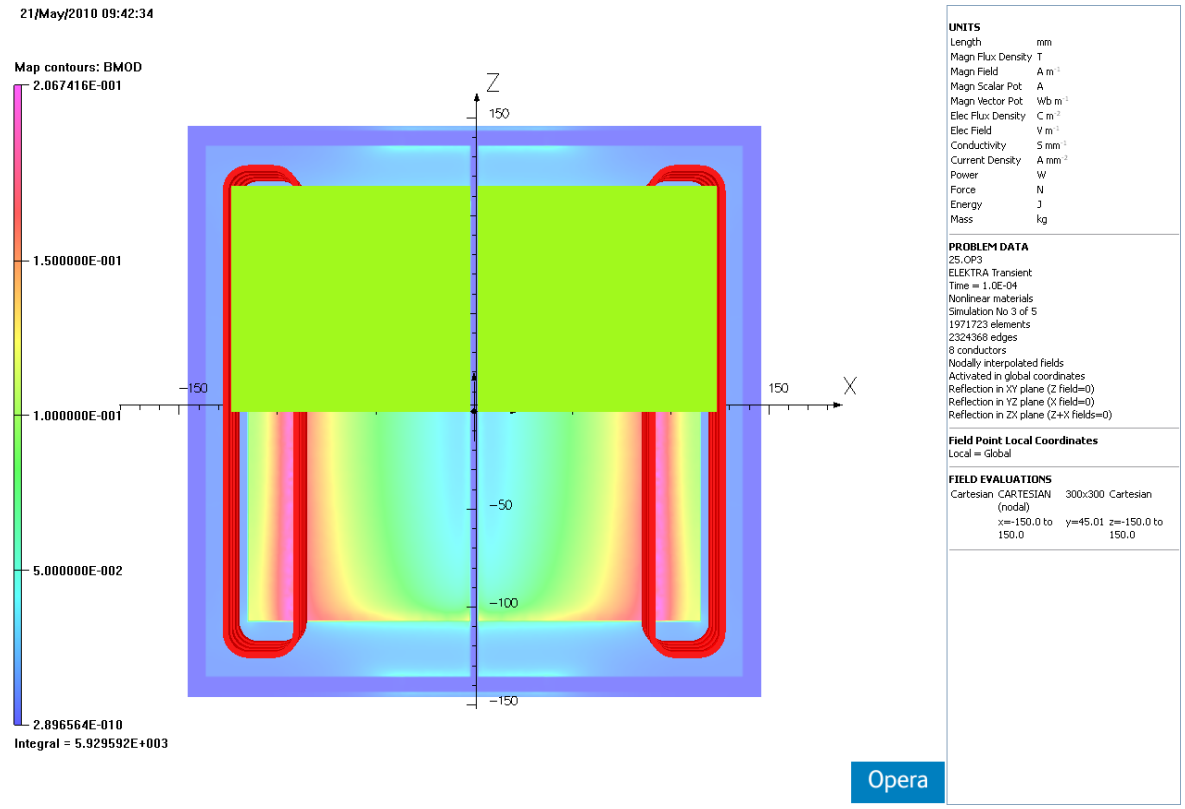

Figure 36 - Magnetic flux density on the x-z plane at y=45 (edge of the ferrite).

Homogeneity of the Magnetic Field

The field quality has been tested by integrating the magnetic field along a distance of 500 mm parallel to the z-axis. This has been done for each mm over one quarter of the area of the good field region, obtaining a map of deviation of the integrated field. The single results refer always to the reference trajectory in the centre of the magnet, which is assumed as a straight line in the calculations. Due to deflection the real particle trajectory is a bend line. Figure 37, Figure 38 and Figure 39 show the field quality at different time steps for rising, maximum and falling current.

The field quality of less than 1% is only reached within an area of 90×54 mm^2 instead of the specified 120×60 mm^2, but the necessary field quality and good field region for the MEDAUSTRON injection bumper are not fixed yet. If the homogeneity of the magnetic field is not sufficient further studies are needed.

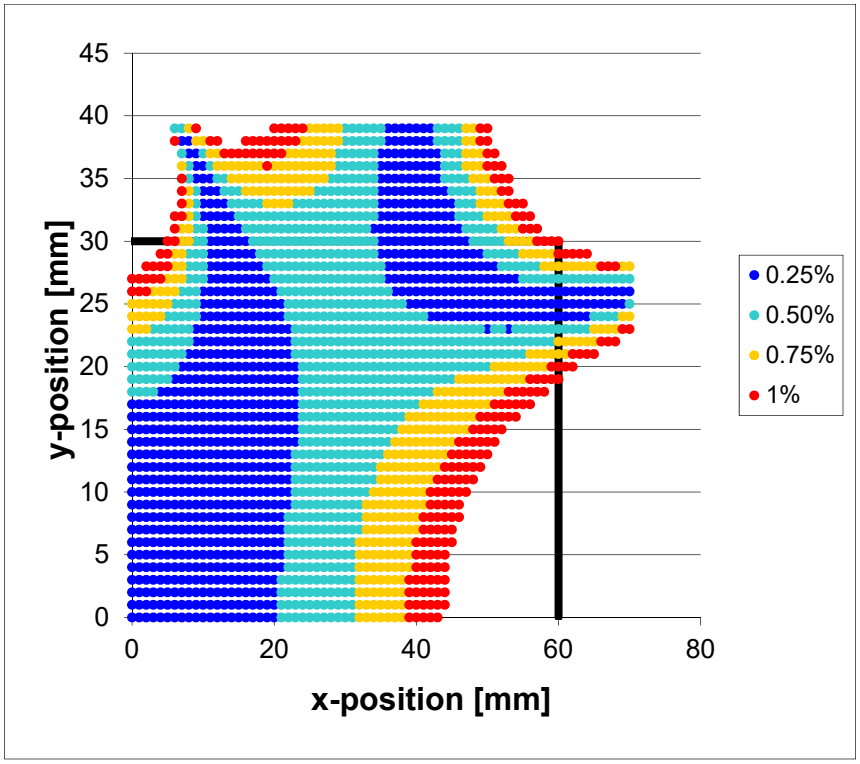

Figure 37 - Homogeneity of the magnetic field during current rise at 50 µs.

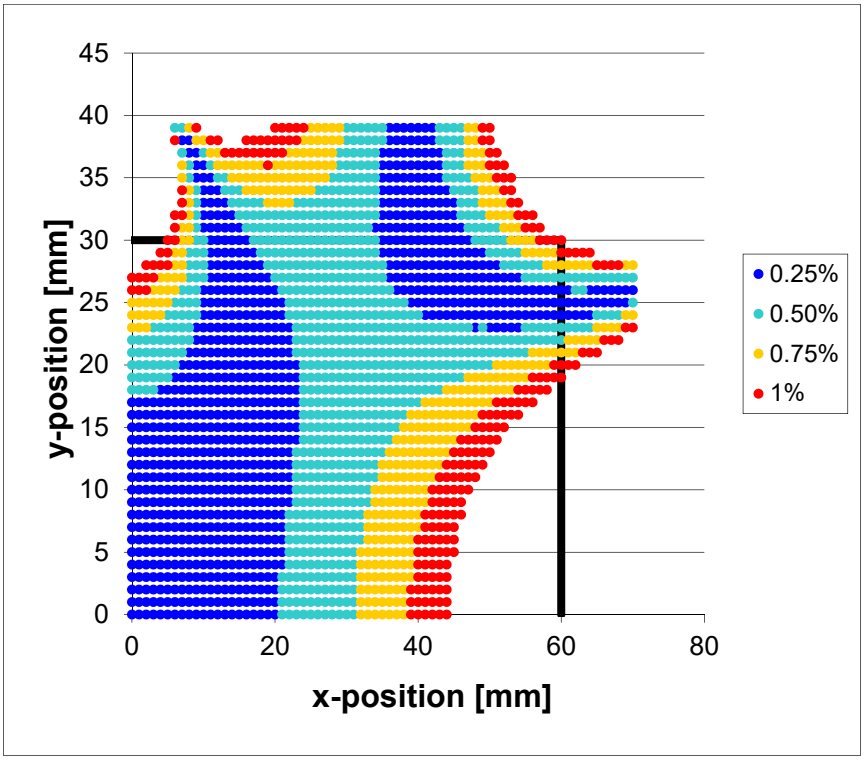

Figure 38 - Homogeneity of the magnetic field at the maximum current of 530 A at 100 µs.

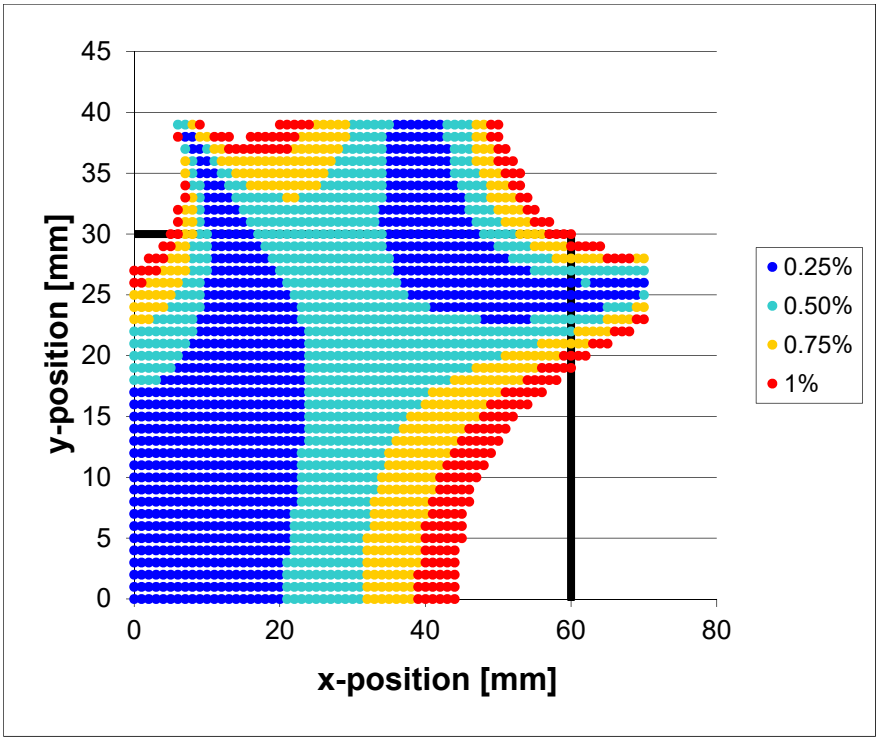

Figure 39 - Homogeneity of the magnetic field during current fall at 150 µs.

2.2.5 Summary

The CERN parameter list predicted for the CNAO injection bumper a maximum current of 454 A. However the magnets built by DANFYSIK were measured at 500 A. The magnetic field produced by these currents should provide a deflection angle of 10 mrad for protons and $^{12}C^{6+}$-ions with a kinetic energy of 7 MeV/[A]. For the MEDAUSTRON application the required deflection angle shall also be true for injection energies up to 10 MeV/[A].

Using a current of 500 A like DANFYSIK gives a deflection angle of 15.1 mrad for protons at 10 MeV/[A] but for $^{12}C^{6+}$-ions the required angle of 10 mrad is missed by 0.9 mrad even for injection energies of 7 MeV/[A].

For $^{12}C^{6+}$ the current has to be raised to 600 A to obtain an angle of 10 mrad for injection energies of 7 and 8 MeV/[A]. For kinetic energies of 9 and 10 MeV/[A] the required deflection angle is missed by 0.4 mrad and 0.9 mrad respectively.

Heat losses due to the higher current are not expected but it has not been verified in the simulations. It is also not verified if the actual power supply system can provide the increased current of 600 A.

The inhomogeneous field measured by DANFYSIK does not appear in the simulations. This is clarified by the use of different materials in the yoke by DANFYSIK.

To lower the flux density in the yoke a change of increasing the cross-section of the vertical blocks of the ferrite by 4 mm to the outer side is proposed. This also allows a lower current of 530 A and saturation drops to 200 mT. Note that the field quality of 1% is not reached over the specified good field region of 120x60 mm^2. Changes of important parameters are shown in Table 11.

Table 11 - Changes of important parameters from the CNAO model to the MEDAUSTRON model.

Changes	CNAO model	MEDAUSTRON model
Cross-section yoke vertical [mm]	20	24
Cross-section yoke horizontal [mm]	20	20
Current [A]	500	530
Current density [A/mm^2]	16.67	17.67
Maximum integrated field [Tm]	0.00717	0.007594
Maximum field [T]	0.0278	0.0294
Aperture w*h [mm^2]	166*90	166*90
Pole gap [mm]	90	90
Good field (±1%) region [mm^2]	40*50	90*54

2.3 Dump Bumper

When DANFYSIK built and measured the dump bumpers [20], measurements showed that the required magnetic field strength was not reached as specified [21]. Therefore it was necessary to make new simulations on the magnets and adapt them.

The CNAO dump bumper magnets S3-010A-BDS and S8-016A-BDE are used as a baseline for the MEDAUSTRON vertical dump bumpers MKD-A and MKD-B.

Figure 40 - Complete Assembly of the CNAO dump bumper magnet.

[20] "Quality Assurance Report" CAN-SPDF-007WXX-00234, 15th May 2007, N. Hauge (DanFysik)
[21] "Final Design, Special Magnets" CAN-TNDP-006WXX-00231, 21th July 2003, J. Borburgh et.al (CNAO-CERN)

2.3.1 Parameter List

Table 12 - Magnet parameter list predicted by CERN for the CNAO dump bumpers built by DANFYSIK.

Dump Bumper		
Name	S3-010A-BDS	S8-016A-BDE
Info	2 different items powered in series, resonant power supply generator	
Function	Start beam dump	End beam dump
Dismantling	Vertical	Vertical
Effective magnetic length [m]	0.3	0.3
Total physical length [m]	0.225	0.225
Ferrite physical length [m]	0.15	0.15
Maximum integrated field ∫Bdl [Tm]	0.0173	0.0346
Maximum field B [T]	0.0577	0.1153
Maximum beam rigidity [Tm]	6.3464	6.3464
Deflection angle [mrad]	2.7	5.4
Yoke	Ferrite, C-shape	Ferrite, C-shape
Pole gap [mm]	166	166
Aperture w × h *[mm2]	90 × 166	90 × 166
Vacuum chamber	Metalized ceramic, racetrack, 7 mm thick	Metalized ceramic, racetrack, 7 mm thick
Coil	1, copper conductor, 6 turns	1, copper conductor, 12 turns
Conductor size [mm2]	3 × 20	3 × 10
Space between turns [mm]	6	3
Good field region (rectangle) [mm2]	60 × 120	60 × 120
Field quality [%]	± 2.5	± 2.5
Current for maximum field [A] (nominal)	1265	1265
Voltage [V] (max.)	3300	3300
Current density [A/mm2]	21.08	42.17
Number of turns	6	12
Average turn length [m]	0.492	0.492
Cooling	Air	Air
Water temperature rise °C	-	-
Water pressure [bar]	-	-
Water flow [l/min]	-	-
DC power dissipation [W]	-	-
Magnet resistance [Ω]	~ 0.25 (PULSED)	~ 0.25 (PULSED)

Estimated inductance [µH]	8	32
Estimated stored energy [J]	6.4	25.6
Maximum coil voltage to ground [V]	~ 3300	~ 3300
Rise time [µs]	32 to 50, 48 pref.	32 to 50, 48 pref.
Rise shape	Linear shape or cosine	Linear shape or cosine
Flat top [µs]	> 6	> 6
Uniformity on flat top [%]	Margin 0 + 10	Margin 0 + 10
Fall time [µs]	Some ms	Some ms
Fall Shape	Whatever shape	Whatever shape
Overshoot [%]		
Repetition rate [sec]	1.2	1.2

2.3.2 CNAO Design

A beam-dumping scheme based on a rapid bump that is excited over a few tens of turns has been adopted. In this way, microsecond technology is used rather than the more expensive nanosecond technology of a fast kicker that would be needed for a single-turn dump. The rapid bump is excited by two bumper dipoles (S3-010A-BDS and S8-016A-BDE). As the two magnets are used to create a closed orbit bump, it seems preferable to power the magnets in series. In order to account for the different optics (β) functions at the two locations, the integrated kick strengths have a ratio of 1:2. This is implemented by using the same magnet yoke design but with a different number of windings i.e. 6 turns for the start beam dump and 12 turns for the end beam dump to provide deflection angles of 2.7 mrad and 5.4 mrad respectively.

Despite this complication, the bumper dipoles are simpler, smaller, and more reliable than a fast kicker and they avoid the complications of a vacuum tank with high-voltage feedthroughs. Since the dumping action takes many turns, the voltages are lower and the power converter is simplified.

The dump bumper is required to deflect the beam vertically. Due to the vertical dimension of the vacuum chamber, the magnet gap width must be larger than 88 mm. The magnets are constructed each in one piece as an open C-core, closed by an eddy-current screen. The main parameters are given in Table 12 and the design is shown in Figure 41, Figure 42 and Figure 43.

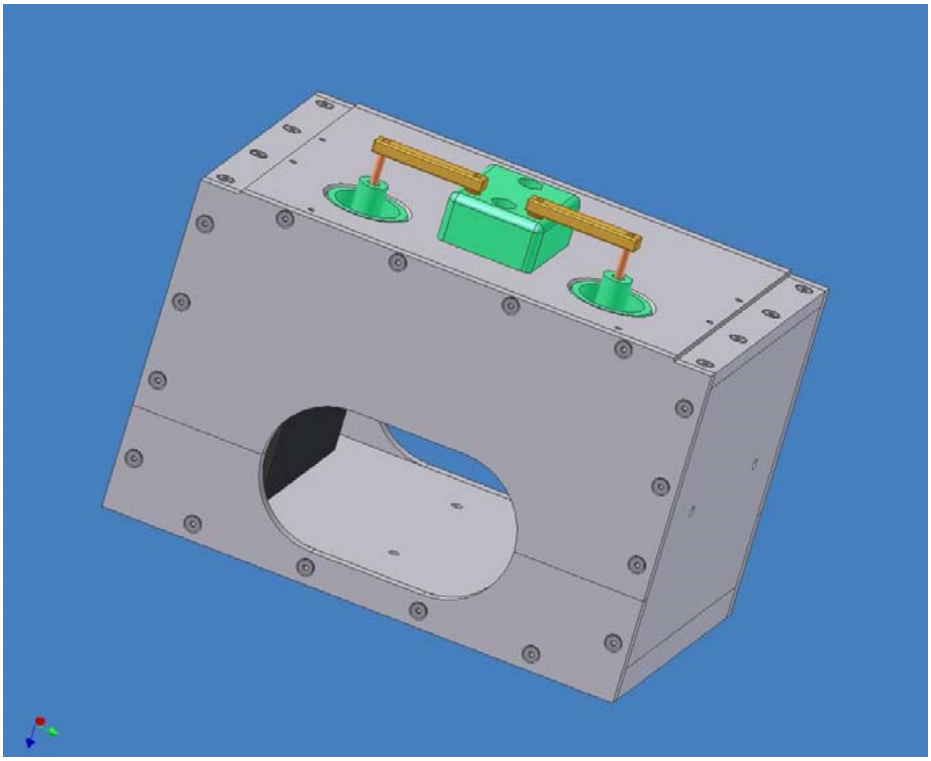

Figure 41 - Dump bumper magnet module assembled. Both 6-turns and 12-turns magnets look alike when assembled.

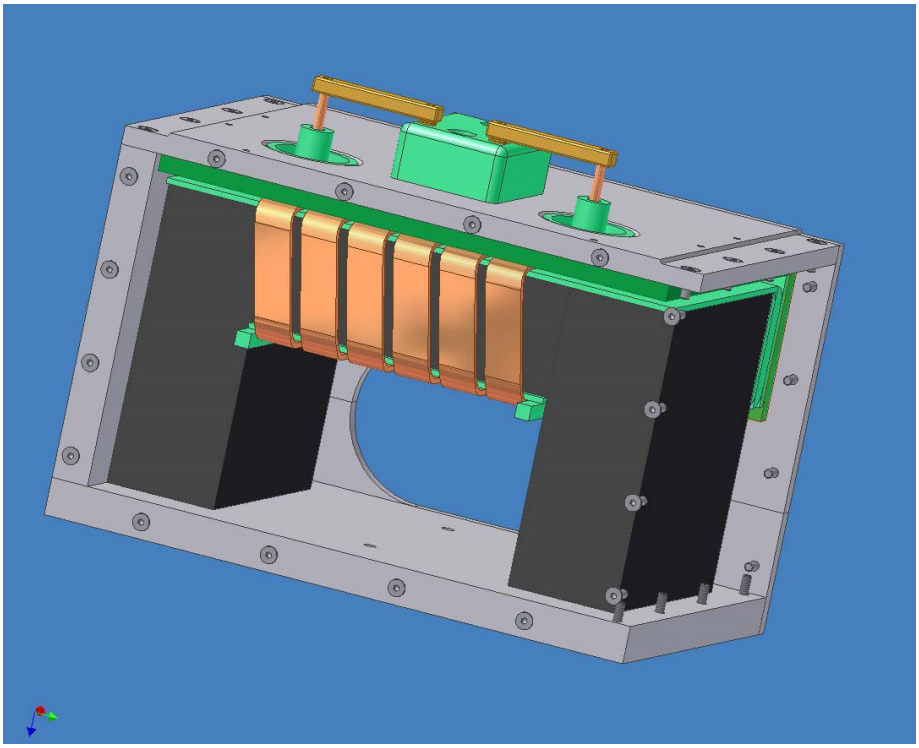

Figure 42 - 6-turns dump bumper start S3-010A-BDS, front and side covers removed.

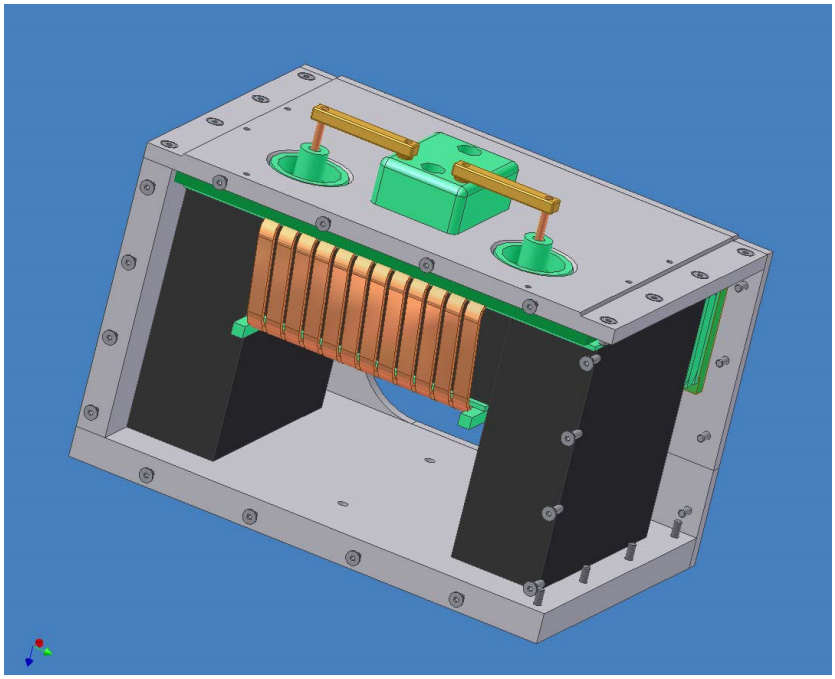

Figure 43 - 12-turns dump bumper end S8-016A-BDE, front and side covers removed.

The two magnets are pulsed in series and present a total inductance of ~40 µH (~8 µH and ~32 µH for S3-010A-BDS and S8-016A-BDE, respectively). Once maximum current has been reached, representing the end of the dump cycle, a flattop of 6 µs is required. Figure 44 shows the magnet current for the CNAO design and is used in the simulations for MEDAUSTRON.

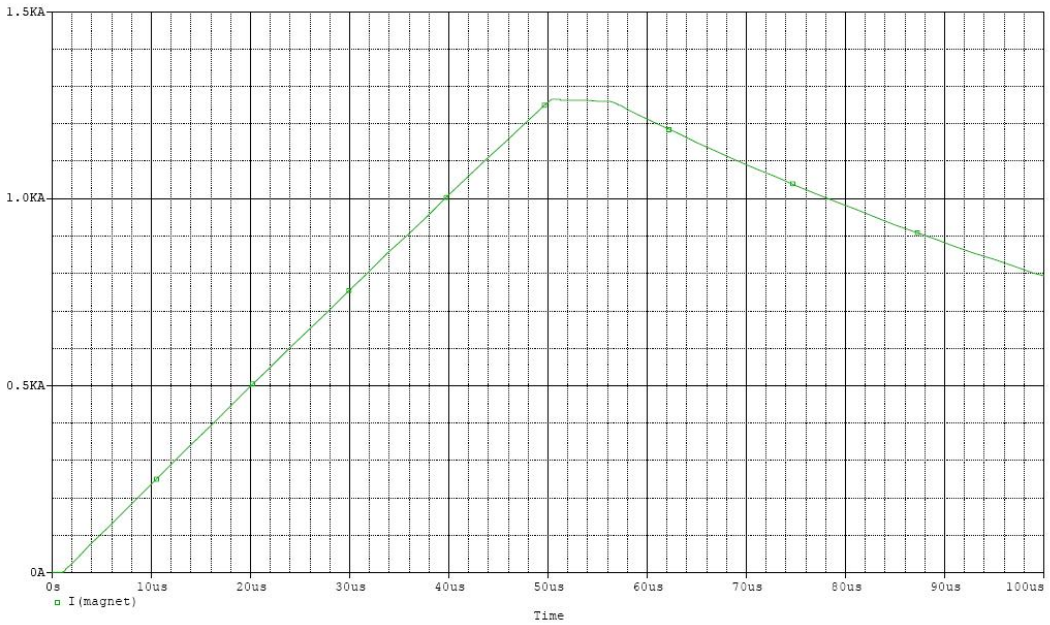

Figure 44 - Dump bumper magnet current vs. time.

The model was designed by using technical drawings from CNAO and DANFYSIK [22], Simplifications, symmetry and settings for TOSCA as well as the material properties have been done and set as described in 2.1.2. Since it was not possible to use ELEKTRA for solving the field equations due the models exceeded the calculation capacities of ELEKTRA simulations were done in TOSCA. This simplification was validated in section 2.1.3. The model as designed in the OPERA Modeller is shown in Figure 45, Figure 46 and Figure 47.

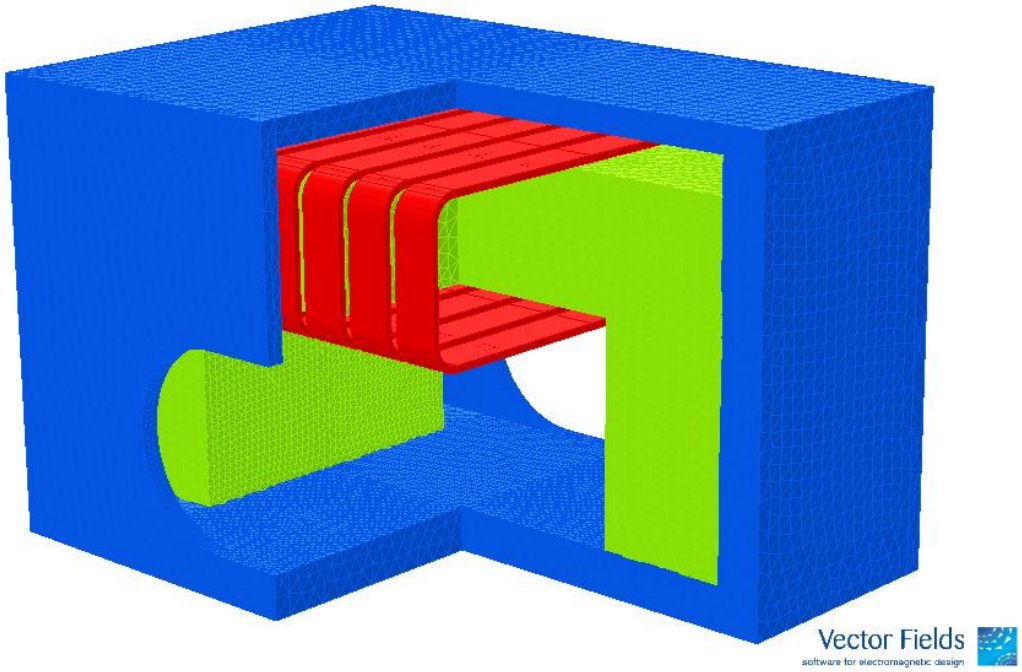

Figure 45 - A 3-D view of three quarters of the 6-turn dump bumper magnet in VECTORFIELDS (green parts are the yoke, blue is the aluminium and red are the conductors).

[22] The files of the technical drawings can be found under
\\cern.ch\dfs\Projects\medaustron\CNAOdocs\docs\Special magnets\special magnets and PS - as built documentation\ 14878-102_103 Dump Bumper\Drawings\Drawings-14878-102\Workspace
and
\\cern.ch\dfs\Projects\medaustron\CNAOdocs\docs\Special magnets\special magnets and PS - as built documentation\ 14878-102_103 Dump Bumper\Drawings\Drawings-14878-103\Workspace
Technical Drawings used:
DanFysik, Magnet with Safety Cover, 14878-102-007.A, 13th July 2006
DanFysik, Final Assembly, 14878.102.009.B, 11th November 2005
DanFysik, Moulded Assembly, 14878.102.010.B, 17th August 2006
DanFysik, Moulding Arrangement, 14878.102.011.B, 20th April 2006
DanFysik, Top Ferrite, 14878.102.020.B, 23rd January 2006
DanFysik, Side Ferrite, 14878.102.021.B, 31st August 2005
DanFysik, Coil - 6 Turns, 14878.102.051.B, 11th November 2005
DanFysik, Upper End Plate, 14878.102.063.B, 26th October 2005
DanFysik, Lower End Plate, 14878.102.064.B, 26th October 2005
DanFysik, Top Ferrite, 14878.103.020.A, 23rd June 2005
DanFysik, Side Ferrite, 14878.103.021.A, 23rd June 2005
DanFysik, Coil - 12 Turns, 14878.103.051.B, 11th November 2005

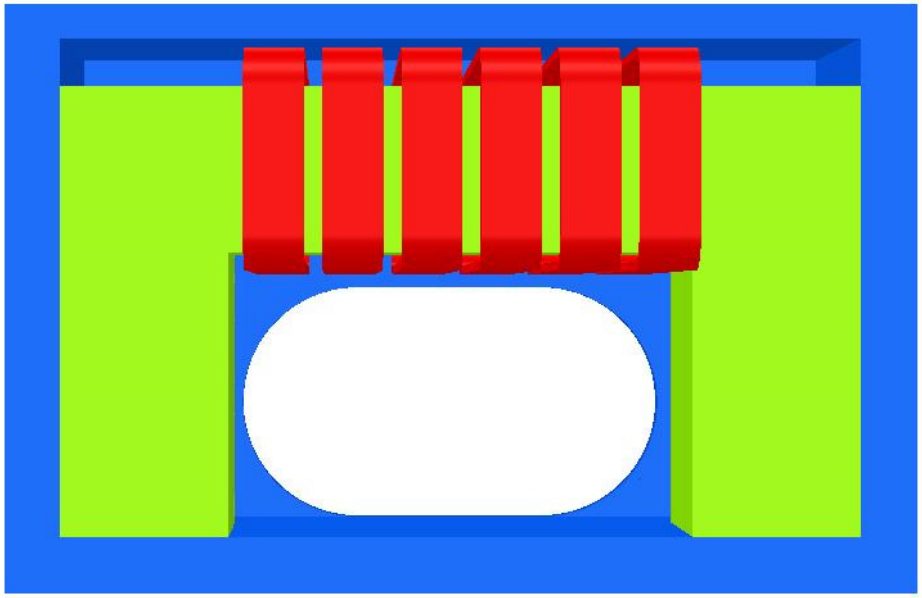

Figure 46 - Cut through the 6-turn dump bumper in VECTORFIELDS (green parts are the yoke, blue is the aluminium and red are the conductors).

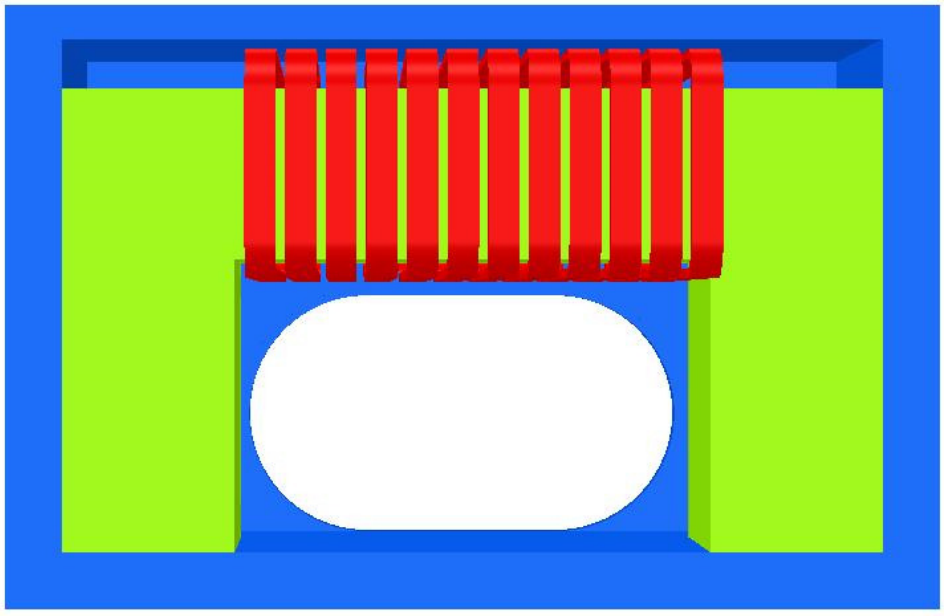

Figure 47 - Cut through the 12-turn dump bumper in VECTORFIELDS (green parts are the yoke, blue is the aluminium and red are the conductors).

2.3.3 DANFYSIK Measurements Compared to Simulation

CNAO Measurements

Measurements have been done by using a strip line air probe in the centre of the magnet (along the z-axis in simulations, which is the particle reference trajectory). The magnet has been excited with a low voltage 5 kHz sine wave using a current of 1265 A as specified in [20].

The maximum magnetic field measured by DANFYSIK for the 6-turn dump bumper is B_0=24.4 mT and the effective magnetic length is L_{eq}=244 mm [20].

For the 12-turn dump bumper B_0=85 mT and L_{eq}=246 mm [20]. For both magnets the field is homogeneous in an area of 60 × 120 mm^2.

Simulations in VECTORFIELDS

To verify these measurements for MEDAUSTRON, DC-simulations in OPERA-TOSCA have been done setting the relative permeability of aluminium to μ_r=0.0001 H/m to simulate the shielding effects (see section 2.1.3.).

Magnetic Field and Magnetic Length

The results of the DANFYSIK measurements for the CNAO magnets and the simulations compared to the specified values for CNAO are shown in Table 13.

Table 13 – Measurements of the CNAO dump bumpers and TOSCA-simulations for MEDAUSTRON.

S3-010A-BDS; 6 turn magnet	Parameter list [21]	DANFYSIK measurements [20]	OPERA-TOSCA simulation
Effective magnetic length [m]	0.3	0.244	0.2236
Maximum integrated field ∫Bdl [Tm]	0.0173	0.01244	0.01261
Maximum field B [T]	0.0577	0.051	0.0564

S8-016A-BDE; 12 turns magnet	Parameter list [21]	DANFYSIK measurements [20]	OPERA-TOSCA simulation
Effective magnetic length [m]	0.3	0.246	0.2233
Maximum integrated field ∫Bdl [Tm]	0.0346	0.02091	0.02259
Maximum field B [T]	0.1153	0.085	0.1012

For the S3-010A-BDS (6-turn) magnet there also have been made measurements at CERN, which have given an effective magnetic length of 0.216 m [23]. This value fits well into the TOSCA simulations, since the magnet was measured at CERN with a 50 kHz low voltage sine wave. The equivalent frequency of the magnets current rise and fall time as shown in Figure 44 is ~2.5 kHz and results in an increased effective magnetic length, because of a higher skin depth, due to the lower frequency. Less eddy currents are induced that oppose the magnetic field and therefore the integrated field is increased.

Comparing the specified values with the DANFYSIK measurements as well as with the measurements and the simulations at CERN (see Table 13, except the CERN measurements), it is shown that the required integrated field and the effective magnetic length is too short and the magnets for MEDAUSTRON have to be redesigned to achieve the specified values.

Saturation

As it could be expected the highest magnetic fields occur in the yokes in the inner corners at the endings of the magnets. For the 6-turn dump bumper the field can there obtain a maximum strength of 290 mT. See Figure 48 and Figure 49.

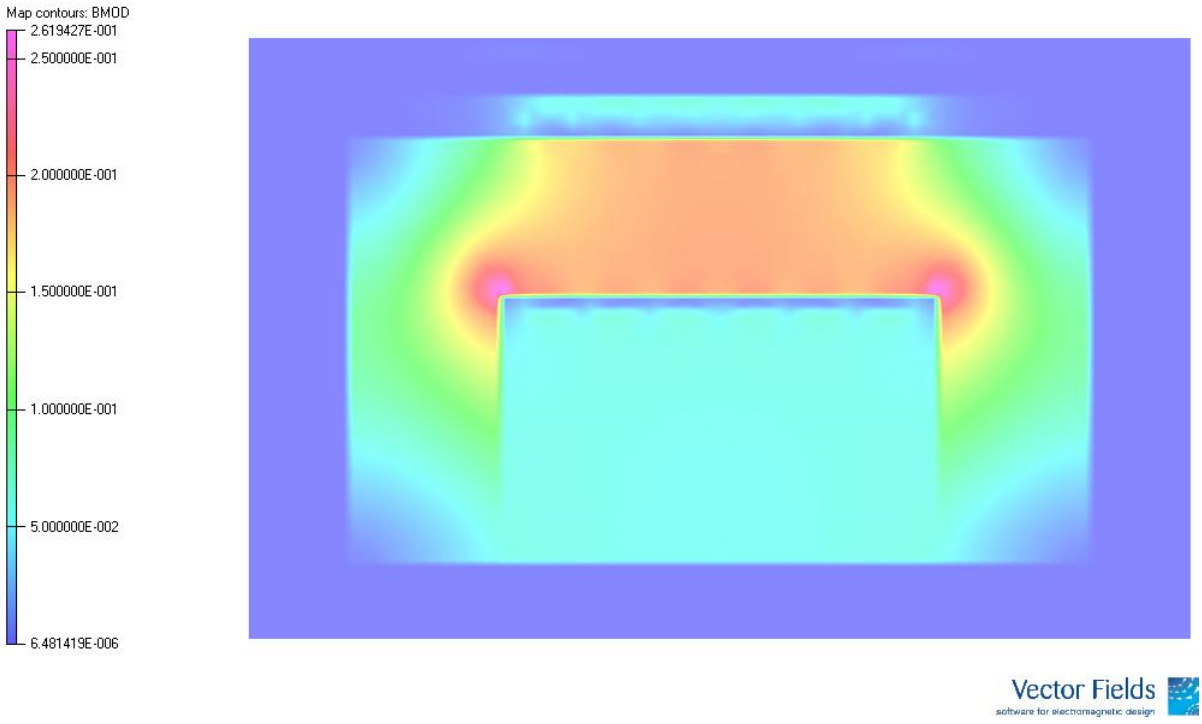

Figure 48 - Magnetic field within the centre of the yoke of the 6-turn dump bumper in the x-y plane at z=0 mm.

[23] Luc Sermeus, private communication, 2nd April 2009

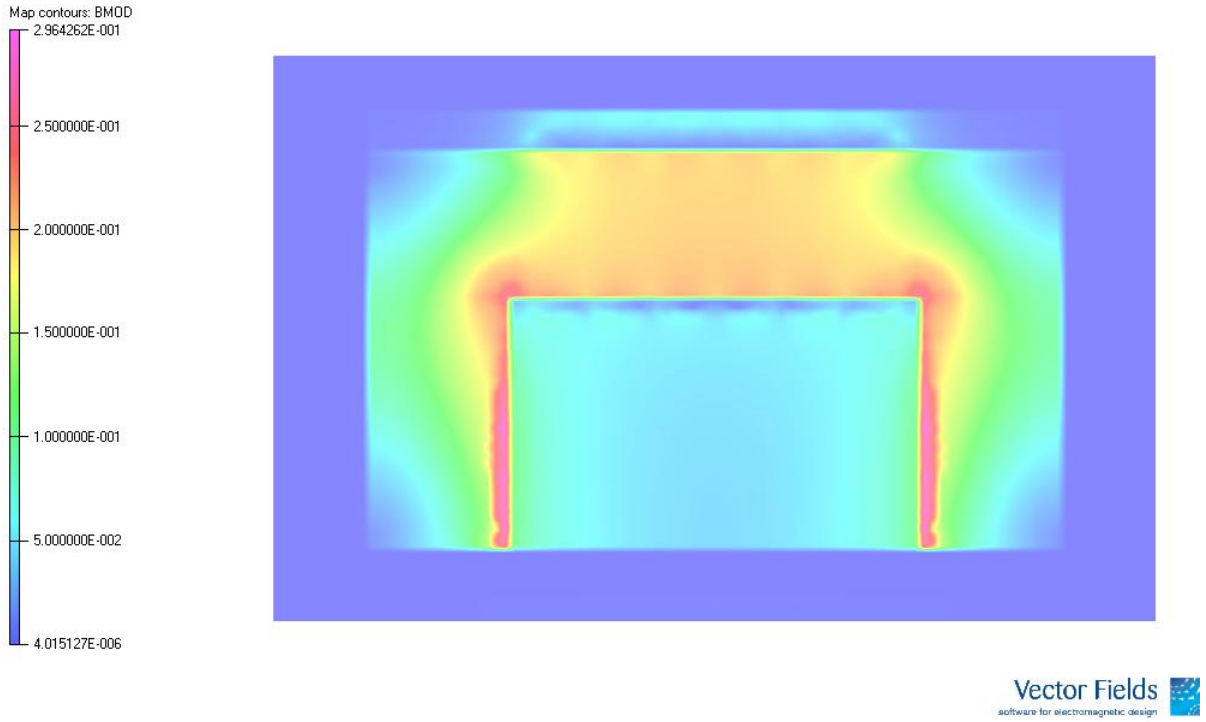

Figure 49 - Magnetic field at the endings of the yoke of the 6-turn dump bumper in the x-y plane at z=74 mm.

The maximum field in the 12-turn dump bumper can also be found at the endings of the yoke and reaches strength of 420 mT. In the centre the maximum field is 330 mT (see Figure 50 and Figure 51). Magnetic Ceramics gives for saturation for CMD 5005 a value of 320 mT (which can also be seen in Figure 8), i.e. the yoke is fully saturated.

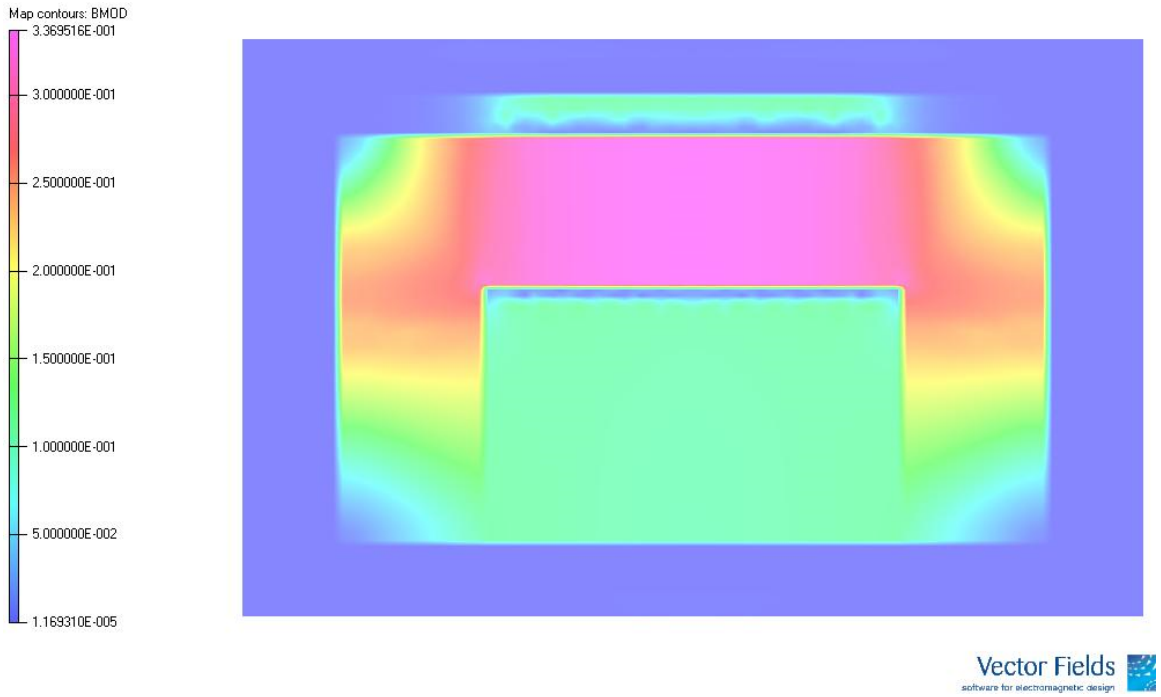

Figure 50 - Magnetic field within the centre of the yoke of the 12-turn dump bumper in the x-y plane at z=0 mm.

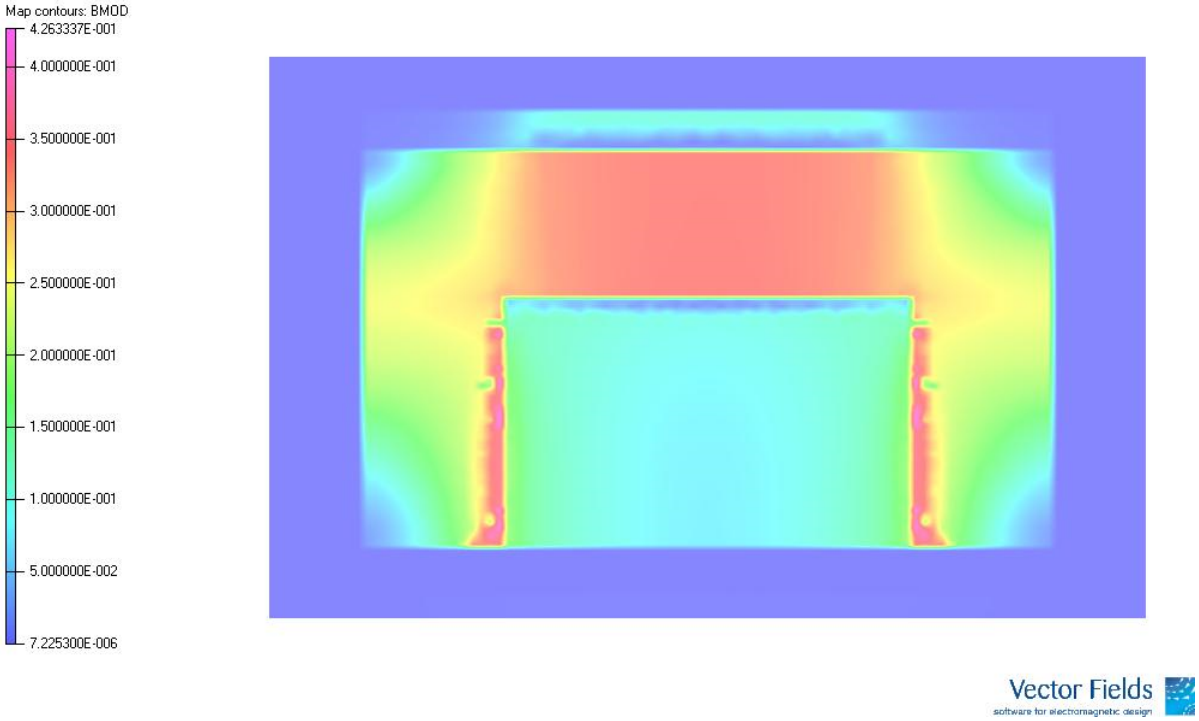

Figure 51 - Magnetic field at the endings of the yoke of the 12-turn dump bumper in the x-y plane at z=74 mm.

2.3.4 Adjustments for MEDAUSTRON

Magnetic Field and Magnetic Length

Since the magnets are identical except of the number of windings, simulations have been done mainly for the 12-turn magnet. To keep the magnets powered in series all changes done for the 12-turn magnet also apply for the 6-turn magnet. Provided that the magnet stays in linear regime, it is possible to divide the results of the 12-turn magnet by two to obtain the values for the 6-turn magnet. To achieve the deflection angle of 5.4 mrad and the integrated magnetic length of 34.6 mTm respectively, several structural changes will be proposed [24].

The CNAO designs are based on the 6-turn magnet, which provoked saturation in the ferrite of the 12-turn magnet. To avoid saturation, the cross-section of the ferrite is doubled. This change in the design results in an increased integrated magnetic field, which can be seen in Table 14. All future simulations are done with the double cross-section.

Table 14 – Results of the magnetic field for the 12-turn magnet for the original CNAO design and the change for the double cross-section.

12 turns magnet	Parameter list [21]	Simulation (CNAO design)	Simulation (double cross-section)
Effective magnetic length [m]	0.3	0.2233	0.224
Maximum integrated field ∫Bdl [Tm]	0.0346	0.02259	0.02526
Maximum field B [T]	0.1153	0.1012	0.113

There are several different options that can be combined to change the design and achieve the required specifications. The effects of the different actions are shown in Table 15.

- Stretch the complete magnet. The magnet is stretched by 60 mm. This change increases the total physical length from 0.225 m to 0.285 m. This increase needs to be approved for space availability in the main ring of the accelerator and further studies are needed by the beam optics group. This change is indicated in Table 15 by '60 mm'.
- Reduce the thickness of the aluminium end plates (perpendicular to beam direction) from 8 mm to 5 mm. This results in a gain of 6 mm space inside the magnet by which the coils and the ferrite can be stretched. In Table 15 this is indicated by 'thin-plate' and the gained physical distance for the ferrite within the magnet).

[24] Changes are done in consultation of Luc Sermeus, private communication, 2nd April 2009

- Between coil and ferrite is some space. The ferrite length can be increased by 12 mm and so the distance between coil and ferrite will be shortened. A distance of 3 mm should be kept for insulating glass fibre plate and resin potting. 'Thick-ferrite' and the gained physical distance for the ferrite within the magnet indicate this action in Table 15.
- Additionally stretch the coil and the ferrite by 12 mm each. Therefore the distance to the aluminium end plates will then be shortened. However, 5 mm of distance between coil and aluminium plates should be kept for the resin and glass fibre plate. Indicated in Table 15 by 'coil-length' and the gained physical distance for the ferrite within the magnet.
- Increase the current. This depends on the limitations of the power supply. For increasing the current too much, components in series/parallel might be needed or making two separate power supplies operating at lower voltage. Currents used in the simulations are indicated in Table 15 by the used current.
- If it is not possible to find the space for the physically stretched magnets, it is also possible to increase the number of windings for each magnet. This increases the inductance and the pulse rise time. In addition it is then very difficult to build both magnets identical due to high current densities in the 12-turn magnet (MKD-B). If they are not identical, each magnet needs its own power supply and they have to be synchronized.

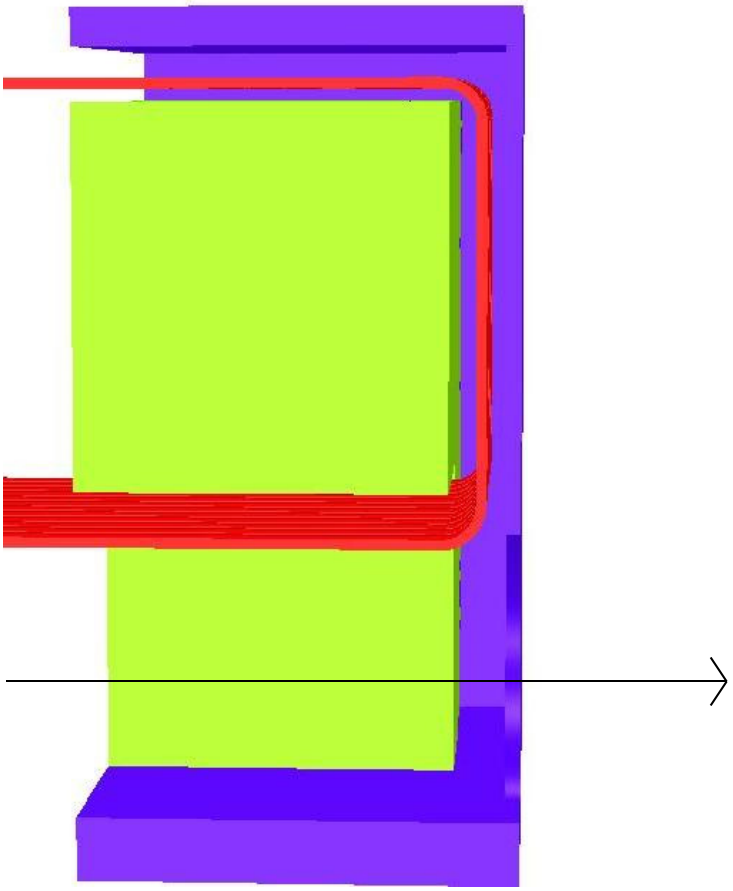

Figure 52 - Cut through the quarter of the modified dump bumper along the beam direction (blue is aluminium, green is ferrite and red is the coil, the arrow indicates the beam direction). Picture is cut on the left-hand side.

Table 15 - Results for TOSCA-DC Simulations varying different parameters. Specified values are: *Bdl*=34.6 mTm; B_0=0.1153 T and L_{eq}= 300 mm

TOSCA 12 Turns Dump Double 1265 A	
Bdl (600 mm) [mTm]	25.258
B_0 [T]	0.113
Leq [mm]	223.917
TOSCA 12 Turns Dump Double 1265 A + 60 mm	
Bdl (600 mm) [mTm]	32.155
B_0 [T]	0.115
Leq [mm]	278.763
TOSCA 12 Turns Dump Double 1265 A + 60 mm + thin-plate 6 mm gain	
Bdl (60 0mm) [mTm]	32.723
B_0 [T]	0.115
Leq [mm]	283.445
TOSCA 12 Turns Dump Double 1265 A + 60 mm + thick-ferrite 12 mm gain	
Bdl (600 mm) [mTm]	32.641
B_0 [T]	0.115
Leq [mm]	282.63
TOSCA 12 Turns Dump Double 1265 A + 60 mm + thick-ferrite 12 mm gain + thin-plate 6 mm gain	
Bdl (600 mm) [mTm]	33.188
B_0 [T]	0.116
Leq [mm]	287.165
TOSCA 12 Turns Dump Double 1265 A + 60 mm + thick-ferrite 12 mm gain + thin-plate 6 mm gain + coil-length 12 mm gain	
Bdl (600 mm) [mTm]	33.62
B_0 [T]	0.116
Leq [mm]	290.653
TOSCA 12 Turns Dump Double 1300 A + 60 mm + thick-ferrite 12 mm gain + thin-plate 6 mm gain + coil-length 12 mm gain	
Bdl (600 mm) [mTm]	34.549
B_0 [T]	0.119
Leq [mm]	290.652
TOSCA 12 Turns Dump Double 1350 A + 60 mm + thick-ferrite 12 mm gain + thin-plate 6 mm gain + coil-length 12 mm gain	
Bdl (600 mm) [mTm]	35.878
B_0 [T]	0.123
Leq [mm]	290.652

Only by using all different options for modification the specified values can be achieved.

For completeness a simulation of the 6-turn magnet (MKD-A) has been made. As it was expected the maximum magnetic field and the integrated magnetic length are half of the maximum of the integrated field and the integrated length respectively of the 12-turn magnet (see Table 16).

Table 16 - Results for TOSCA-DC Simulations for the 6-turn magnet MKD-A.

Specified values are: Bdl=17.3 mTm; B_0=0.0577 T and L_{eq}= 300 mm

TOSCA 6 Turns Dump Double 1350 A + 60 mm + thick-ferrite 12 mm gain + thin-plate 6 mm gain + coil-length 12 mm gain	
Bdl (600 mm) [mTm]	17.943
B_0 [T]	0.062
Leq [mm]	290.672

Saturation

In the original CNAO design the ferrite for the 12-turn magnet has been saturated. Therefore the simulations for MEDAUSTRON have been done with a double cross-section of the ferrite. As it already can be seen in Table 14 by a higher magnetic field, the saturation effects vanish. Figure 53, Figure 54 and Figure 55 show the saturation of the 12-turn magnet with double cross-section. The highest magnetic field can be found at the endings of the yoke obtaining strength of 400 mT in very small parts of the edges. Though the ferrite is saturated at 320 mT, it has no effect in the linearity between rising current and magnetic field as shown in Figure 56.

The 6-turn dump bumper was not saturated in the original CNAO design and will therefore also not being saturated with double cross-section.

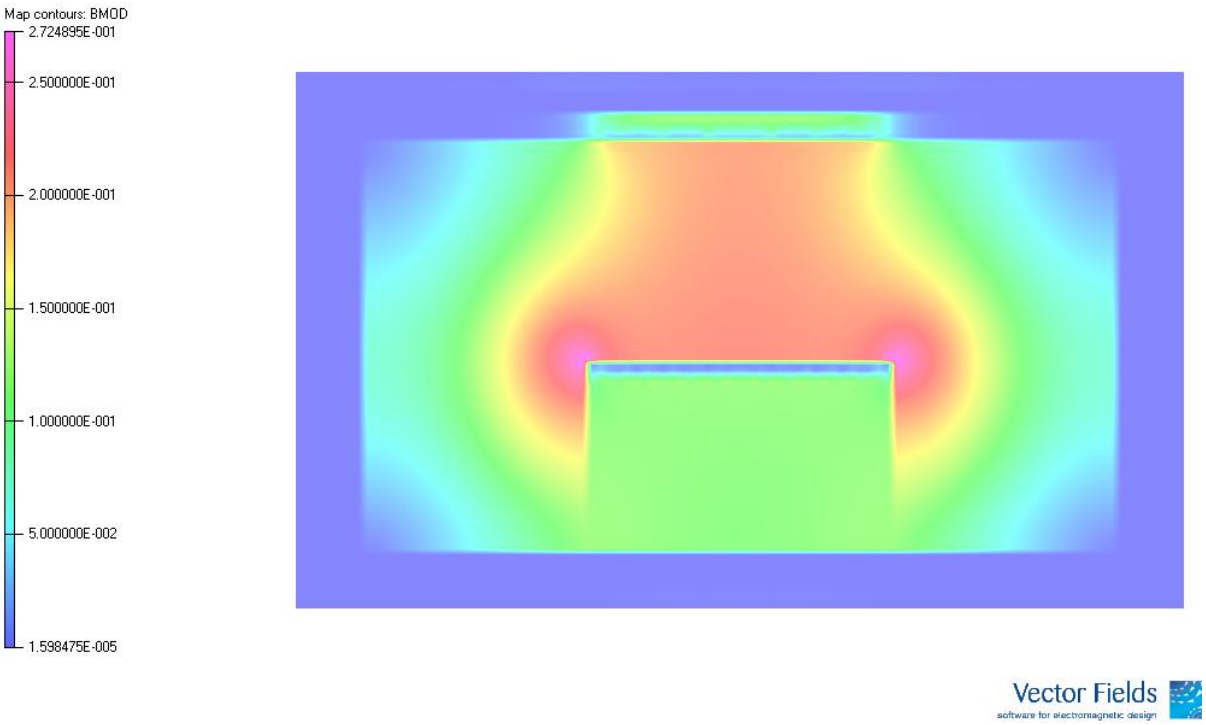

Figure 53 - Magnetic field within the centre of the yoke of the 12-turn dump bumper with double cross-section in the x-y plane at z=0 mm.

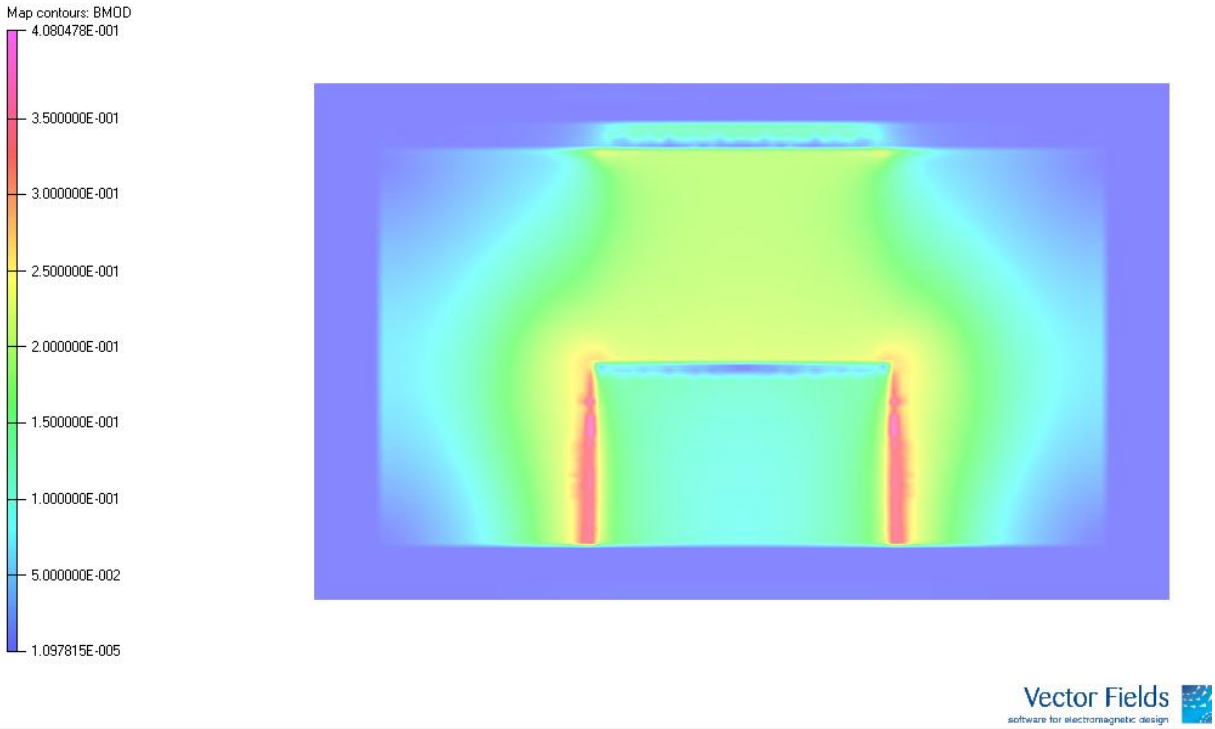

Figure 54 - Magnetic field at the endings of the yoke of the 12-turn dump bumper with double cross-section in the x-y plane at z=74 mm.

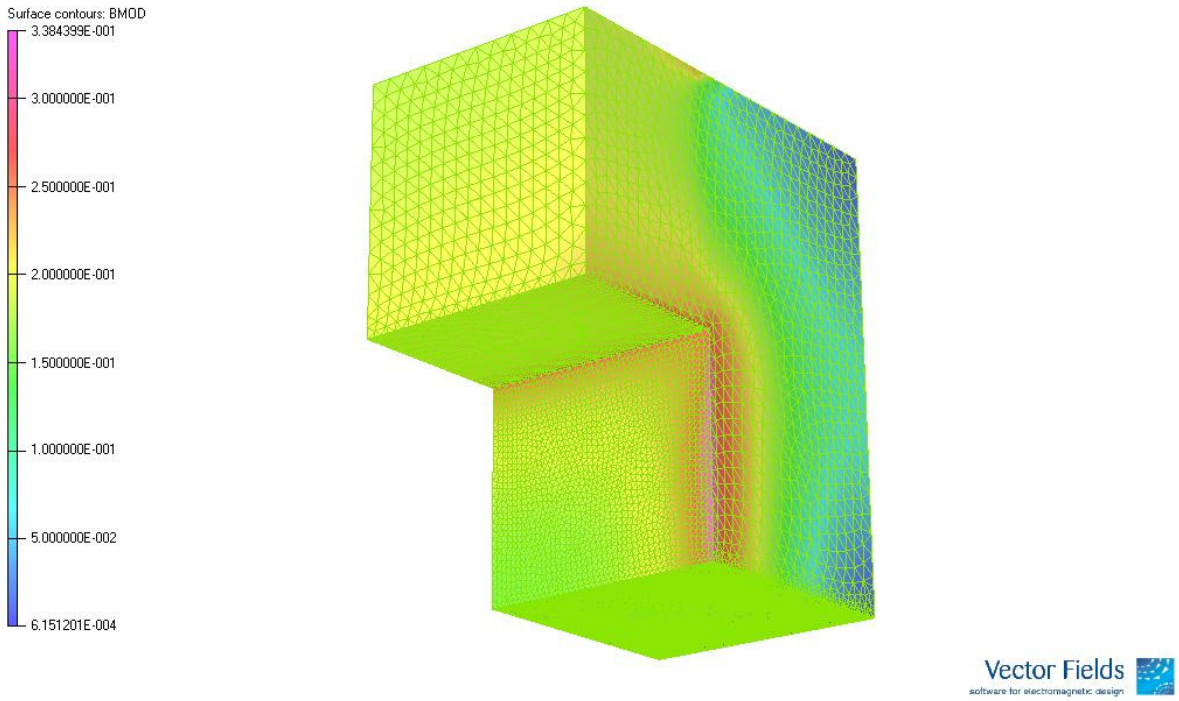

Figure 55- A 3-D view of a quarter of the yoke of the 12-turn dump bumper with double cross section showing the magnetic field.

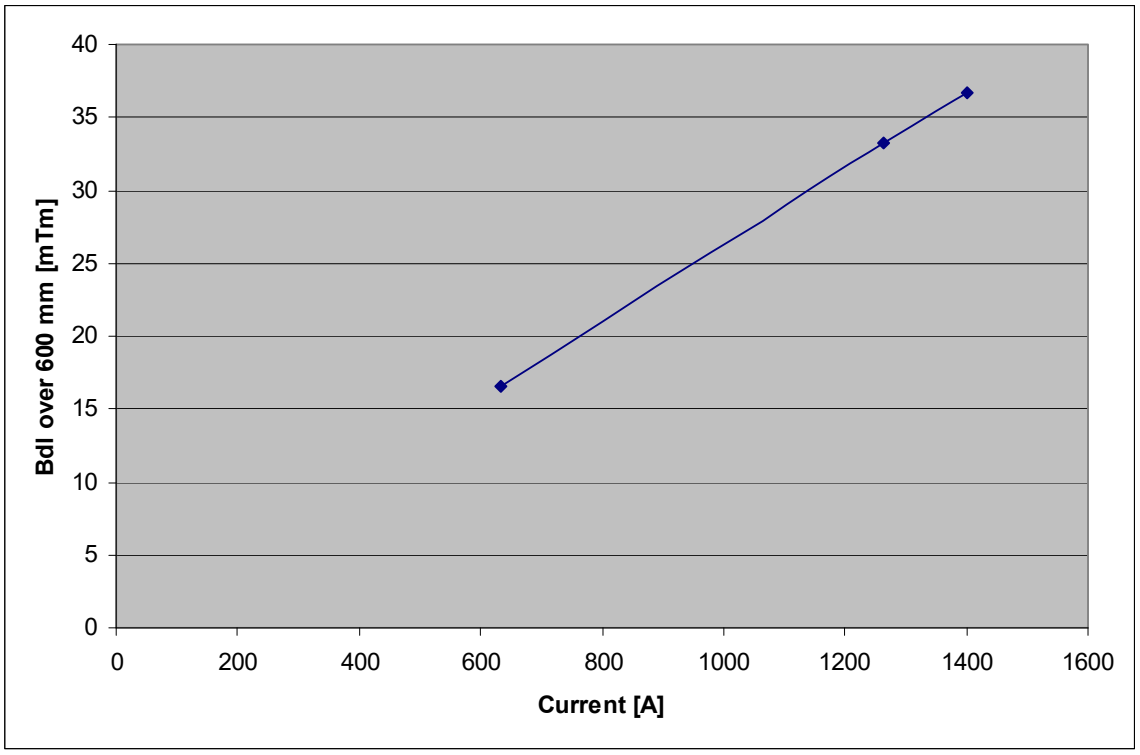

Figure 56 - Behaviour of the integrated field over 600 mm at rising current.

Homogeneity of the Magnetic Field

As shown in the line map of Figure 57 the magnetic field is homogeneous for the 12-turn dump bumper within the specified area of 60 × 120 mm^2 in the plane z=0. The magnetic field in the reference trajectory is 123.4 mT and the maximum deviation is Δ2.9 mT within the specified good field region, which equivalents a Δ angle kick of Δ0.16 mrad.

The line map of the 6-turn dump bumper is shown in Figure 58 and also homogeneous. In the reference trajectory the magnetic field is 61.7 mT. The maximum deviation is Δ1.3 mT and equivalents a Δ angle kick of Δ0.04 mrad.

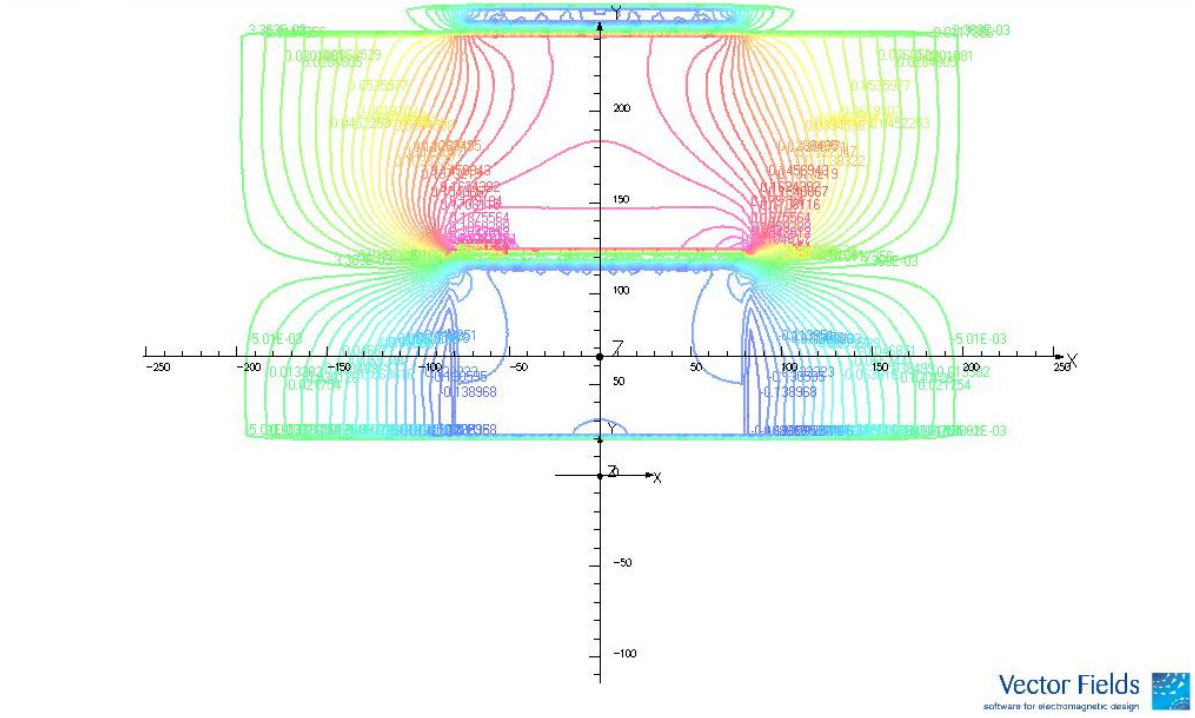

Figure 57 - Equivalent field-lines of the B-field in the x-y plane at z=0 of the 12-turn dump bumper.

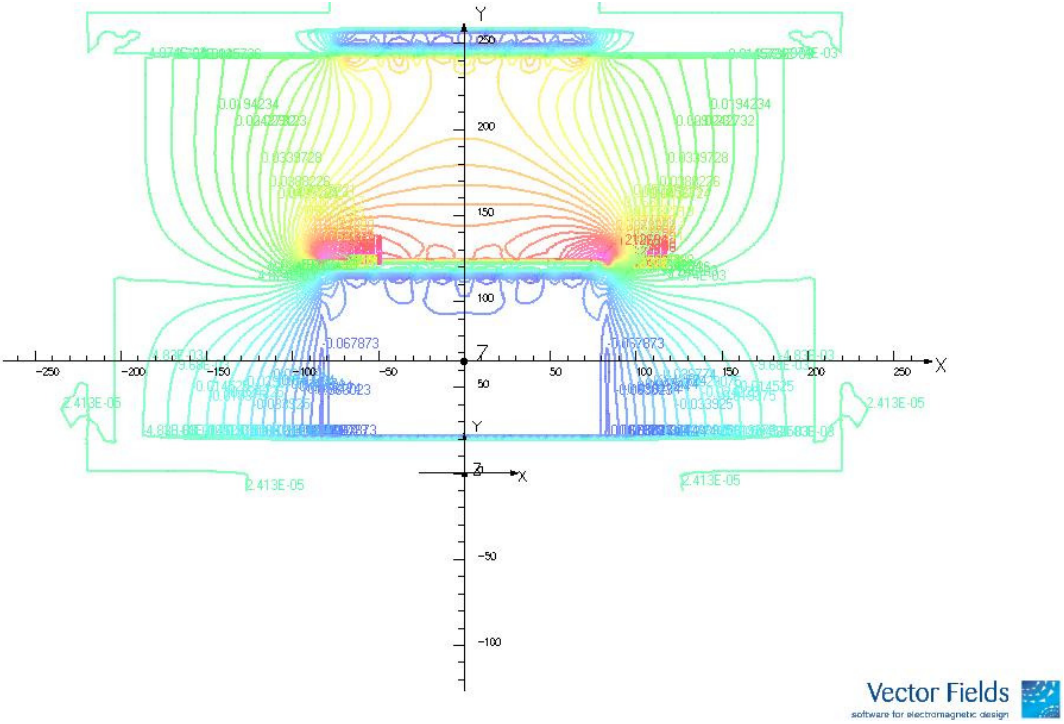

Figure 58 - Equivalent field-lines of the B-field in the x-y plane at z=0 of the 6-turn dump bumper.

Magnetic Inductance

Since the magnet has been modified, also the magnetic inductance has changed. The inductance *L* is calculated by the stored Energy *W* and the current *I.*

$$L=2W/I^2$$

For the 12-turn dump bumper the stored energy is 36.94 J while it is 9.29 J for the 6-turn magnet. This results in a magnetic inductance of 41 µH and 10 µH respectively. The total inductance for both magnets rises then from 40 µH to 51 µH. Using

$$U=LdI/dt$$

with a ramp time of 50 µs and a current of 1350 A, a voltage of 1400 V is needed.

Survey and Positioning

For lengthening the magnet the beam optics group will need to make further studies, if this is possible. Therefore this section shows the positioning of the magnet with surrounding elements and their possibility to move.

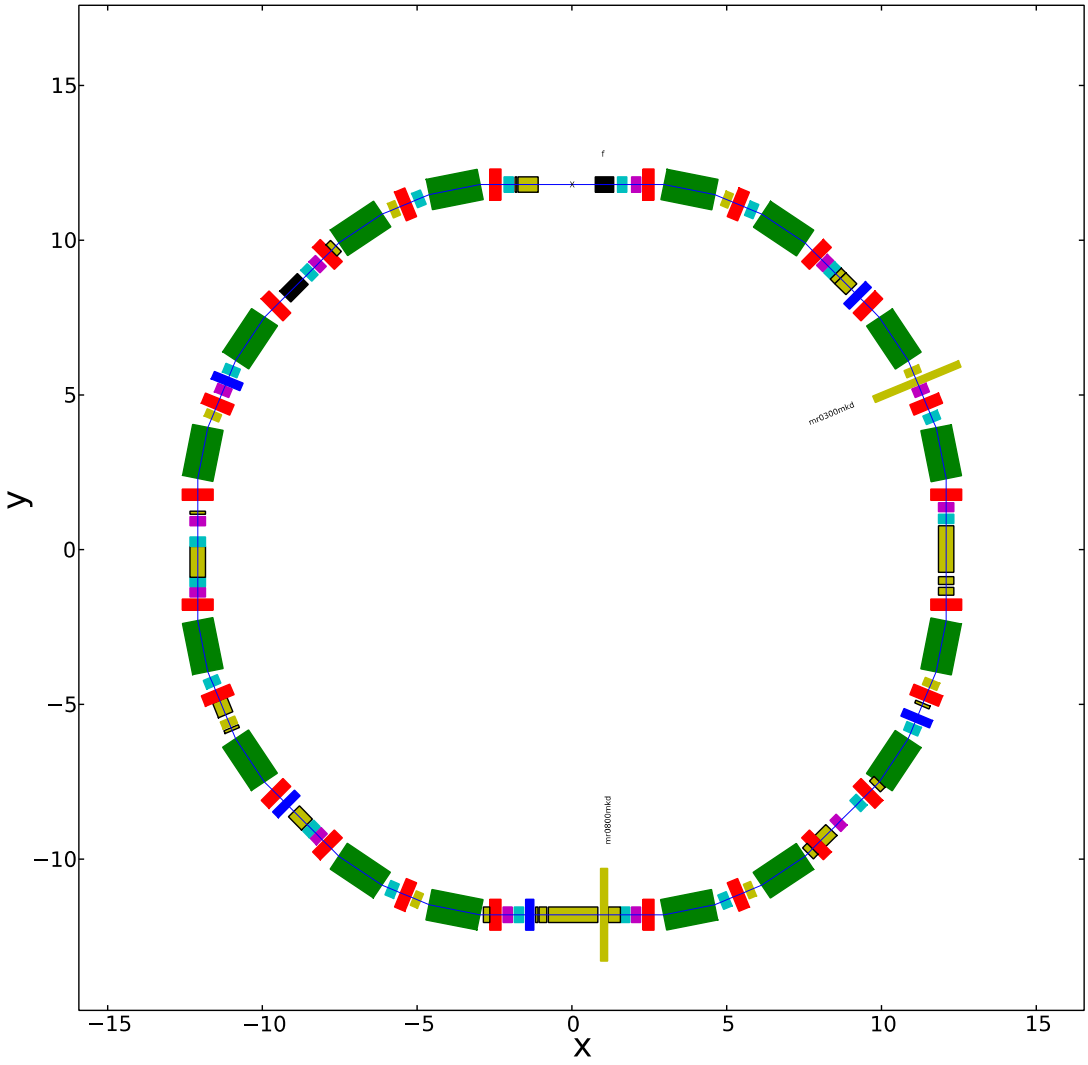

Figure 59 - Dump bumper shown as wide yellow lines with labels

In Figure 59 the position of the dump bumpers in the main ring sectors 3 and 8 are shown as wide yellow lines with the current specified total physical length for MKD-A and MKD-B of 0.225m each. Table 17 and Table 18 give all the elements and their physical length in the two sectors around the magnets and say if the elements can be moved or if they have to stay in their places.

Table 17 - Elements in the main ring sector 3. (N=not moveable; Y=moveable; L=limited moveable)

MR Sector 3		
Name	Physical length [m]	Moveable
mr0300mbh	1.6772	N
mr0300vac	0.25715	Y
mr0300mcv	0.252	L
mr0301vac	0.122	Y
mr0300mkd	0.225	L
mr0302vac	0.05	Y
mr0300mki	0.295	L
mr0303vac	0.148	Y
mr0300mqd	0.36	L
mr0304vac	0.139	Y
mr0300puv	0.3	L
mr0305vac	0.21015	Y

Table 18 - Elements in the main ring sector 8. (N=not moveable; Y=moveable; L=limited moveable)

MR Sector 8		
Name	Physical length [m]	Moveable
mr0800mbh	1.6772	N
mr0800vac	0.31915	Y
mr0800mqf	0.36	L
mr0801vac	0.08	Y
mr0800mch	0.292	L
mr0802vac	0.059	Y
mr0800puh	0.3	Y
mr0803vac	0.0072	Y
mr0800cta	0.4	Y
mr0804vac	0.01	Y
mr0800mkd	0.225	L
mr0805vac	0.0858	Y
mr0800rfc	1.6	Y
mr0806vac	0.05	Y
mr0800mqs	0.25	L
mr0807vac	0.032	Y
mr0800sch	0.082	Y
mr0808vac	0.056	Y
mr0800mxr	0.26	L
mr0809vac	0.07	Y
mr0801puh	0.3	L
mr0810vac	0.069	Y
mr0801mch	0.292	L
mr0811vac	0.07	Y
mr0801mqf	0.36	L
mr0800vvs	0.21	Y/L
mr0812vac	0.10915	Y

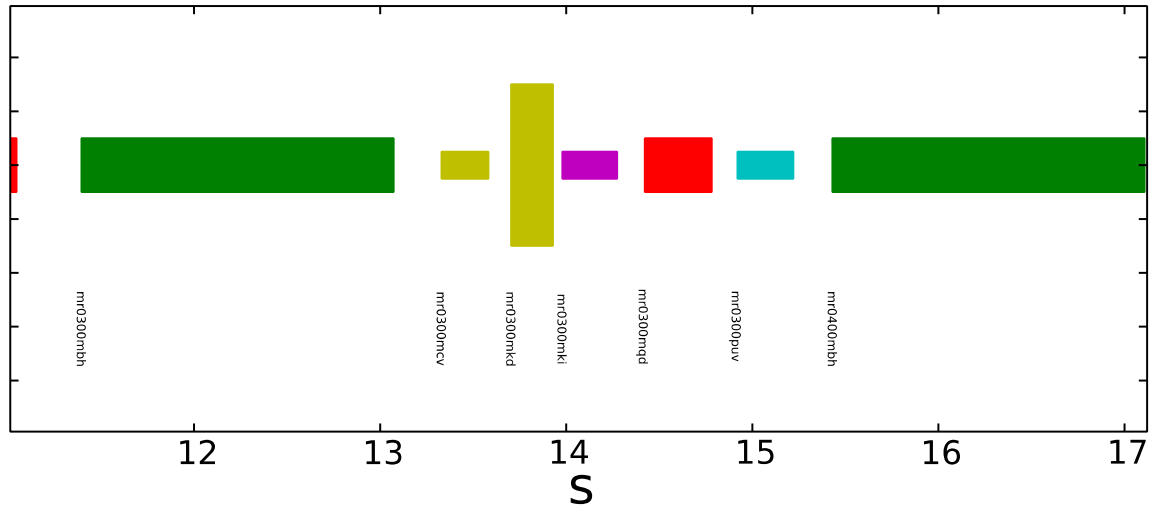

Figure 60 - Position of MKD-A in main ring sector 3.

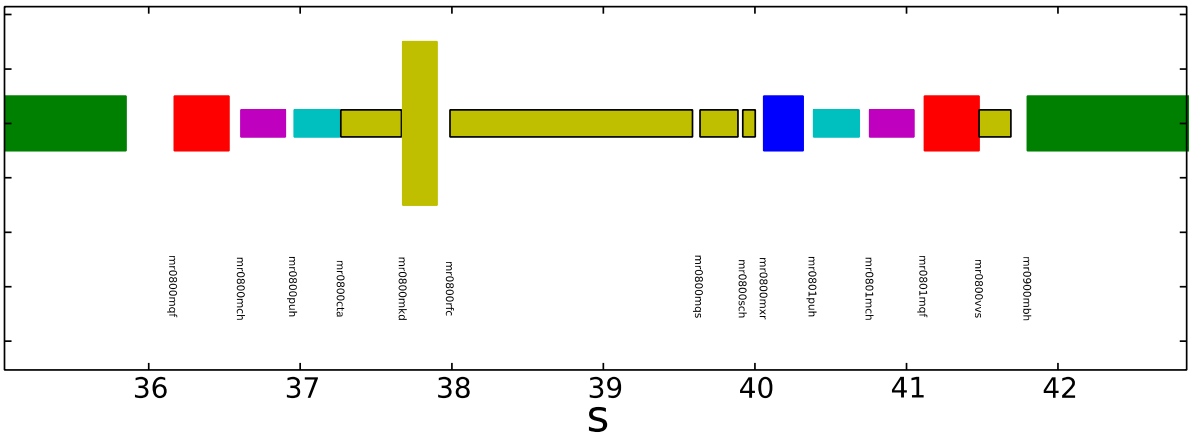

Figure 61 - Position of MKD-B in main ring sector 8.

Figure 60 and Figure 61 show the exact position of the two dump bumpers (wide yellow lines) with the elements next to them.

The extraction optics for the vertical closed orbit offset due to kicks of 5.4 mrad and 2.7 mrad respectively can be seen in Figure 62.

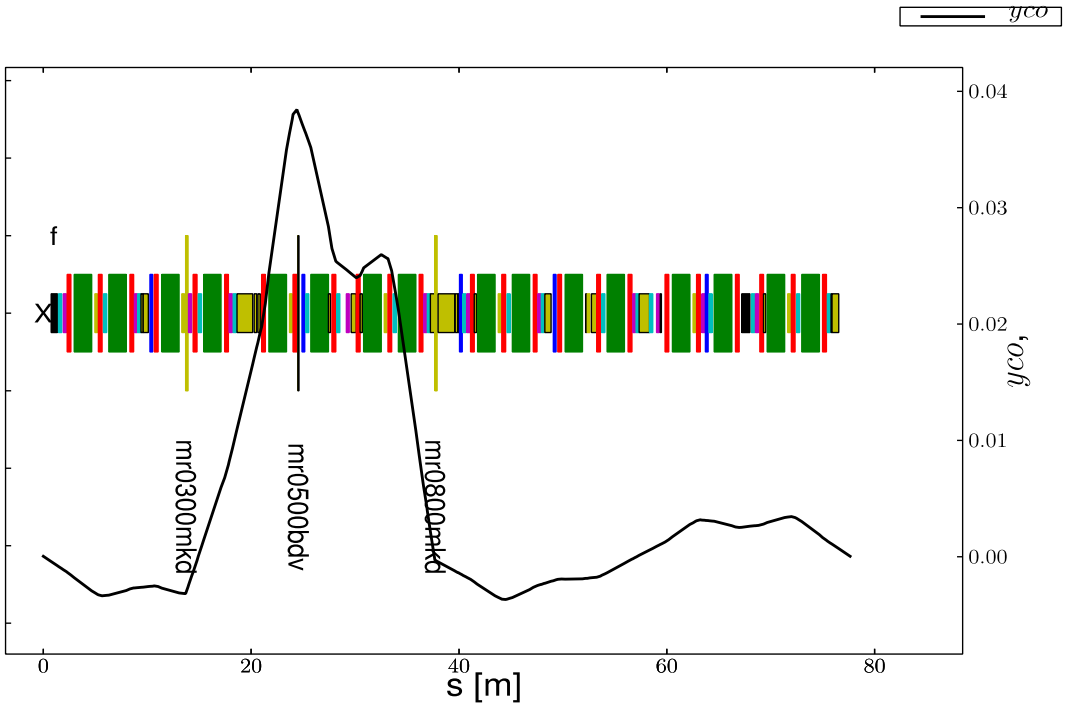

Figure 62 - The black line shows the vertical orbit bump along synchrotron sectors overlaid by the accelerator lattice (extraction optics). The light green lines indicate the location of dump bumpers, the vertical black line the dump position.

2.3.5 Summary

To reach the current specifications, the design of the magnets has to be changed. A combination of the different options given above is needed.

- Double the cross-section of the ferrite.
- Increase the total physical length of each magnet by 60 mm.
- Reduce the thickness of the aluminium end plates by 3 mm each. Therefore ferrite and coil length can be increased by 6 mm.
- Increase the coil length and the ferrite length by additional 12 mm.
- Increase the ferrite length by further 12 mm.
- Increase the current from 1265 A to 1350 A.

Note that the simulations are only done in VECTORFIELDS-TOSCA i.e. DC-simulations. By using a relative permeability of 0.0001 H/m instead of 1 H/m for the material properties of aluminium, eddy currents were simulated and as mentioned in section 2.3.3, results are fitting to CERN measurements. The approximation to ELEKTRA AC-simulations by changing the material properties can be done as shown in section 2.1.3.

The increase of the total physical length of 60 mm needs to be approved.

It needs to be verified if the power supply system is able to provide the increase from 1265 A to 1350 A and to handle the higher inductance of 51 µH.

Changes can also be seen in Table 19.

Table 19 - Changes of important parameters for the MEDAUSTRON dump bumpers (counts for both magnets)

Changes	CNAO model	MEDAUSTRON model
Total physical length [m]	0.225	0.285
Ferrite length [m]	0.15	0.18
Current [A]	1265	1350
Average turn length [m]	0.492	0.51
Estimated inductance for both magnets [uH]	40	51
Ferrite lengths in the cross-section are doubled in vertical and horizontal direction compared to CNAO model		

2.4 Chopper Dipole

As the injection bumpers and the dump bumpers also the four identical chopper dipoles were designed at CERN [25] and built and measured by DANFYSIK [26]. With reference to the report of the measurements the chopper dipoles were working fine except the field quality, which was not reached in the whole specified good field region. However the main problem was a very high inductance for the four-coupled magnets, which results in a high voltage and therefore a very costly power supply system. Hence the goal was to reduce the inductance in order to reduce the voltage, which significantly improves the requirements for the solid-state switches and thus the overall reliability. As a nice to have side effect money on the building cost for the power supply is saved as well. Reliability is the key design parameter for the MEDAUSTRON MKC as it will be classified as a safety device and medical product.

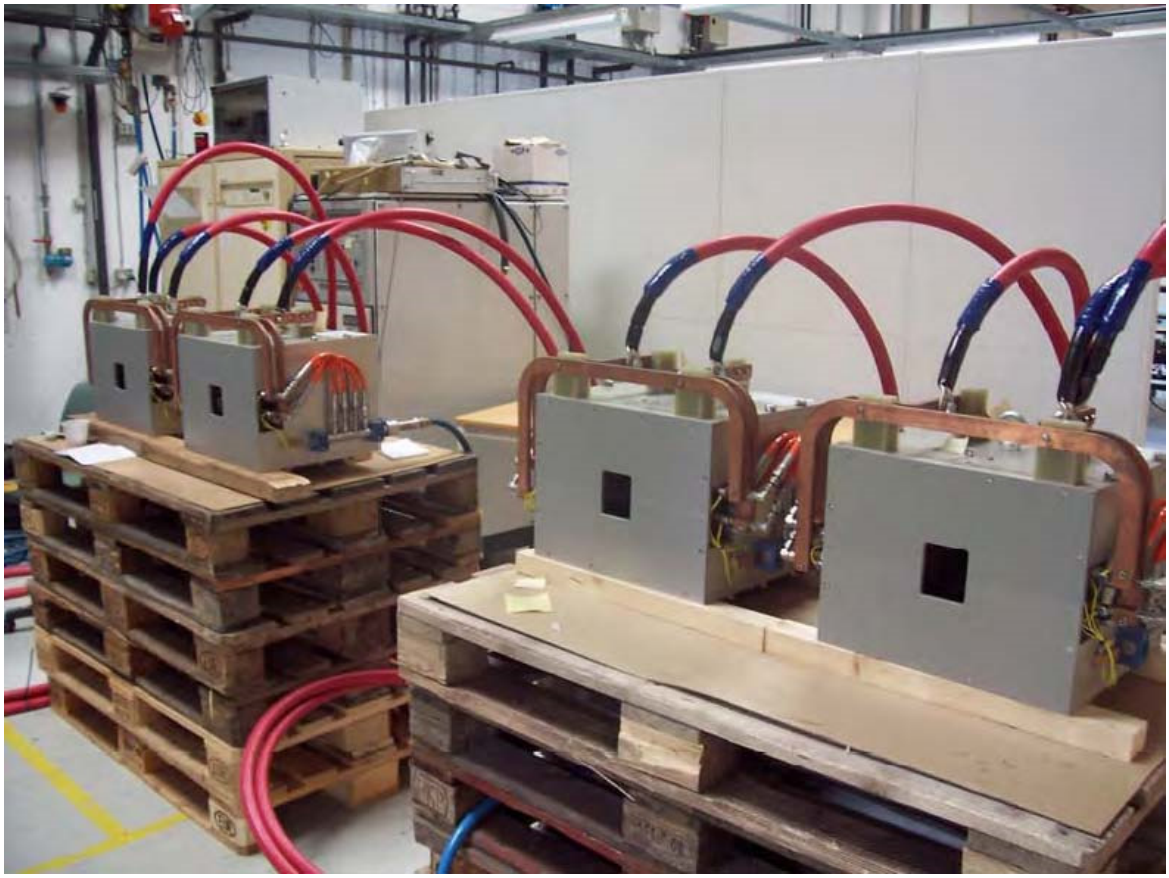

Figure 63 - Complete Assembly of the CNAO chopper dipole magnets.

[25] "Final Design, Special Magnets" CAN-TNDP-006WXX-00231, 21th July 2003, J. Borburgh et.al (CNAO-CERN)
[26] "Quality Assurance Report" CNA-SPDF-007WXX-00234, 15th August 2007, N. Hauge (DanFysik)

2.4.1 Parameter List

Table 20 - Magnet parameter list predicted by CERN for the CNAO chopper dipoles build by DANFYSIK.

	CNAO-CERN – Chopper Dipoles
Info	4 items powered in series, current controlled power converter and programmable with a resonant HV branch
Dismantling	-
Effective magnetic length [m]	0.3
Total physical length [m]	0.35
Ferrite physical length [m]	0.205
Maximum integrated field ∫Bdl [Tm]	0.0419
Maximum field B [T]	0.141
Deflection angle [mrad]	6.6
Pole gap [mm]	90
Aperture w × h [mm^2]	166 x 90
Vacuum chamber	Ceramic, Racetrack, 7 mm thick
Good field region (rectangle) [mm^2]	66 x 66
Field quality [%]	Δ 0.2%
Coil	2, copper conductor, water cooled, double layer pancake 2 × 4 turns, saddle-shaped
Conductor size [mm^2]	8 x 15, ø 4.5 mm water hole
Current for maximum field [A] (nominal)	644
Voltage [V] (nominal)	7450 (pulsed) & 41 (DC)
Current density [A/mm^2]	6.24
Number of turns	16 (8 per coil)
Water temperature rise [°C]	8
Water pressure [bar]	4
Water flow [l/min]	3.2
DC power dissipation [W]	1322 (661 per coil)
Magnet resistance [Ω]	0.0032 (0.016 per coil) (DC)
Estimated inductance [µH]	250
Estimated stored energy [J]	51.8
Maximum coil voltage to ground [V]	1790
Rise time [µs]	90 (max)
Fall time [µs]	90 (max)
Repetition rate [sec]	0.0001

Since DANFYSIK changed parts of the design including the Aperture, the parameter list used by DANFYSIK is given in Table 21. The changes are the total physical length, the aperture, the conductor size and therefore the current density, the cooling requirements, the ramp time, the inductance and the voltage, as well as the stored energy.

Table 21 - Parameter list given by DANFYSIK.

	DANFYSIK - Chopper Dipoles
Name	H3-001A / 005° / 009A / 013A-CHD
Info	4 items powered in series, current controlled power converter and programmable with a resonant HV branch
Function	Extracted beam chopper
Dismantling	Vertical
Effective magnetic length [m]	0.3
Total physical length [m]	0.346
Ferrite physical length [m]	0.205
Maximum integrated field ∫Bdl [Tm]	0.0419
Maximum field B [T]	0.141
Deflection angle [mrad]	6.6
Yoke	Ferrite, window frame
Pole gap [mm]	90
Aperture w × h [mm^2]	133 x 90
Coil	2, copper conductor, water cooled, double layer pancake 2 × 4 turns, saddle-shaped
Conductor size [mm^2]	8 x 8, ø 4.0 mm water hole
Space between turns [mm]	2
Good field region (rectangle) [mm^2]	-
Field quality [%]	-
Current for maximum field [A] (nominal)	644
Voltage [V] (nominal)	3.8 V per magnet (total ex. cables)
Current density [A/mm^2]	12.7
Number of turns	16 (8 per coil)
Average turn length [m]	1
Cooling	Water
Water temperature rise °C	5.6
Water pressure [bar]	0.7
Water flow [l/min]	1.5 per circuit - 6 total.
DC power dissipation [W]	2300, 1150 per coil
Magnet resistance [Ω]	0.0054 (0.0027 per coil)
Estimated inductance [µH]	143

Estimated stored energy [J]	30
Maximum coil voltage to ground [V]	> 2900
Rise time [µs]	260
Fall time [µs]	260
Overshoot [%]	< 7
Repetition rate [sec]	0.1

2.4.2 CNAO and DANFYSIK Design

All treatment rooms will be able to switch the beam on and off for routine operational reasons by means of the beam Chopper. The Chopper works by making a closed-orbit bump that bypasses a dump block mounted inside of the vacuum chamber. The extra narrow beam and the absence of tails on the 'bar' of charge makes the horizontal plane the preferred choice for the bump that is excited by four equal bumper dipoles in series. The four dipoles surround two dipole magnets and the bump is closed to a few µm. This can be neglected and the downstream trajectory of the beam is unaffected at all times. For this reason, the stability and over-shoot of the power converter are not critical issues. The chopper dipoles must provide kicks of 6.6 mrad. For the highest rigidity beam, this represents an integrated field of 0.0419 Tm.

The required deflection is 6.6 mrad horizontally in an effective magnetic length of 0.3 m. The magnet is of window frame construction with two water-cooled saddle coils of 8 turns each. Some details of the original CERN design are shown in Figure 64, Figure 65 and Figure 66.

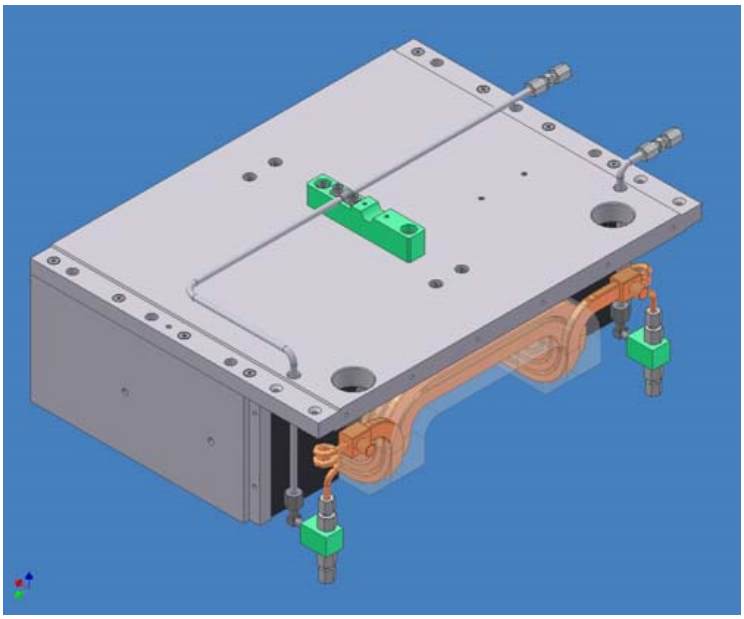

Figure 64 - Chopper top half (CERN design).

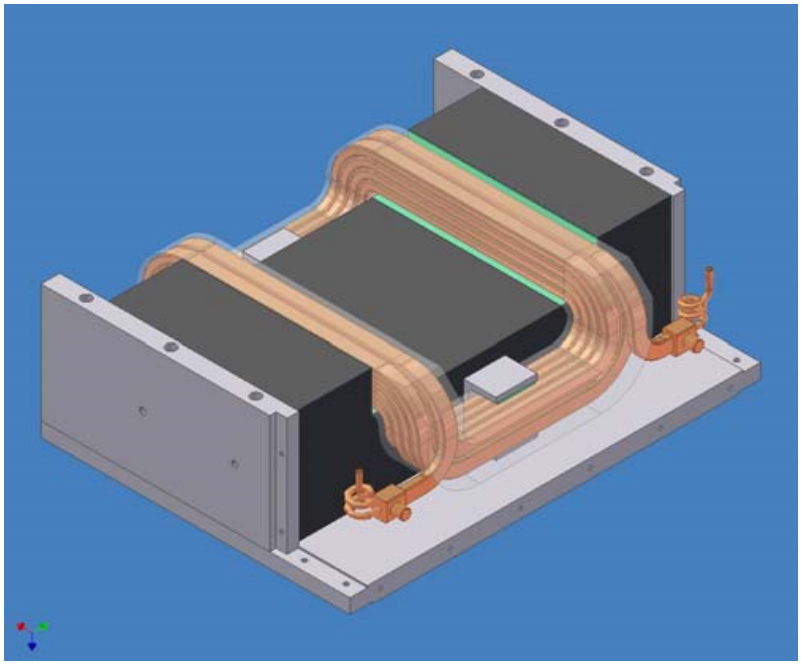

Figure 65 - Chopper bottom half (CERN design).

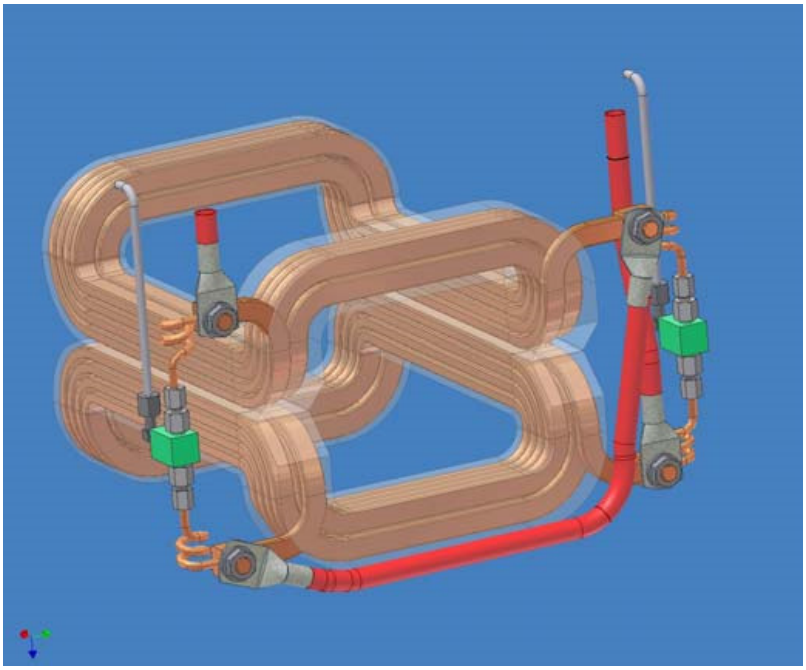

Figure 66 - Assembled chopper coils (CERN design).

Together with the coil size DANFYSIK changed powering and cooling connections, which can be seen in Figure 67. Otherwise then in the CERN design this design misses a second layer on one end of the bedstead.

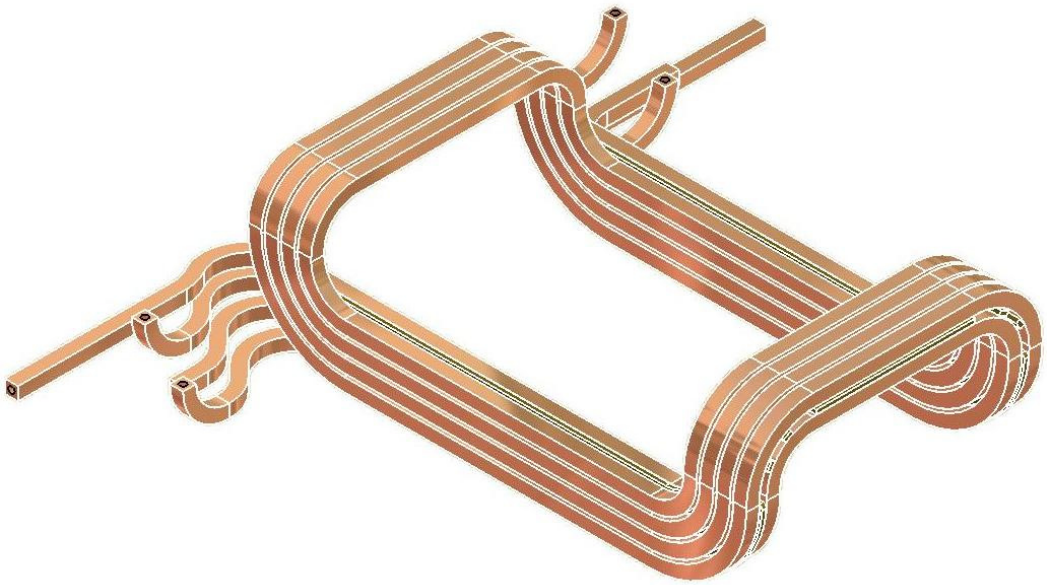

Figure 67 - Top half coil design (DANFYSIK).

The original CERN design foresees a ramp time of 90 µs, while the built DANFYSIK magnets are ramped with 260 µs. For MEDAUSTRON, security issues and the chosen treatment strategy will determine the ramp time, since this is the last possibility to interrupt the beam before it is delivered to the treatment rooms.

For the design in OPERA-ELEKTRA the dimensions are taken from the technical drawings of DANFYSIK [27], but have been simplified as the two injection bumpers and the dump bumpers

[27] The files of the technical drawings can be found under
\\cern.ch\dfs\Projects\medaustron\CNAOdocs\docs\Special magnets\special magnets and PS - as built documentation\ 14878-105 Chopper\Drawings-14878-105\Workspace
Technical Drawings used:
DanFysik, Chopper Dipole Magnet, 14878.105.065.C, 6th August 2007
DanFysik, Assembly Bottom, 14878.105.066.B, 15th June 2006
DanFysik, Coil, 14878.105.067.C, 15th June 2006
DanFysik, Coil Assembly, 14878.105.070.A, 16th February 2006
DanFysik, Coil Layer 1, 14878.105.071.A, 15th February 2006
DanFysik, Coil Layer 2, 14878.105.072.A, 15th February 2006
DanFysik, Coil Layer 3, 14878.105.073.A, 15th February 2006
DanFysik, Coil Layer 4, 14878.105.074.A, 15th February 2006
DanFysik, Bottom Plate, 14878.105.085.B, 15th June 2006
DanFysik, Frame Side, 14878.105.087.A, 1st May 2006
DanFysik, Top Plate, 14878.105.091.A, 1st May 2006
DanFysik, Front Plate, 14878.105.092.A, 22nd June 2006
DanFysik, Ferrite Top/Bottom, 14878.105.101.B, 15th June 2006
DanFysik, Side Ferrite, 14878.105.102.A, 5th April 2006
DanFysik, Frame Side, 14878.105.121.A, 1st May 2006

as described in 2.1.2. Compared to the technical drawings also the conductor has been simplified by the double layer on both ends of the conductors. Shown in Figure 68.

The ramp time has been taken from the CERN design with 90 µs.

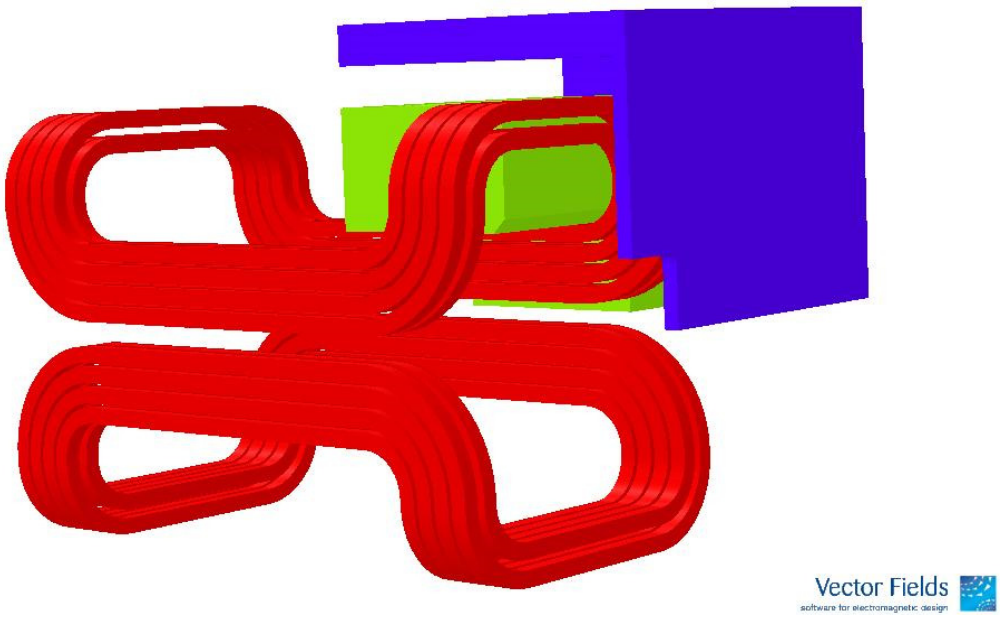

Figure 68 – One eighth of the DANFYSIK 3-D-model in VECTORFIELDS.

2.4.3 DANFYSIK Measurements Compared to Simulation

DANFYSIK Measurements

Measurements have been made at a current of 644 A and a voltage of 3.8 V using a Hall probe. The field quality measured in the upper half of the magnet over a total length of 880 mm on various positions for the four magnets can be seen in Figure 69.

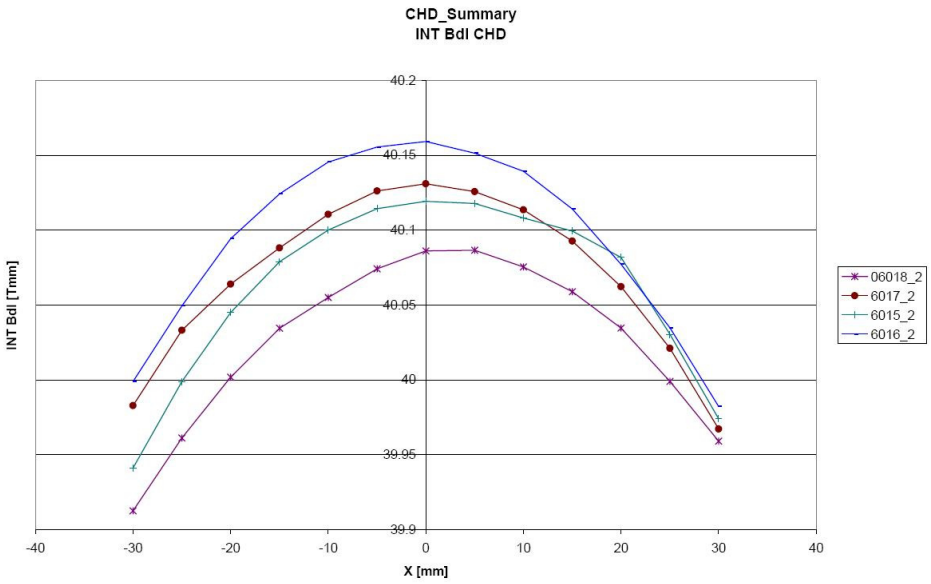

Figure 69 - Integrated field over 880 mm at various x-y position measured by DANFYSIK.

The maximum magnetic field is B_0=150.15 mT and the effective length is 276.16 mm. See also the full report [26].

Simulations in VECTORFIELDS

To verify these measurements for MEDAUSTRON, AC-simulations in OPERA–ELEKTRA have been done.

Magnetic Field, Length and Field Quality

The results of the DANFYSIK measurements for the CNAO magnets and the simulations compared to the specified values for CNAO are shown in Table 22.

The maximum field and the integrated length are increased while the effective length is slightly decreased. Also the field quality over the integrated length is less than the specified Δ0.2% predicted by CERN, which is shown in Figure 70 and Figure 71 for Δ0.5% for a time step of 170 µs after the maximum current has been reached.

Table 22 - Compared results of DANFYSIK specifications, measurements and simulation results.

	DANFYSIK Specification	**DANFYSIK Measurements**	**DANFYSIK Simulations**
Effective magnetic length [m]	0.3	0.276	0.272
Maximum integrated field ∫Bdl [Tm]	0.0419	0.04	0.0477
Maximum field B [T]	0.141	0.145	0.1755
Aperture w × h [mm^2]	133 x 90	133 x 90	133 x 90
Good field region (rectangle) [mm^2]	-	45 x 45	
Conductor size [mm^2]	8 x 8, ø 4.0 mm	8 x 8, ø 4.0 mm	8 x 8, ø 4.0 mm
Current for maximum field [A] (nominal)	644	644	644
Voltage [V] (nominal)	> 2900	-	-
Current density [A/mm^2]	12.7	-	-
Number of turns	16 (8 per coil)	16 (8 per coil)	16 (8 per coil)
Estimated inductance [µH]	143	-	-
Rise time [µs]	260	-	-
Fall time [µs]	260	-	-

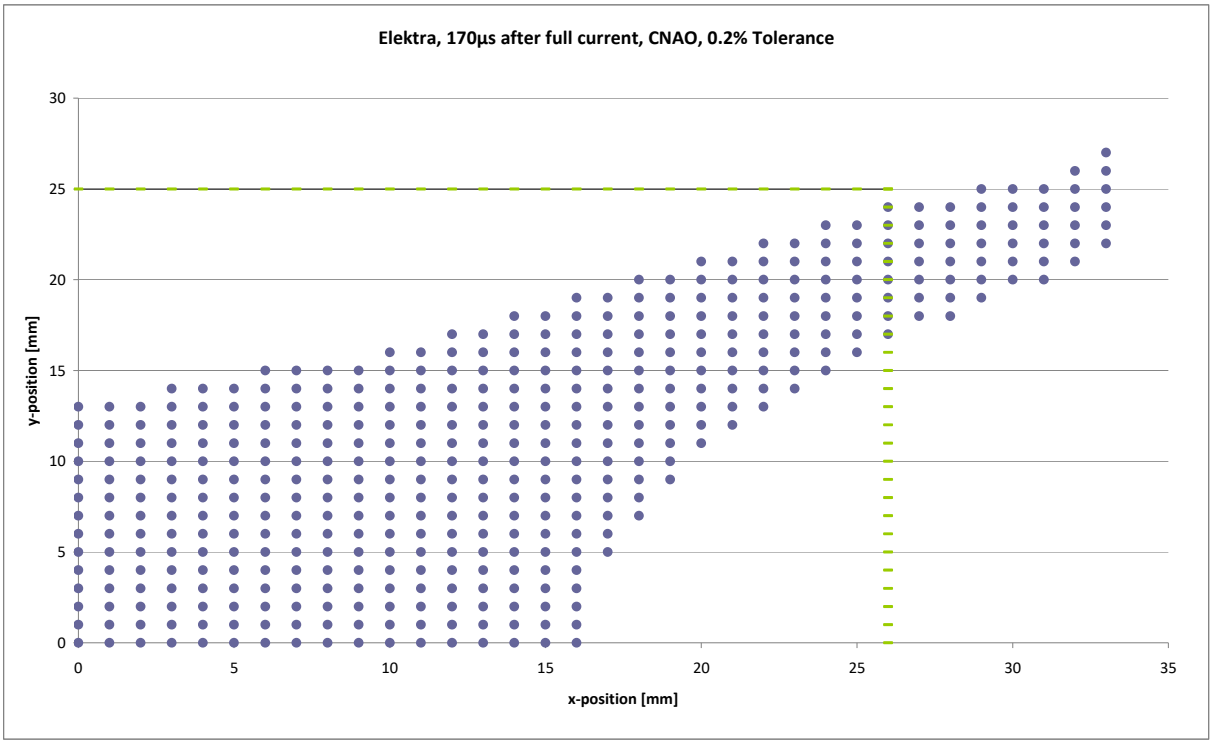

Figure 70 – Integrated field over 500 mm. The dots show the x-y position in a quarter of the magnet within a tolerance of Δ0.2%. The green lines indicate the vacuum chamber.

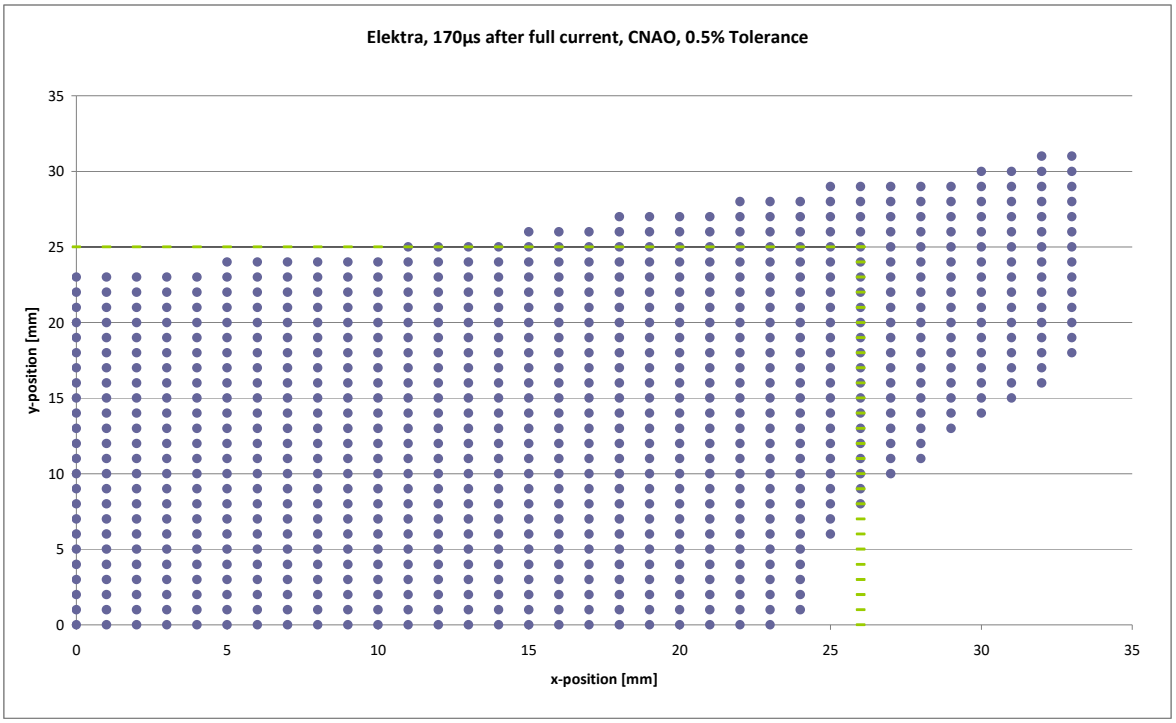

Figure 71 – Integrated field over 500 mm. The dots show the x-y position in a quarter of the magnet within a tolerance of Δ0.5%. The green lines indicate the vacuum chamber.

Saturation

The yoke is saturated with the maximums in the inner corners, at the chamfer and top and end surfaces, up to 376 mT. Most of the other parts are saturated up to 320 mT, which is the value of saturation given by Ceramics Magnetics Inc. See Figure 72.

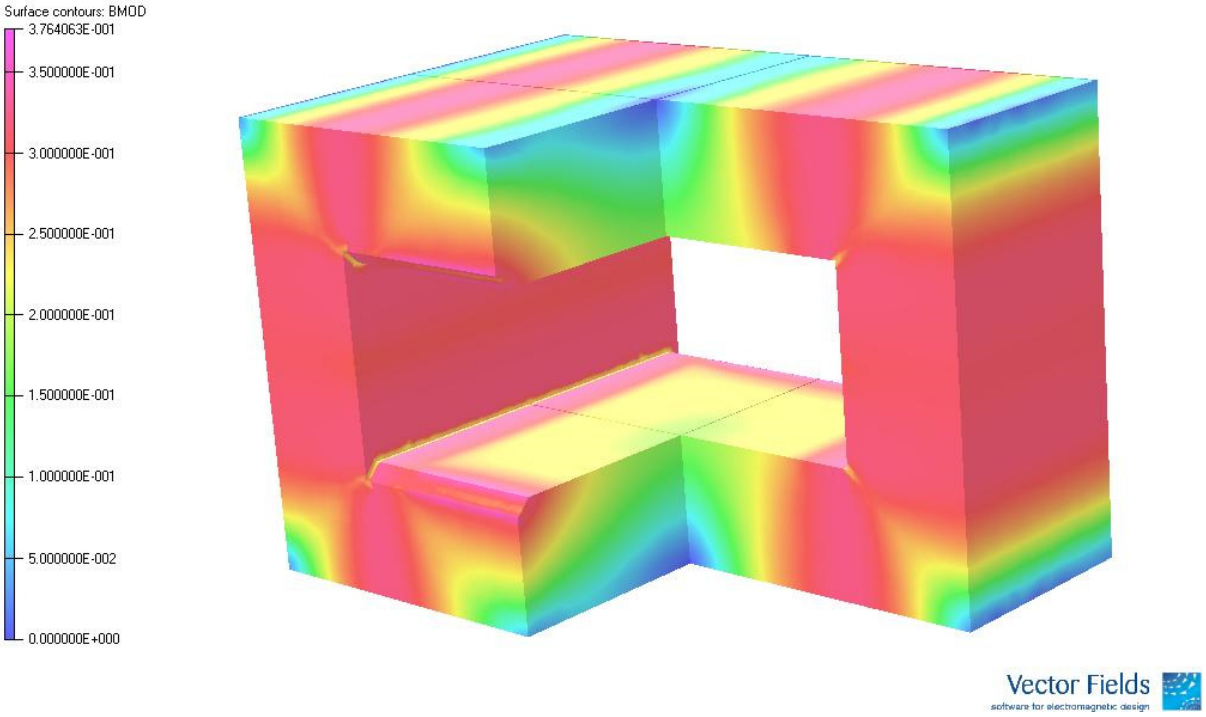

Figure 72 – Saturation shown in three quarter of the yoke.

2.4.4 Modifications proposed for MEDAUSTRON

New Design

The CNAO magnets fulfil the requirements of the magnetic field and also the field quality within Δ0.5%. Since the chopper dipoles have to be ramped very fast, the high inductance of 143 µH and the current of 644 A requires a high voltage, which leads to a costly power supply. The voltage is calculated by

$$U = -L\frac{dI}{dt}$$

Assuming a rise time of 90 µs, as proposed in the CERN special magnets report [21], a voltage of ~4.1 kV is necessary for all four copper magnets. Hence, reducing the inductance was the main issue in the proposed new design by keeping the standards of the magnetic field.

The permeability constant μ_0, the number of turns N, the effective magnetic length L_{eq} as well as the width w and the height h of the aperture calculate the inductance L.

$$L = \mu_0 N^2 \frac{L_{eq} \cdot w}{h}$$

Yoke and Shielding Box

The yoke consists as in the CNAO model of CMD5005 and is shaped as window frame with a total ferrite length of 250 mm and an aperture in width and height of 156 x 68 mm^2. The thickness of the ferrite equals 70 mm in width (x-direction) and 76 mm in height (y-direction). See Figure 73. Along the width of the aperture (x-direction) there are on the top and on the bottom chamfers for the coil as well as to break the saturation on the edges. The chamfer is in y and z-direction 11 mm, which gives a slant surface of almost 16 mm.

In a longitudinal distance of 43 mm from the yoke there are ferrite plates at both ends of the yoke also consisting of CMD5005 to control the fringe fields. The longitudinal length of these plates is 8 mm each and width and height are 336 x 260 mm^2. In the centre of these plates there is a gap for the vacuum chamber with width (x-direction) and height (y-direction) of 66 x 70 mm^2. The corners of these gaps are rounded with a radius of 5 mm (see Figure 73). The vacuum chamber has to be fitted in y-direction to the gap in the yoke, which is slightly smaller than the gap in the both endplates. Since these ferrite plates are also the endplates, the magnet has a total physical length 352 mm.

At the sides as well as at the top and the bottom the yoke is boxed in aluminium plates, which keeps a distance of 20 mm all around the yoke. The side plates have a longitudinal length of 352 mm, thickness in x-direction is 20 mm and the height in y-direction is 260 mm. The top and bottom plates also have a longitudinal length of 352 mm. They are 376 mm wide (x-direction) and the thickness (y-direction) is 20 mm. On the top, bottom and the sides they are touching the ferrite endplates (see Figure 74).

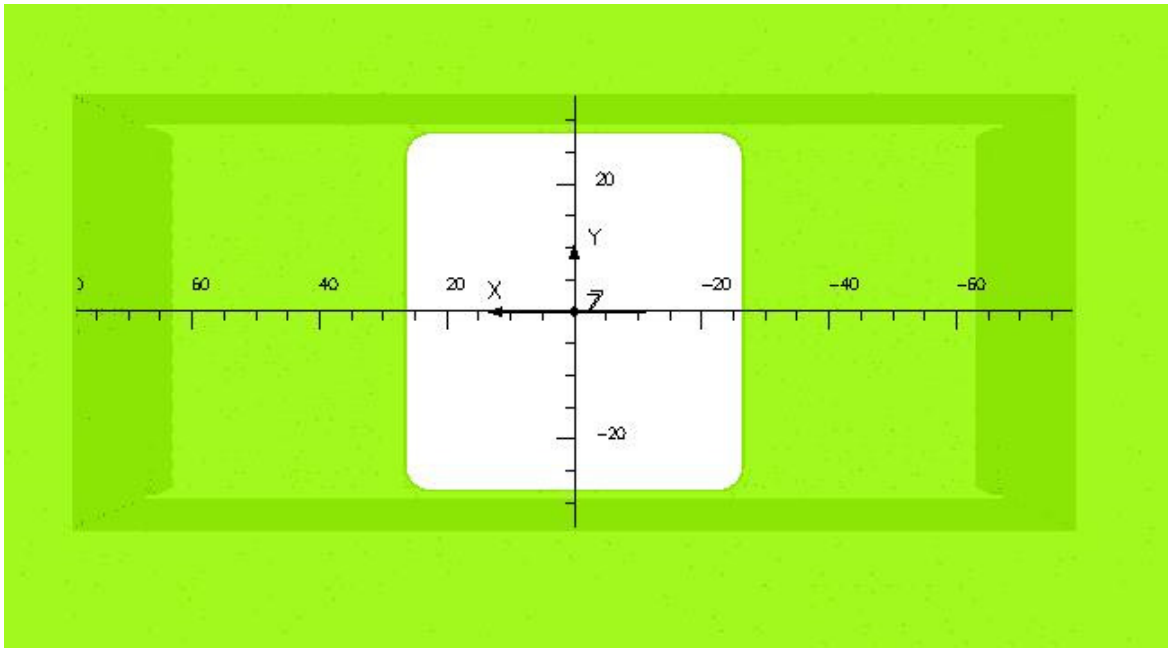

Figure 73 - Aperture of the ferrite for the MEDAUSTRON project.

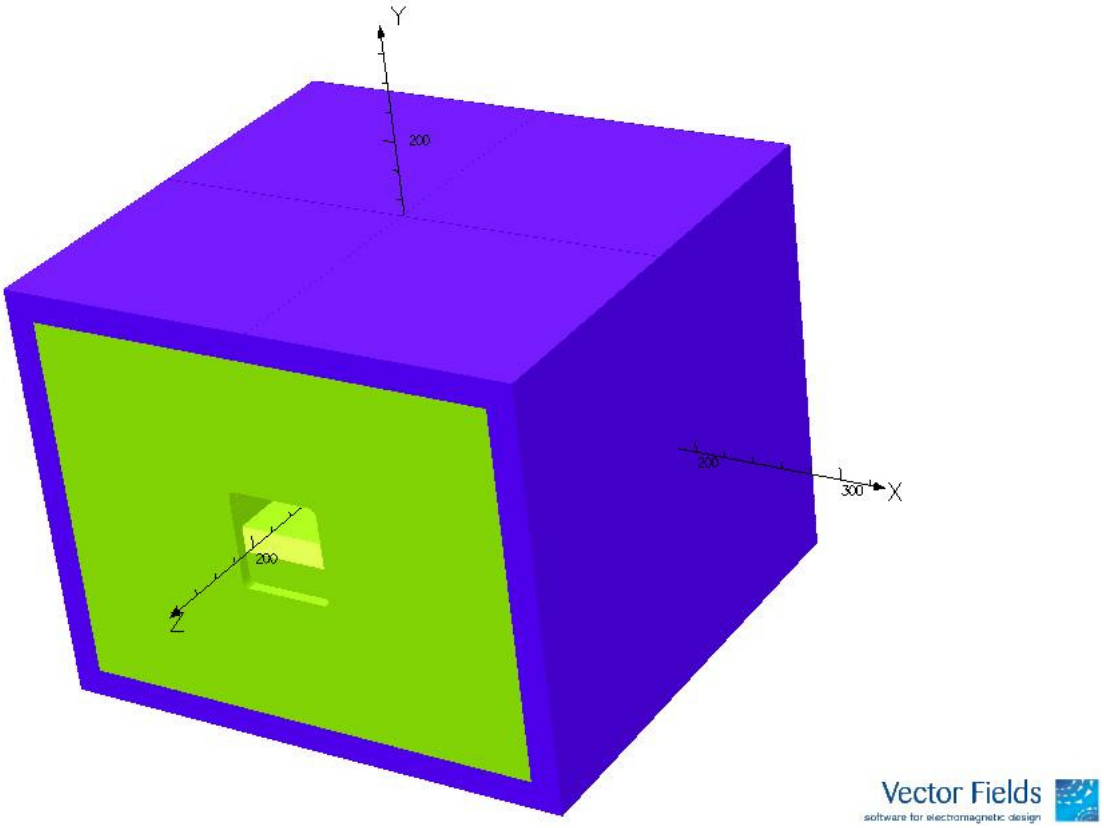

Figure 74 - Complete chopper magnet (green is ferrite and blue the aluminium shielding box).

Coil Design

The coil consists of 2 copper conductors while one conductor represents the upper half of the coil and the other conductor the bottom half. The two conductors are mirrored at the x-z plane with a space of 2 mm between the two halves. The conductors are water-cooled and have a double layer bedstead design of 3 turns each which gives 6 turns for one half i.e. 12 turns in total. To simplify the construction in the model there are 12 separately build bedstead coils.

Since the two halves are identical only one of them will be described from now on.

The cross section of one turn is 9 x 9 mm^2. In the middle there is a hole for the water-cooling with a radius of 2 mm. This hole is not build in the model. Between the three layers in y-direction of one half there is everywhere a distance of 2 mm between the turns as well as the two layers in x-direction. For one half there are three inner turns and three outer turns. This gives two turns near to the mid-plane (inner and outer), two turns in the middle of the conductor (inner and outer) and two turns near to the ferrite (inner and outer). See also Figure 75 and Figure 76. The values for each of these turns are given in Table 23.

Table 23 - Values for each turn of one conductor in mm (i.e. half of the complete conductor).

Inner Turns	Length	Arc Radius	Upright Length	Upright Arc Radius	Inner width
Mid-plane Turn	274	16	0	16	112
Middle Turn	252	16	0	16	112
Ferrite Turn	230	16	0	16	112
Outer Turns	Length	Arc Radius	Upright Length	Upright Arc Radius	Inner width
Mid-plane Turn	274	16	0	27	134
Middle Turn	252	16	0	27	134
Ferrite Turn	230	16	0	27	134

The two halves of the conductor are then placed in the centre of the magnet. The two turns at the top of the top half have then a distance of 2 mm to the ferrite, so have the top turns in the bottom half. The three outer turns have on both sides also a distance of 2 mm to the yoke. In longitudinal length the upright part of the two shortest turns have a distance of 6 mm to the yoke; the two longest turns have a distance of 6 mm to the ferrite endplates. Between the turns there are always 2 mm, except at the arc radius from the horizontal to the upright part of the windings. Using this kind of step and stair-coils helps to control the fringe fields at the end of the magnet, which gives a better field quality in the end.

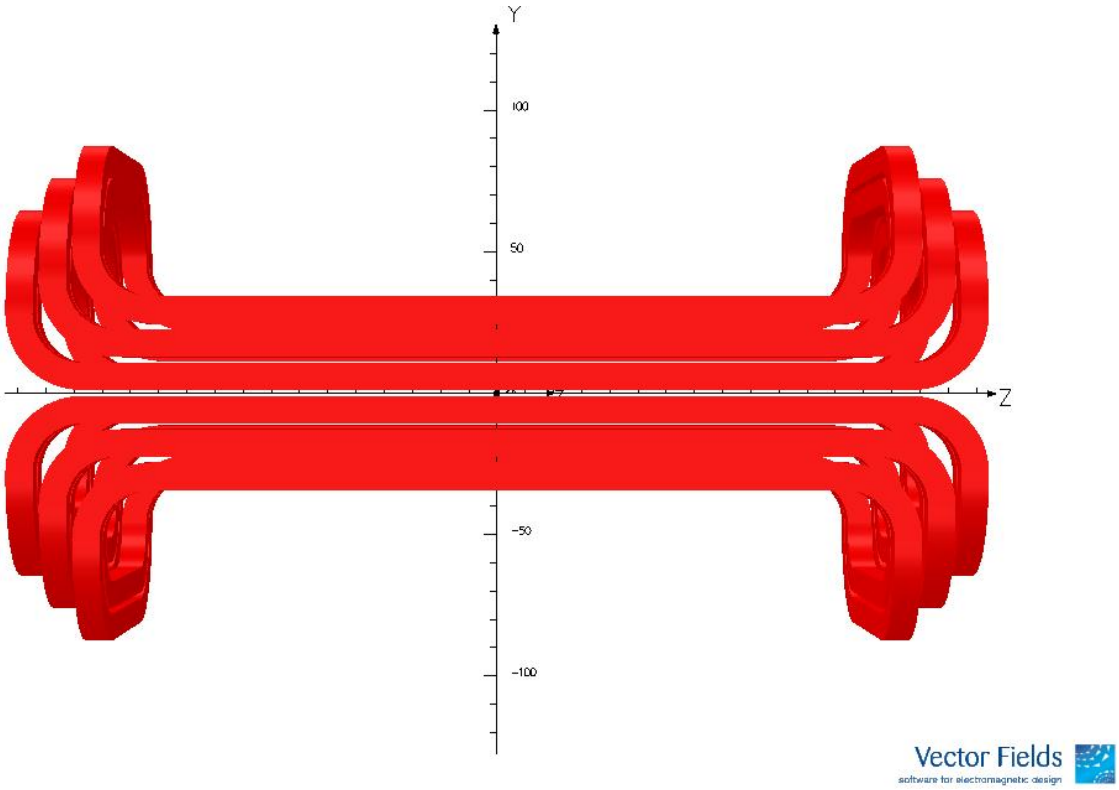

Figure 75 - Upper and lower half of the conductor.

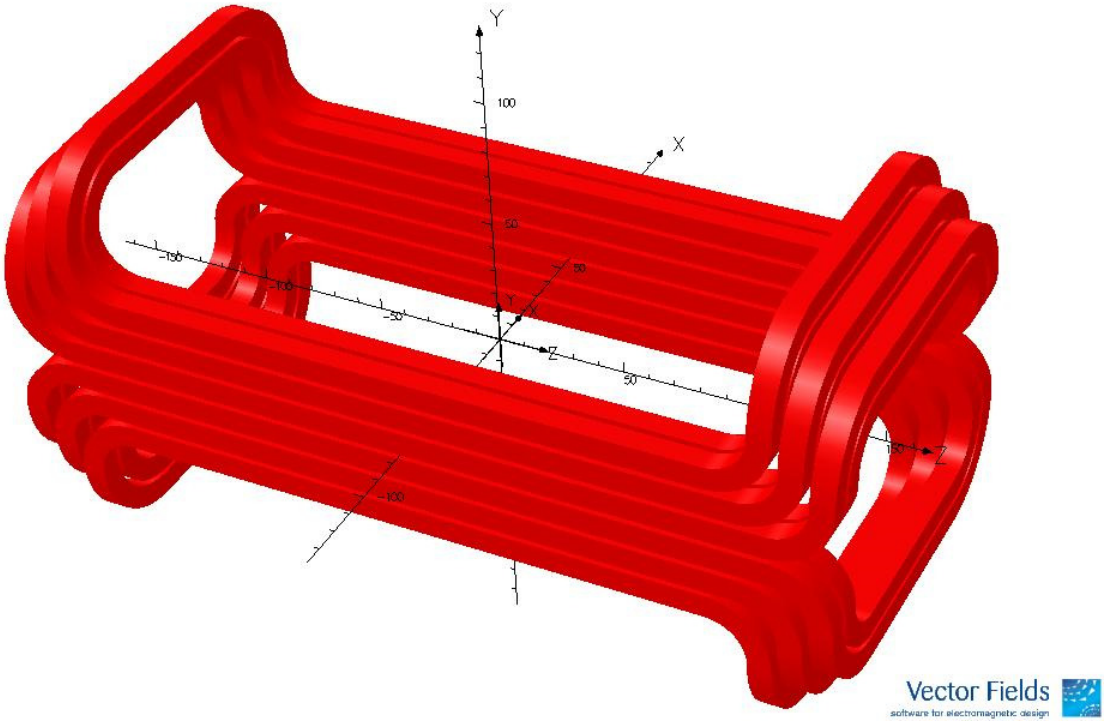

Figure 76 - Upper and lower half of the conductor.

Magnetic Field and Magnetic Length

Due to the changes in the magnet a higher current of 710 A is needed to achieve the required *Bdl*. On the other hand the inductance drops from 143 µH to 105 µH. The total physical length increases by 6 mm to 352 mm. The values of the magnetic length and some other data can be read in Table 24.

Table 24 - DANFYSIK specification and measurements and the results of the MEDAUSTRON chopper dipole simulations.

	DANFYSIK Specification	**DANFYSIK Measurements**	**Chopper Dipole MEDAUSTRON**
Effective magnetic length [m]	0.3	0.276	0.278
Maximum integrated field ∫Bdl [Tm]	0.0419	0.04	0.0438
Maximum field B [T]	0.141	0.145	0.157
Aperture w × h [mm^2]	133 x 90	133 x 90	112 x 68
Good field region (rectangle) [mm^2]	-	45 x 45	-
Conductor size [mm^2]	8 x 8, ø 4.0 mm	9 x 9, ø 4.0 mm	9 x 9, ø 4.0 mm
Current for maximum field [A] (nominal)	644	644	710
Voltage [V] (nominal)	> 2900 (1400)	-	> 3350
Current density [A/mm^2]	12.7	-	8.77
Number of turns	16 (8 per coil)	16 (8 per coil)	12 (6 per coil)
Estimated inductance [µH]	143	-	118
Rise time [µs]	260	-	90
Fall time [µs]	260	-	90

Saturation

As could be expected there is a high flux density in the corners and at the edges of the chamfer. In most areas the flux density is less than 0.25 T. This can also be seen in Figure 77.

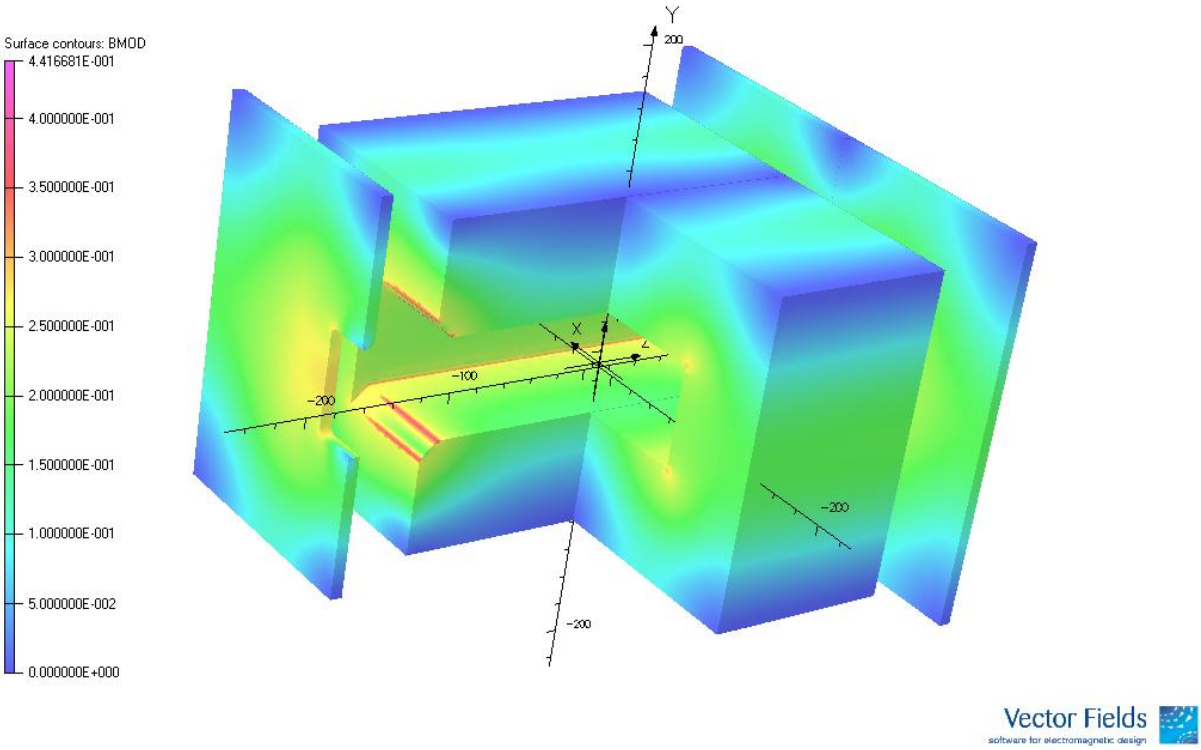

Figure 77 - Saturation of three quarter of the yoke and the ferrite endplates.

Homogeneity of the Magnetic Field

For the field quality CERN specified Δ0.2%. DANFYSIK did not reach this value and also in the adjustments for MEDAUSTRON this value could not be achieved. While the magnetic field in the centre of the magnet at the plane z=0 is in the vacuum chamber within the 0.2% tolerance (see Figure 78) the end fields are responsible for the degraded integral field quality over the integrated length as can be seen in Figure 79. In Figure 80 the magnetic field is shown with a Δ0.5% tolerance of the magnetic field referring to the centre of the magnet. For the cut in the x-y plane at z=0 the magnetic field is within this tolerance of the good field region. Almost the complete cross section of the vacuum chamber is within this tolerance. The tolerance in the vacuum chamber is less than Δ0.6%.

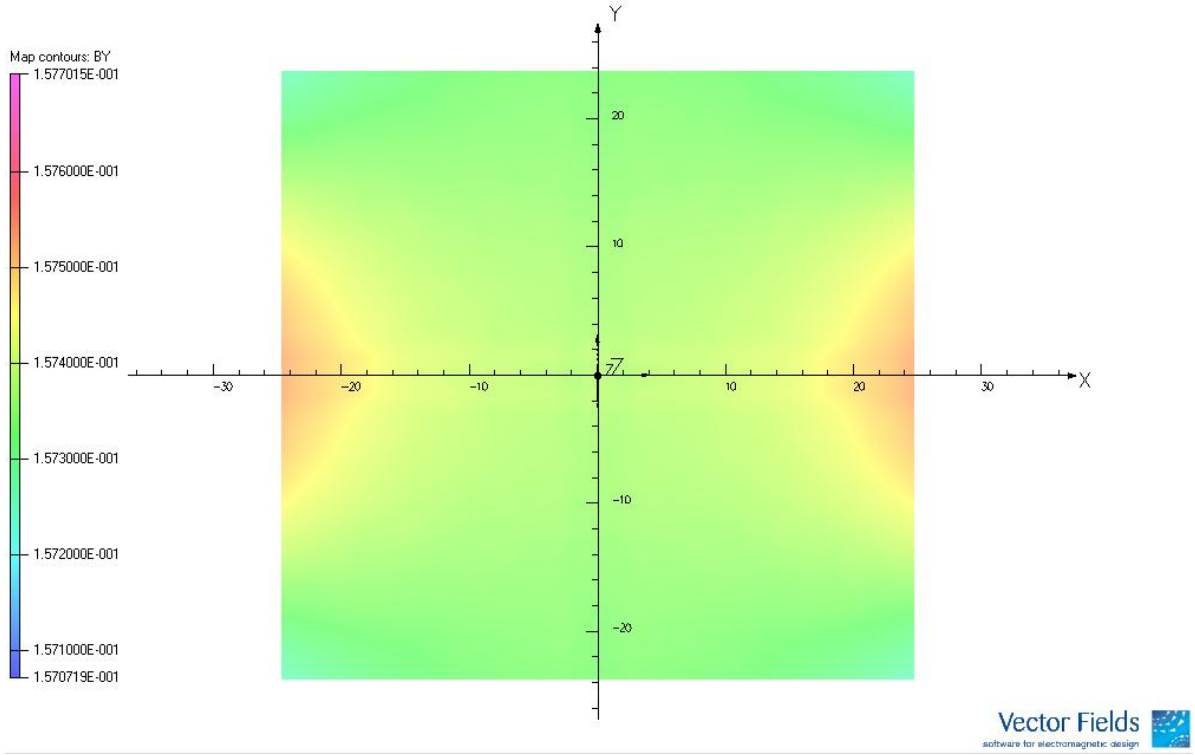

Figure 78 - Magnetic field at the plane z=0 inside the vacuum chamber. A Δ0.2% tolerance of the magnetic field referring to the centre of the magnet is displayed.

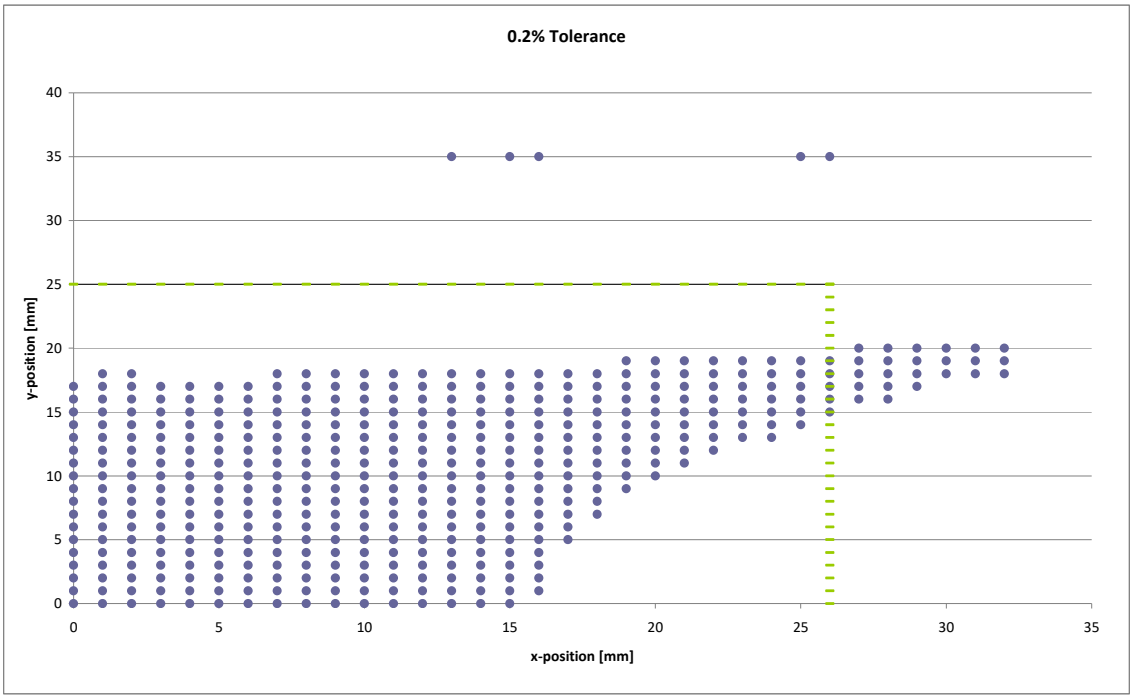

Figure 79 - Integrated field over 500 mm. The dots show the x-y position in a quarter of the magnet within a tolerance of Δ0.2%. The green lines indicate the vacuum chamber.

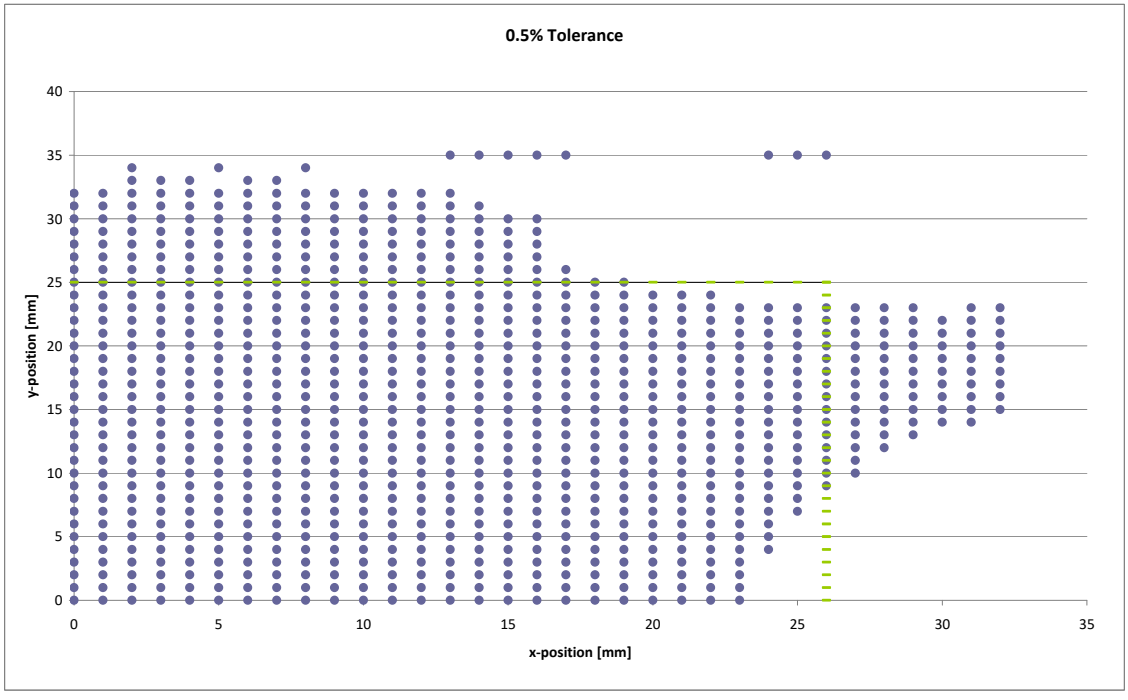

Figure 80 - Integrated field over 500 mm. The dots show the x-y position in a quarter of the magnet within a tolerance of Δ0.5%. The green lines indicate the vacuum chamber.

Stretched Magnet

The fringe fields are messing the field quality of the modified magnet, as shown. By stretching the magnet by 40 mm, the fringe fields are less dominant and therefore the field quality is increased.

Magnetic Field and Magnetic Length

Stretching the magnet will increase the integrated field. Therefore less current is needed, but the inductance will be increased due to the higher *Bdl* and the dropped maximum field, which gives an increased effective length. The total physical length is then 392 mm. The new values of the magnet are listed in Table 25.

Note that the voltage needed in the MEDAUSTRON design is higher than the voltage for DANFYSIK but has a different rise time. Calculating the voltage for the DANFYSIK chopper for a rise time of 90 µs gives 4100 V.

Table 25 - DANFYSIK specification and the two different designs for MEDAUSTRON.

	DANFYSIK Specification	**Chopper Dipole MEDAUSTRON**	**Stretched Chopper Dipole MEDAUSTRON**
Effective magnetic length [m]	0.3	0.278	0.318
Maximum integrated field ∫Bdl [Tm]	0.0419	0.0438	0.0434
Maximum field B [T]	0.141	0.157	0.136
Aperture w × h [mm^2]	133 x 90	112 x 68	112 x 68
Good field region (rectangle) [mm^2]	-	-	-
Conductor size [mm^2]	8 x 8, ø 4.0 mm	9 x 9, ø 4.0 mm	9 x 9, ø 4.0 mm
Current for maximum field [A] (nominal)	644	710	615
Voltage [V] (nominal)	> 2900 (1400)	> 3350	> 3450
Current density [A/mm^2]	12.7	8.77	7.6
Number of turns	16 (8 per coil)	12 (6 per coil)	12 (6 per coil)
Estimated inductance [µH]	143	105	118
Rise time [µs]	260	90	90
Fall time [µs]	260	90	90

Saturation

As in the first design the flux density is highest in the corners and at the edges of the chamfer. In most areas the flux density is less than 0.25 T as in the short version. In the endplates saturation is increased to 0.28 T. See Figure 81.

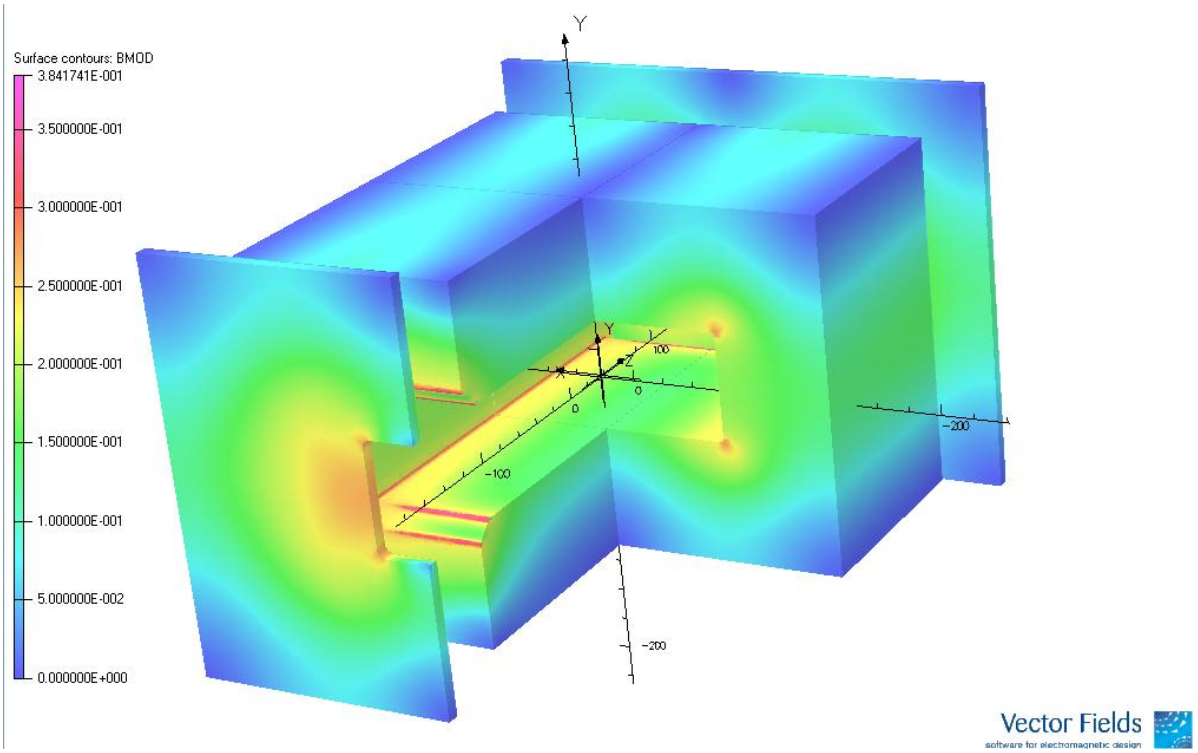

Figure 81 - Saturation of three quarter of the yoke and the ferrite endplates.

Homogeneity of the Magnetic Field

Also in the stretched model the tolerance of Δ0.2% could not be achieved. In the centre of the magnet the field is also within Δ0.2% but the fringe fields now, do not dominate the magnetic field that much as before, so that the complete vacuum chamber is now within a tolerance of Δ0.5%. See Figure 82, Figure 83 and Figure 84.

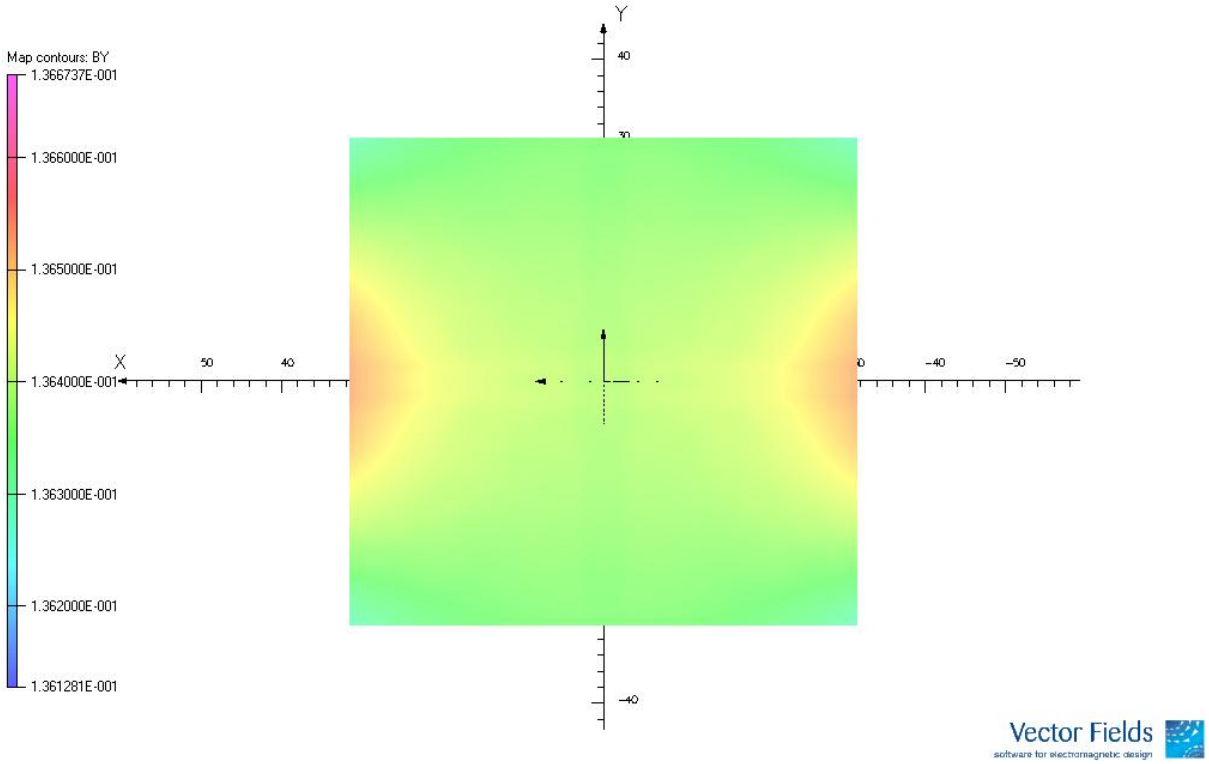

Figure 82 - Magnetic field at the plane z=0 inside the vacuum chamber for the stretched magnet. A 0.2% tolerance is displayed.

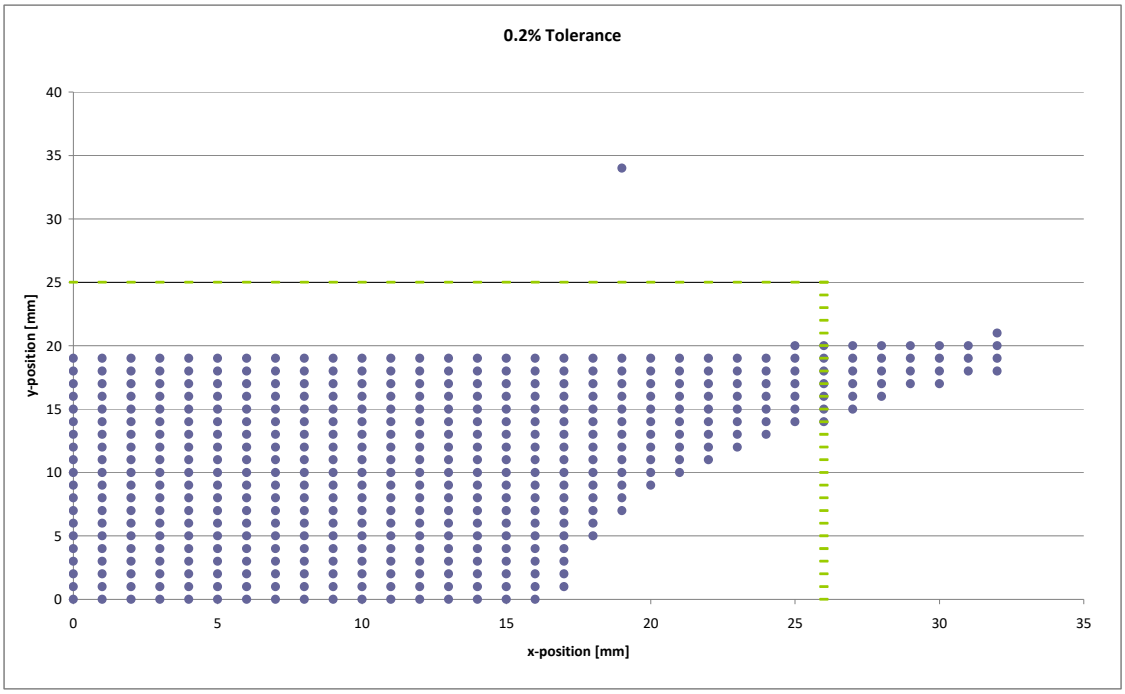

Figure 83 - Integrated field over 500 mm. The dots show the x-y position in a quarter of the magnet within a tolerance of Δ0.2%. The green lines indicate the vacuum chamber.

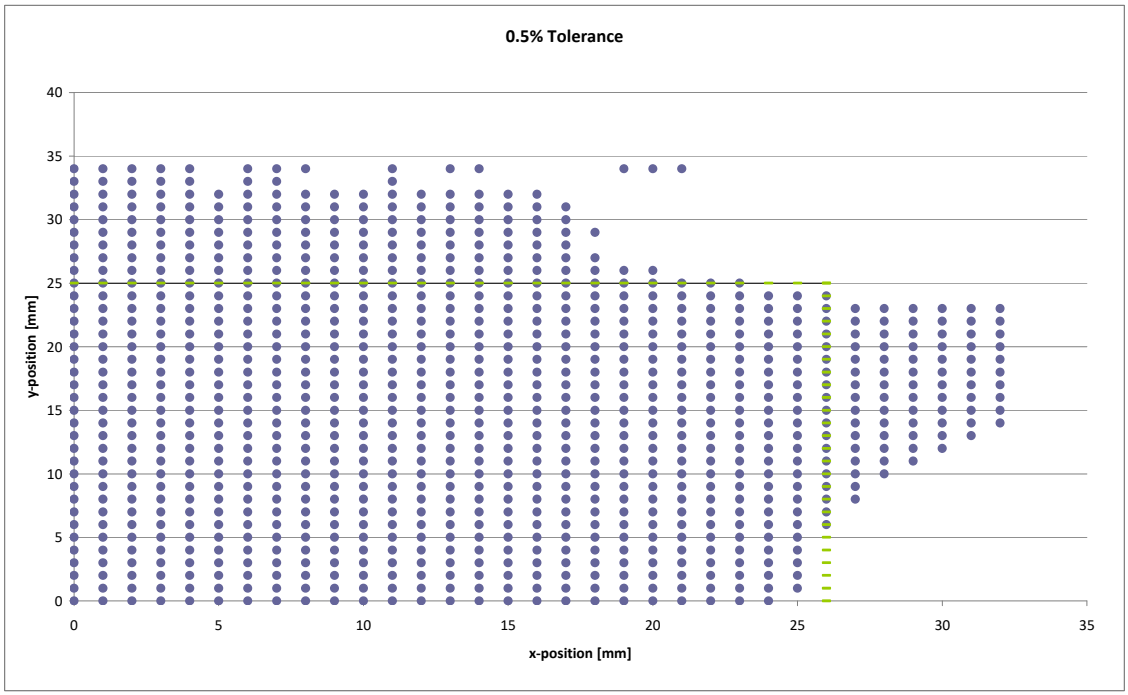

Figure 84 - Integrated field over 500 mm. The dots show the x-y position in a quarter of the magnet within a tolerance of Δ0.5%. The green lines indicate the vacuum chamber.

Low Energy Particles

Since the MEDAUSTRON accelerator will also provide low energy particles, the question arises, if the field quality requirements are also achieved, using a very low current.

That the field quality is the same is shown in simulations with a current of 162 A for the preferred stretched version of the chopper dipole. B_0 is then 35.9 mT and the integrated length is 11.4 mTm.

Figure 85 and Figure 86 show the field quality with tolerances of Δ0.2% and Δ0.5% respectively. As can be seen, the field quality is equal to the full powered magnet at 615 A.

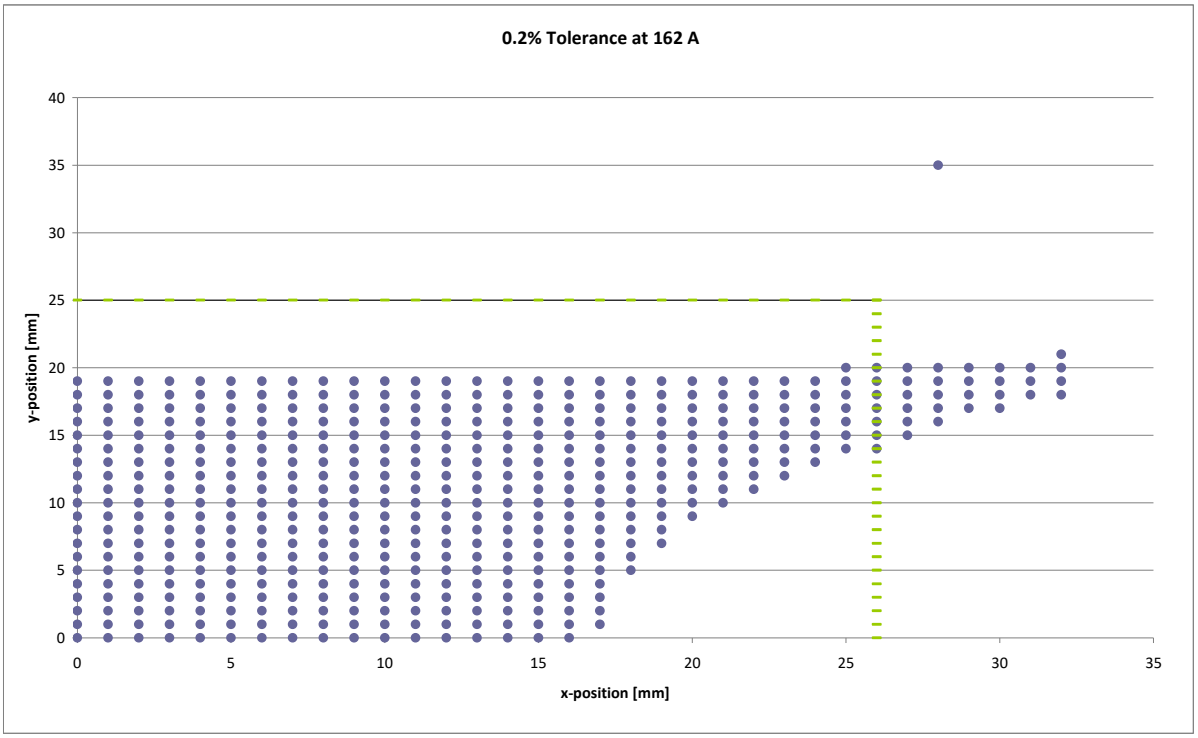

Figure 85 - Integrated field over 500 mm at a current of 162 A. The dots show the x-y position in a quarter of the magnet within a tolerance of Δ0.2%. The green lines indicate the vacuum chamber.

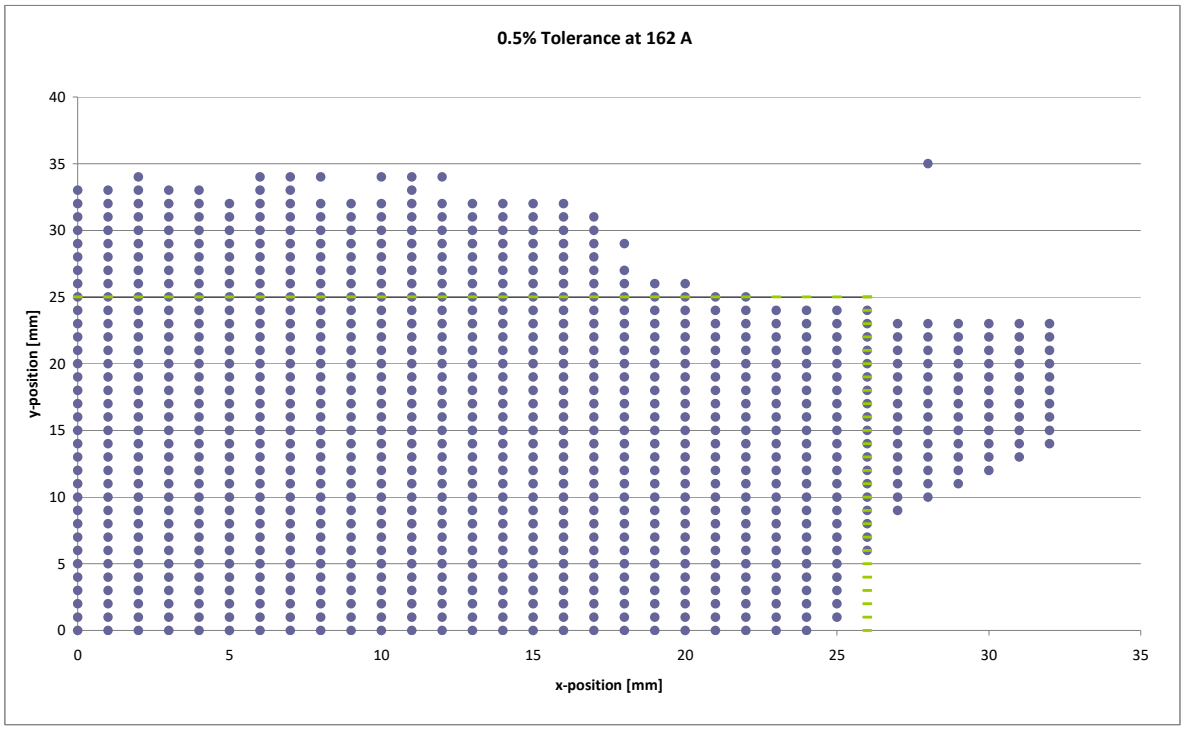

Figure 86 - Integrated field over 500 mm at a current of 162 A. The dots show the x-y position in a quarter of the magnet within a tolerance of Δ0.2%. The green lines indicate the vacuum chamber.

2.4.5 Summary

To save money on the chopper dipoles power supply the inductance has to be reduced and therefore a redesign of the four identical magnets is proposed.

Design Changes

Yoke and shielding box

The yoke consists as in the CNAO model of CMD5005 and is shaped as window frame with a total ferrite length of 250 mm and an aperture in width and height of 156 x 68 mm^2. The thickness of the ferrite equals 70 mm in width (x-direction) and 76 mm in height (y-direction). See Figure 73.

Along the width of the aperture in x-direction there are chamfers (for the coil as well as to break the saturation on the edges) on the top and on the bottom of the ferrite. The chamfer is in y and z-direction 11 mm, which gives a slant surface of almost 16 mm.

There are ferrite plates at both ends of the yoke in a longitudinal distance of 43 mm from the yoke also manufactured out of CMD5005 to control the fringe fields. The longitudinal length of these plates is 8 mm each and width and height are 336 x 260 mm^2. In the centre of these plates is a gap for the vacuum chamber with a width (x-direction) and height (y-direction) of 66 x 70 mm^2. The corners of these gaps are rounded with a radius of 5 mm (see Figure 73). The vacuum chamber has to be fitted in y-direction to the yoke gap, which is slightly smaller than the gap in both endplates. The magnet has a total physical length of 352 mm.

At the sides as well as at the top and the bottom the yoke is boxed in aluminium plates, which keeps a distance of 20 mm to the yoke elements. The side plates have a longitudinal length of 352 mm, the thickness in x-direction is 20 mm and the height in y-direction is 260 mm. The top and bottom plates have a longitudinal length of 352 mm. They are 376 mm wide (x-direction) and the thickness (y-direction) is 20 mm. On the top, bottom and the sides they are in electrical and mechanical contact with the ferrite endplates (see Figure 74).

Coil Design

The coil consists of 2 copper conductors while one conductor represents the upper half of the coil and the other conductor the bottom half. The two conductors are mirrored at the x-z plane with a space of 2 mm between the two halves. The conductors are water-cooled and have a double layer bedstead design of 3 turns each which gives 6 turns for one half i.e. 12 turns in total.

Since the two halves are identical only one of them will be described. The cross section of one turn is 9 x 9 mm^2. In the conductor centre is a hole for the water-cooling with a radius of

2 mm. Between the three layers in y-direction of one half, there is everywhere a distance of 2 mm between the turns as well as the two layers in x-direction. For one half there are three inner turns and three outer turns. This gives two turns near to the mid-plane (inner and outer), two turns in the middle of the conductor (inner and outer) and two turns near to the ferrite (inner and outer). See also Figure 75 and Figure 76. The values for each of these turns are given in Table 26.

Table 26 - Values for each turn of one conductor in mm (i.e. half of the complete conductor).

Inner Turns	Length	Arc Radius	Upright Length	Upright Arc Radius	Inner width
Mid-plane Turn	274	16	0	16	112
Middle Turn	252	16	0	16	112
Ferrite Turn	230	16	0	16	112
Outer Turns	Length	Arc Radius	Upright Length	Upright Arc Radius	Inner width
Mid-plane Turn	274	16	0	27	134
Middle Turn	252	16	0	27	134
Ferrite Turn	230	16	0	27	134

The two halves of the conductor are then placed in the centre of the magnet. The two turns at the top of the top half have then a distance of 2 mm to the ferrite. The three outer turns have on both sides also a distance of 2 mm to the yoke. In longitudinal length the upright part of the two shortest turns have a distance of 6 mm to the yoke; the two longest turns have distance of 6 mm to the ferrite endplate. Between the turns there are always 2 mm, except at the arc radius from the horizontal to the upright part of the windings.

In this version the current is increased and the inductance is decreased compared to the specification of DANFYSIK. Nevertheless less voltage is needed to ramp the four magnets within the same time, while the field quality stayed equal. It is possible to increase the area of the good field region by stretching the complete magnet. Then the fringe fields have less influence on the whole magnetic field. The DANFYSIK design, the MEDAUSTRON design as well as a stretched version of the MEDAUSTRON design (by 40 mm) is compared in Table 27.

Table 27 - DANFYSIK specification and the two different designs for MEDAUSTRON.

	DANFYSIK Specification	**Chopper Dipole MEDAUSTRON**	**Stretched Chopper Dipole MEDAUSTRON**
Effective magnetic length [m]	0.3	0.278	0.318
Maximum integrated field ∫Bdl [Tm]	0.0419	0.0438	0.0434
Maximum field B [T]	0.141	0.157	0.136
Aperture w × h [mm^2]	133 x 90	112 x 68	112 x 68
Good field region (rectangle) [mm^2]	-	-	-
Conductor size [mm^2]	8 x 8, ø 4.0 mm	9 x 9, ø 4.0 mm	9 x 9, ø 4.0 mm
Current for maximum field [A] (nominal)	644	710	615
Voltage [V] (nominal)	> 2900 (1400)	> 3350	> 3450
Current density [A/mm^2]	12.7	8.77	7.6
Number of turns	16 (8 per coil)	12 (6 per coil)	12 (6 per coil)
Estimated inductance [µH]	143	105	118
Rise time [µs]	260	90	90
Fall time [µs]	260	90	90

Since the ferrite is not saturated (i.e. almost linear calculations) the reduced current when stretching the magnet almost sets off the increased inductance and therefore the required voltage remains the same. Note that the voltage needed in the MEDAUSTRON design is higher than the voltage for DANFYSIK but has a different rise time. Calculating the voltage for the DANFYSIK chopper for a rise time of 90 µs gives 4100 V.

For low energy particles and therefore a reduced current the field quality stays the same as if the magnet is fully powered.

3 Conclusion

Three types of the special magnets for the MEDAUSTRON accelerator have been analysed namely the injection bumpers, the dump bumpers and the chopper dipoles, since measurements of these magnets for the CNAO project showed results which would not fit to the planned MEDAUSTRON baseline.

For all of these magnets improvements and changes have been made.

For the injection bumper the cross section of the ferrite has been increased because of saturation.

For the dump bumper the cross section also needed to be increased due to saturation effects in the 12-turn magnet. Further modifications inside the magnets as well as stretching these two magnets were needed since the necessary integrated field for the deflection angles of 2.7 mrad and 5.4 mrad respectively could not be reached in the CNAO design.

To reduce the cost of the power supply for the for the chopper dipoles, the inductance had to be reduced. Therefore it was necessary to redesign the complete magnet.

Injection Bumper

The CERN parameter list for the CNAO injection bumper predicted a maximum current of 454 A. However the magnets build by DANFYSIK were measured at 500 A. The magnetic field produced by these currents should provide a deflection angle of 10 mrad for protons and $^{12}C^{6+}$-ions with a kinetic energy of 7 MeV/[A]. In this thesis deflection angles for injection energies of up to 10 MeV/[A] have been studied.

Using a current of 500 A like DANFYSIK gives a deflection angle of 15.1 mrad for protons at 10 MeV/[A] but for $^{12}C^{6+}$-ions the required angle of 10 mrad is missed by 0.9 mrad even for injection energies of 7 MeV/[A].

For $^{12}C^{6+}$ the current has to be raised to 600 A to obtain an angle of 10 mrad for injection energies of 7 and 8 MeV/[A]. For kinetic energies of 9 and 10 MeV/[A] the required deflection angle is missed by 0.4 mrad and 0.9 mrad respectively.

Heat losses due to the higher current are not expected but it has not been verified in the simulations. It is also not verified if the actual power supply system can provide the increased current of 600 A.

The inhomogeneous field measured by DANFYSIK does not appear in the simulations. One explanation could be the usage of different ferrite materials in the magnet yoke legs.

To lower the flux density in the ferrite yoke a change of increasing the cross-section of the vertical blocks by 4 mm to the outer side is proposed. Additionally this allows a lower current of 530 A and the magnetic field drops to 200 mT. Note that the anticipated field quality of 1%

is not reached over the whole good field region. Changes of important parameters are shown in Table 28.

It is also shown that it is possible to make a good approximation to AC simulation by using TOSCA if the relative permeability is lowered to simulate shielding effects.

Table 28 - Changes of important parameters from the CNAO model to the MEDAUSTRON model.

Changes	CNAO model	MEDAUSTRON model
Cross-section yoke vertical [mm]	20	24
Cross-section yoke horizontal [mm]	20	20
Current [A]	500	530
Current density [A/mm^2]	16.67	17.67
Maximum integrated field [Tm]	0.00717	0.007594
Maximum field [T]	0.0278	0.0294
Aperture w*h [mm^2]	166*90	166*90
Pole gap [mm]	90	90

Dump Bumper

To reach the current specifications, the design of the magnets has to be changed. A combination of the different options given above is needed.

- Double the cross-section of the ferrite.
- Increase the total physical length of each magnet by 60 mm.
- Reduce the thickness of the aluminium end plates by 3 mm each. Therefore ferrite and coil length can be increased by 6 mm.
- Increase the coil length and the ferrite length by additional 12 mm.
- Increase the ferrite length by further 12 mm.
- Increase the current from 1265 A to 1350 A.

Note that the simulations are only done in VECTORFIELDS-TOSCA i.e. DC-simulations. By using a relative permeability of 0.0001 H/m instead of 1 H/m for the material properties of aluminium, eddy currents were simulated and as mentioned in section 2.3.3, results are fitting to CERN measurements. The approximation to ELEKTRA AC-simulations by changing the material properties can be done as shown in section 2.1.3.

The increase of the total physical length of 60 mm needs to be checked for space availability and further studies are needed by the beam optics group.

The power supply system needs to be checked if it is able to provide the increased current from 1265 A to 1350 A and to handle the higher inductance of 51 µH.

All changes are summarized in Table 29.

Table 29 - Changes of important parameters for the MEDAUSTRON dump bumpers (for both magnets)

Changes	CNAO model	MEDAUSTRON model
Total physical length [m]	0.225	0.285
Ferrite length [m]	0.15	0.18
Current [A]	1265	1350
Average turn length [m]	0.492	0.51
Estimated inductance for both magnets [µH]	40	51
Ferrite lengths in the cross-section are doubled in vertical and horizontal direction compared to CNAO model		

Chopper Dipole

To save money on the power supply for the chopper dipoles the inductance has to be reduced and a redesign of the four identical magnets is proposed.

Design Changes

Yoke and shielding box

The yoke consists as in the CNAO model of CMD5005 and is shaped as window frame with a total ferrite length of 250 mm and an aperture in width and height of 156 x 68 mm^2. The thickness of the ferrite equals 70 mm in width (x-direction) and 76 mm in height (y-direction). See Figure 73.

Along the width of the aperture in x-direction there are chamfers (for the coil as well as to break the saturation on the edges) on the top and on the bottom of the ferrite. The chamfer is in y and z-direction 11 mm, which gives a slant surface of almost 16 mm.

There are ferrite plates at both ends of the yoke in a longitudinal distance of 43 mm from the yoke also manufactured out of CMD5005 to control the fringe fields. The longitudinal length of these plates is 8 mm each and width and height are 336 x 260 mm^2. In the centre of these plates is a gap for the vacuum chamber with a width (x-direction) and height (y-direction) of 66 x 70 mm^2. The corners of these gaps are rounded with a radius of 5 mm (see Figure 73).

The vacuum chamber has to be fitted in y-direction to the yoke gap, which is slightly smaller than the gap in both endplates. The magnet has a total physical length of 352 mm.

At the sides as well as at the top and the bottom the yoke is boxed in aluminium plates, which keeps a distance of 20 mm to the yoke elements. The side plates have a longitudinal length of 352 mm, the thickness in x-direction is 20 mm and the height in y-direction is 260 mm. The top and bottom plates have a longitudinal length of 352 mm. They are 376 mm wide (x-direction) and the thickness (y-direction) is 20 mm. On the top, bottom and the sides they are in electrical and mechanical contact with the ferrite endplates (see Figure 74).

Coil Design

The coil consists of 2 copper conductors while one conductor represents the upper half of the coil and the other conductor the bottom half. The two conductors are mirrored at the x-z plane with a space of 2 mm between the two halves. The conductors are water-cooled and have a double layer bedstead design of 3 turns each which gives 6 turns for one half i.e. 12 turns in total.

Since the two halves are identical only one of them will be described. The cross section of one turn is 9 x 9 mm^2. In the middle there is a hole for the water-cooling with a radius of 2 mm. Between the three layers in y-direction of one half there is everywhere a distance of 2 mm between the turns as well as the two layers in x-direction. For one half there are three inner turns and three outer turns. This gives two turns near to the mid-plane (inner and outer), two turns in the middle of the conductor (inner and outer) and two turns near to the ferrite (inner and outer). See also Figure 75 and Figure 76. The values for each of these turns are given in Table 30.

Table 30 - Values for each turn of one conductor in mm (i.e. half of the complete conductor).

Inner Turns	Length	Arc Radius	Upright Length	Upright Arc Radius	Inner width
Mid-plane Turn	274	16	0	16	112
Middle Turn	252	16	0	16	112
Ferrite Turn	230	16	0	16	112
Outer Turns	Length	Arc Radius	Upright Length	Upright Arc Radius	Inner width
Mid-plane Turn	274	16	0	27	134
Middle Turn	252	16	0	27	134
Ferrite Turn	230	16	0	27	134

The two halves of the conductor are then placed in the centre of the magnet. The two turns at the top of the top half have then a distance of 2 mm to the ferrite. The three outer turns have on both sides also a distance of 2 mm to the yoke. In longitudinal length the upright part of the two shortest turns have a distance of 6 mm to the yoke; the two longest turns have distance of 6 mm to the ferrite endplate. Between the turns there are always 2 mm, except at the arc radius from the horizontal to the upright part of the windings.

In this version the current is increased but the inductance is decreased compared to the specification of DANFYSIK. Nevertheless less voltage is needed to ramp the four magnets within the same time, while the field quality stayed equal. It is possible to increase the area of the good field region by stretching the complete magnet. Then the fringe fields have less influence on the whole magnetic field. The DANFYSIK design, the MEDAUSTRON design as well as a stretched version of the MEDAUSTRON design by 40 mm is compared in Table 31.

Table 31 - DANFYSIK specification and the two different designs for MEDAUSTRON.

	DANFYSIK Specification	**Chopper Dipole MEDAUSTRON**	**Stretched Chopper Dipole MEDAUSTRON**
Effective magnetic length [m]	0.3	0.278	0.318
Maximum integrated field ∫Bdl [Tm]	0.0419	0.0438	0.0434
Maximum field B [T]	0.141	0.157	0.136
Aperture w × h [mm^2]	133 x 90	112 x 68	112 x 68
Good field region (rectangle) [mm^2]	-	-	-
Conductor size [mm^2]	8 x 8, ø 4.0 mm	9 x 9, ø 4.0 mm	9 x 9, ø 4.0 mm
Current for maximum field [A] (nominal)	644	710	615
Voltage [V] (nominal)	> 2900 (1400)	> 3350	> 3450
Current density [A/mm^2]	12.7	8.77	7.6
Number of turns	16 (8 per coil)	12 (6 per coil)	12 (6 per coil)
Estimated inductance [µH]	143	105	118
Rise time [µs]	260	90	90
Fall time [µs]	260	90	90

In general the magnets can be built with any length depending on the field quality wanted. Since the ferrite is not saturated (i.e. almost linear calculations) the increased inductance almost compensates the less needed current when stretching the magnet. Note that the voltage needed in the MEDAUSTRON design is higher than the voltage for DANFYSIK but has a different rise time. Calculating the voltage for the DANFYSIK chopper for a rise time of 90 µs gives 4100 V.

For low energy particles and therefore a reduced current the field quality stays the same as if the magnet is fully powered.

4 Bibliography

Literature

Alexander Wu Chao, Maury Tigner, “Handbook of Accelerator Physics and Engineering”, World Scientific, Stanford, California, Ithaca, New York, 1998

H. Wiedemann, “Particle Accelerator Physics I”, Springer, second edition, Palo Alto, California, 1998

Rende Steerenberg, “Introduction to Accelerator Physics”, CERN, Geneva, 2010

Henke, Elektromagnetische Felder, Springer, second edition, Berlin, 2004

Marlene Marinescu, “Elektrische und magnetische Felder“, Springer, Berlin, 1996

Stanley Humphries, Jr., “Principles of Charged Particle Acceleration“, Albuquerque, New Mexico, 1999

Philip J. Bryant, Kjell Johnson, “The Principles of Circular Accelerators and Storage Rings“, Press Syndicate oft he University of Cambridge 1993

Helmut Nowotny, “Elektrodynamik und Relativitätstheorie”, 6th edition, Technische Universität Wien 2003

List of Tables

List of Figures

5 Appendix

5.1 Abstract

Introduction

MEDAUSTRON, a facility for ion therapy and research headquartered in Wiener Neustadt, Austria radiates patients with protons or carbon ions. For injection, acceleration in the synchrotron and extraction of particles a variety of magnets is needed, which are designed and produced in cooperation with CERN. 2d und 3d FEM simulations are applied to improve and verify the magnets. As a baseline for the MEDAUSTRON accelerator the construction drawings of CNAO, a similar facility in Italy, have been used.

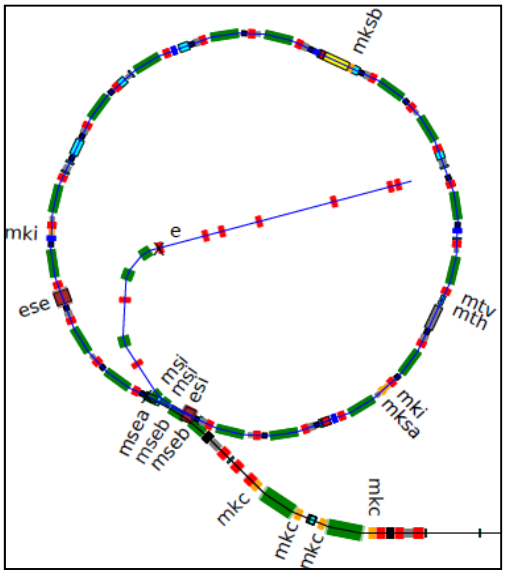

Figure 87 - MEDAUSTRON accelerator.

Injection Bumpers

The two identical injection bumpers (mki in Figure 87) are located around the injection line and are used to deflect the beam by 10 mrad to bump it from its reference trajectory. Hence the position of the beam is shifted within the phase-space and it is possible to inject new particle bunches in the main ring of the accelerator.

Measurements of the CNAO injection bumpers showed an inhomogeneous field and simulations showed that the required deflection angle of 10 mrad is only achieved for protons but not for carbon ions.

Improvements

Since the ferrite showed beginning saturation effects, the cross-section of the yoke has been increased by 4 mm, which also allows using a higher current. For CNAO a current of 454 A has been specified, which is now increased to 600 A. This provides higher deflection angles so that the injection energy of 7 MeV/[A] can be raised to 10 MeV/[A] for protons. For carbon ions the deflection angle of 10 mrad is missed by 0.9 mrad for injection energies of 10 MeV/[A]. The inhomogeneous field measured by DANFYSIK for the CNAO magnets does not appear in the simulations. This is clarified by the use of different materials in the yoke by DANFYSIK.

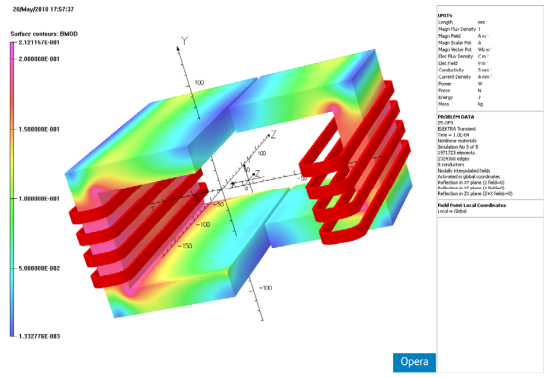

Figure 88 - Saturation of the ferrite for the modified injection bumpers.

Dump Bumpers

To dump the beam in the main ring, two dump bumpers (with the suffix mkd in Figure 89) are installed. As the two magnets are used to create a closed orbit bump, it seems preferable to power the magnets in series. In order to account for the different optics (β) functions at the two locations, the integrated kick strengths have a ratio of 1:2. This is implemented by using the same magnet yoke design but with a different number of windings i.e. 6 turns for the start beam dump and 12 turns for the end beam dump to provide deflection angles of 2.7 mrad and 5.4 mrad respectively.

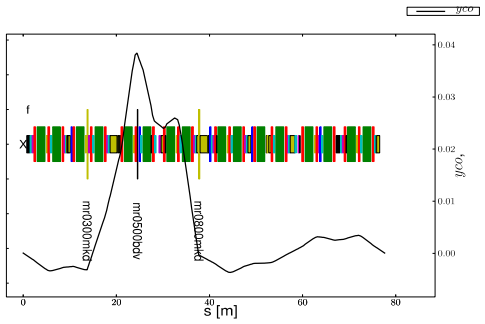

Figure 89 - The black line shows the vertical orbit bump along synchrotron sectors overlaid by the accelerator lattice (extraction optics).

Measurements of the CNAO dump bumpers showed that both magnets - especially mr0300mkd (12 turns) - did not meet the required integrated magnetic lengths.

Improvements

Both magnet designs were based on the 6-turn dump bumper, which led to saturation effects in the 12-turn dump bumper. To avoid saturation the cross-section of the ferrite has been doubled in both magnets. In addition the current had to be increased and the physical dimensions of the magnet had to be changed to reach the required specifications.

The changes in detail are:

- Double the cross-section of the ferrite.
- Increase the total physical length of each magnet by 60 mm.
- Reduce the thickness of the aluminium end plates by 3 mm each. Therefore ferrite and coil length can be increased by 6 mm.
- Increase the coil length and the ferrite length by additional 12 mm.
- Increase the ferrite length by further 12 mm.
- Increase the current from 1265 A to 1350 A.

Changes of important parameters are summarized in Table 32.

Table 32 - Changes of important parameters for the MEDAUSTRON dump bumpers.

Changes	CNAO	MEDAUSTRON
Total physical length [m]	0.225	0.285
Ferrite length [m]	0.15	0.18
Current [A]	1265	1350
Average turn length [m]	0.492	0.51
Estimated inductance for both magnets [µH]	40	51
Ferrite lengths in the cross-section are doubled in vertical and horizontal direction compared to CNAO model		

Chopper Dipoles

The four identical and coupled chopper dipoles (mkc in Figure 90 - MEDAUSTRON accelerator layout.) are located in the extraction line of the accelerator and work as a closed orbit bump bypassing a dump block, which is mounted inside of the vacuum chamber. Hence the chopper works as a safety device to dump the beam before reaching the treatment rooms. Due the magnets are coupled, they have a high overall inductance and because of the fast ramp time a high voltage is needed, which makes the power supply a very costly device.

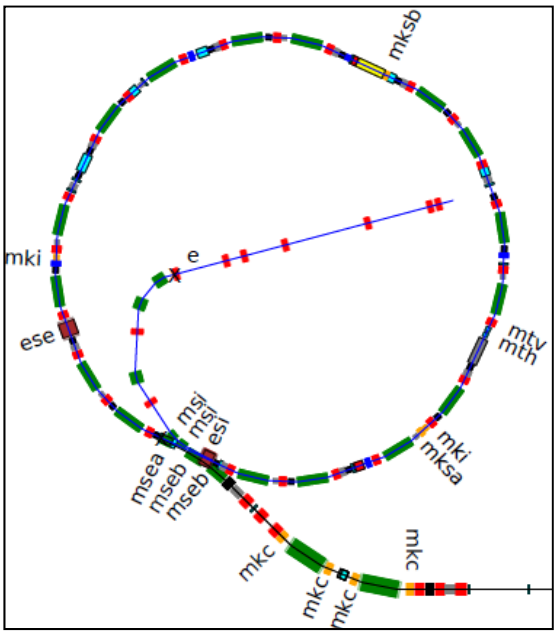

Figure 90 - MEDAUSTRON accelerator layout.

Improvements

The chopper dipoles were originally designed at CERN with coils of 16 turns per magnet, a ramp time of 90 µs, a current of 644 A per magnet and an estimated total inductance of 250 µH. This leads to a needed pulsed voltage of almost 7.5 kV. To reduce the inductance a new coil design has been proposed, which foresees only 12 turns per coil and magnet. (See Figure 91).

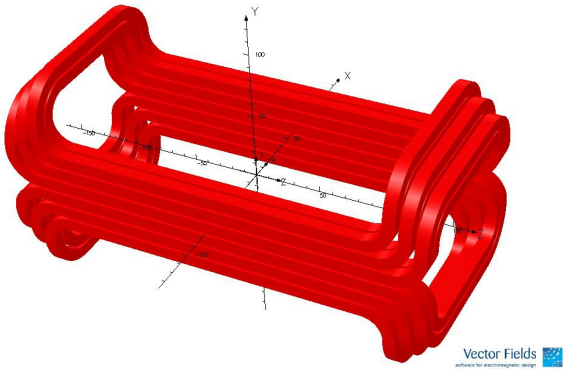

Figure 91 - Proposed coil design of the chopper dipole.

To control the fringe fields the coils have a stair-design and CMD 5005 has replaced the aluminium endplates. Also the ferrite dimensions as well as the dimensions of the magnet have been slightly changed. Due to the reduction of turns of the coil, the current had to be increased to 710 A. The overall inductance is reduced too estimated 118 µH and the field quality could be maintained. Hence the needed pulsed voltage for the chopper dipoles could be reduced to less than 3.5 kV for a ramp time of 90 µs. The power supply therefore can be redesigned saving expensive components in production.

5.2 Kurzfassung

Einleitung

MEDAUSTRON ist eine medizinische Einrichtung für Ionentherapie und Forschung mit Hauptsitz in Wr. Neustadt, Österreich, in der Tumorpatienten mit Kohlenstoff Ionen oder Protonen bestrahlt werden können. Um Teilchen in den Synchrotron-Beschleuniger zu injizieren und extrahieren werden verschiedene Magnete benötigt, welche in Kooperation mit CERN designet und produziert werden. Um das bisherige Design der Magnete zu verifizieren und zu verbessern wurden 2d und 3d FEM Simulationen erstellt. Als Basis für MEDAUSTRON dienen dabei die Konstruktionszeichnungen von CNAO, einer ähnlichen Einrichtung in Italien.

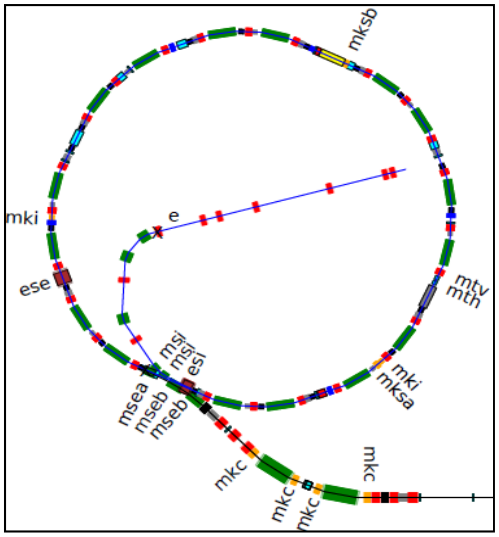

Abbildung 92 – MEDAUSTRON-Beschleunigerring.

Injection Bumpers (Injektions Bumper)

Zwei identische Injection Bumper (mki in Abbildung 92) befinden sich um den Injektionsbereich und werden benötigt, um den Teilchenstrahl um 10 mrad vom Sollorbit auszulenken. Dadurch wird der Teilchenstrahl innerhalb des Phasenraums geschiftet und es ist möglich neue Teilchenpakete in den Beschleunigerring zu injizieren.

Messungen der CNAO Injection Bumper zeigten jedoch einerseits ein inhomogenes Magnetfeld sowie eine ungenügende Ablenkung der schwereren Kohlenstoff Ionen.

Verbesserungen

Das Ferrit im inneren des Magneten zeigte beginnende Sättigungserscheinungen. Daher wurde der Querschnitt des Eisenkerns um 4 mm vergrößert. Damit ist es außerdem möglich den Strom zu erhöhen, ohne in den Sättigungsbereich zu kommen. Der für CNAO spezifizierte Strom wurde von 454 A auf 600 A erhöht, womit auch höhere Ablenkungswinkel erzielt werden können. Die Injektionsenergie kann somit von 7 MeV/[A] auf 10 MeV/[A] für Protonen erhöht werden. Der Ablenkwinkel für Kohlenstoff Ionen von 10 mrad wird bei Injektionsenergien von 10 MeV/[A] um 0.9 mrad verfehlt. Das inhomogene Feld der CNAO Magneten, welches von DANFYSIK gemessen wurde, scheint in den Simulationen nicht auf. Die Inhomogenitäten können jedoch auf verschiedene Materialien, die für die Produktion des Eisenkerns verwendet wurden, zurück geführt werden.

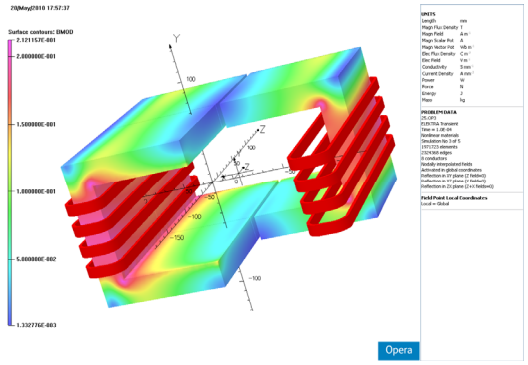

Abbildung 93 – Sättigung des Eisenkerns im modifizierten Injection Bumper.

Dump Bumpers (Strahlfänger)

Um den Strahl zu dumpen werden im Beschleunigerring zwei Dump Bumper installiert (mit dem Suffix mkd in Abbildung 94). Die beiden Magnete bilden einen geschlossenen Orbit-Bump und werden daher in Serie geschalten. Aufgrund der verschiedenen Strahloptik Funktionen (β-Funktionen) an den beiden Positionen, hat der Ablenkwinkel ein Verhältnis von 1:2. Um dies zu erreichen werden die beiden Magnete identisch gebaut, besitzen jedoch eine unterschiedliche Windungszahl (6 bzw. 12 Windungen), um die benötigten Ablenkwinkel von 2.7 und 5.4 mrad zu erreichen.

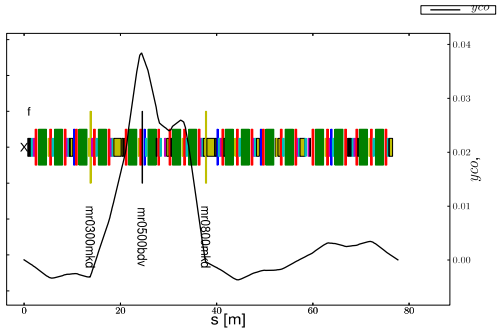

Abbildung 94 – Die schwarze Linie zeigt den vertikalen Orbit-Bump entlang der Synchrotron Elemente (Extraktionsoptik).

Messungen der CNAO Dump Bumpers zeigten, dass die Magnete (im Speziellen mr0300mkd mit 12 Windungen), die spezifizierten integrierten magnetischen Längen nicht erreichten.

Verbesserungen

Bei CNAO basieren beide Magnet-Designs auf dem Dump Bumper mit 6 Windungen. Dies führte zu Sättigungseffekten für den Magneten mit 12 Windungen. Um Sättigung zu vermeiden wurde für beide Magnete der Ferrit-Querschnitt verdoppelt und zusätzlich der Strom erhöht um die benötigten Spezifikationen zu erreichen.

Die Veränderungen im Detail sind:

- Verdoppelung des Ferrit-Querschnitts.
- Erhöhung der totalen physikalischen Länge des Magneten um 60 mm.
- Reduktion der Dicke der Aluminium Endplatten um 3 mm auf beiden Seiten. Dafür werden Ferrit und Spulen um 6 mm verlängert.
- Verlängerung der Spulenlänge und des Ferrits um 12 mm.
- Erhöhung der Ferritlänge um weitere 12 mm.
- Erhöhung des Stroms von 1265 A auf 1350 A.

Änderungen von wichtigen Parametern sind in Tabelle 33 zusammengefasst.

Tabelle 33 – Änderungen von wichtigen Parametern der MEDAUSTRON Dump Bumper.

Änderungen	CNAO	MEDAUSTRON
Totale physikalische Länge [m]	0.225	0.285
Ferrit Länge [m]	0.15	0.18
Strom [A]	1265	1350
Durchschnittliche Windungslänge [m]	0.492	0.51
Geschätzte Induktanz für beide Magnete [µH]	40	51
Ferrit Querschnitt ist im Vergleich zu CNAO vertikal und horizontal verdoppelt		

Chopper Dipoles (Chopper Dipol)

Vier identische und in Serie geschaltete Chopper Dipole (mkc in Abbildung 95) befinden sich in der Extraktionslinie des Beschleunigers und bilden einen geschlossenen Orbit Bump, der einen Dump-Block in der Mitte der Vakuumkammer umgeht. Der Chopper dient als Sicherheitselement um den Strahl vor den Behandlungsräumen abzubrechen. Aufgrund der Kopplung zwischen den Magneten haben diese eine hohe Induktanz und mit der kurzen Schaltzeit wird eine hohe Spannung benötigt, was die Stromversorgungsquelle stark verteuert.

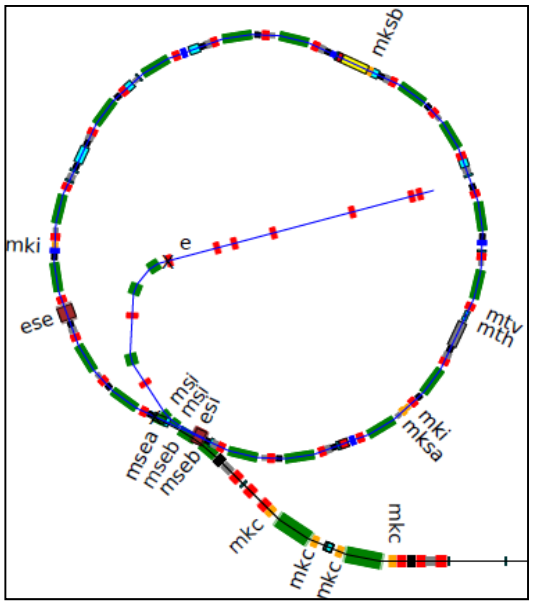

Abbildung 95 - MEDAUSTRON Beschleuniger Layout.

Verbesserungen

Die Chopper Dipole wurden ursprünglich am CERN designet mit einer Windungszahl von 16 Windungen pro Magnet, einer Schaltzeit von 90 µs, einem Strom von 644 A und einer abgeschätzten Induktanz von 250 µH. Die maximale gepulste Spannung beträgt damit knappe 7.5 kV. Um die Induktanz zu reduzieren, wurde ein neues Spulendesign mit 12 Windungen pro Spule und Magnet entworfen. Siehe Abbildung 96.

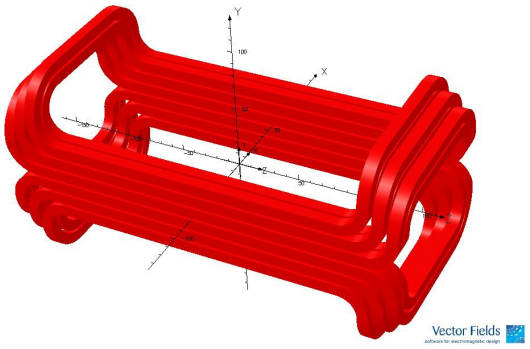

Abbildung 96 – Neues Spulendesign für die Chopper Magneten.

Um die Randfelder besser zu kontrollieren wurden die Windungen stiegen förmig gestaltet und die Aluminium Endplatten wurden durch CMD 5005 ersetzt. Zusätzlich wurden die Dimensionen des Ferrits und des Magneten als Ganzes verändert. Wegen der Reduktion der Windungszahl, musste der Strom auf 710 A erhöht werden. Die Gesamtinduktanz sank im Gegenzug auf abgeschätzte 118 µH. Durch sämtliche Änderungen benötigt der Chopper nun etwas weniger als 3.5 kV gepulste Spannung bei einer Schaltzeit von 90 µs. Damit kann eine neue Stromversorgungsquelle entworfen werden, ohne kostspielige Komponenten für Hochspannung zu verwenden.